NTNU

Kunnskap for en bedre verden

Investigation of polycyclic aromatic hydrocarbons (PAH) absorption from seawater to model microplastic particles

Emilie Rogers

Master i realfag

Innlevert:	mai 2018
Hovedveileder:	Rudolf Schmid, IKJ
Medveileder:	Andrew Booth, Sintef Ocean
	Lisbet Sørensen, Sintef Ocean

Norges teknisk-naturvitenskapelige universitet
Institutt for kjemi

Abstract

Microplastics (MPs) pollution in the aquatic ecosystems has aroused increasing concerns in recent years and are known to sorb polycyclic aromatic hydrocarbons (PAHs) from water, influencing the transport, retardment, and the bioavailability of PAHs. The MPs can also control the concentration of PAHs in the environment.

In this study the sorption behaviour of three polycyclic aromatic hydrocarbons (PAHs); phenanthrene (PHE), 1,3-dimethylnaphthalene (DMN) and fluoranthene (FLA), to different MP polymers; polystyrene (PS), polyethylene (PE) and polyester (PES), at two different temperatures, 10 and 20 °C, was investigated. Sorption equilibrium and isotherms were sought established for the different pairings of MP and PAHs.

It was shown that fluoranthene and phenanthrene sorb on to MPs. The partitioning of 1,3-dimethylnaphthalene to the MPs showed negligible or negative values, and sorption could therefore not be observed. PE (10 µm) and fluoranthene had the largest sorption capacities of the MPs and the PAHS, respectively.

The equilibration times were 5 days for fluoranthene, 9 days for phenanthrene at 10 °C and 7 days for phenanthrene at 20 °C, irrespective of polymer type and size used in the experiments.

In this study, the goodness-of-fit of nonlinear forms of five common isotherm models, Dubinin-Ashtakhov, Freundlich, Langmuir, Dual Langmuir and Redlich-Peterson equations, were compared. One can use the values of R^2, SSE, K and B, obtained from fitting the experimental isotherms, and the visual fit, to assess the sorption potential of PAHs to MPS. Thus, it was suggested that the Redlich-Peterson and the Dubinin-Ashtakhov isotherms were more useful for investigating the sorption behaviour of PAHs to PE-10 and PS-10, indicating adsorption as their main sorption process. The results showed that the linear regression method is more suitable for fitting the experimental sorption isotherms of PAHs to PE-100, indicating possible absorption as the MP's main sorption process.

Sammendrag

Mikroplastforurensning i det akvatiske miljøet har vekket økende bekymringer de siste årene, og er kjent for å sorbere polysykliske aromatiske hydrokarboner (PAH) fra vann. Dette påvirker transporten, retarderingen og biotilgjengeligheten av PAH'ene. Mikroplast (MP) kan også kontrollere konsentrasjonen av PAH'er i miljøet.

I dette studiet ble sorpsjonen av tre PAH'er; fenantren (PHE), 1,3-dimethylnaftalen (DMN) og fluoranten (FLA), til ulike MP-polymerer; polystyren (PS), polyetylen (PE) og polyester (PES), ved to ulike temperaturer, 10 og 20 °C, undersøkt. Sorpsjonslikevekten og isotermer ble etablert for de ulike sammenkoblingene av MP og PAH.

Det ble observert at fluoranten og fenantren har sorpsjon til MP'er. Oppførselen til 1,3-dimetylnaftalen i løsning med MP viste ubetydelige eller negative verdier, og sorpsjon kunne dermed ikke bli observert. PE- (10 µm) og fluoranten hadde den høyeste sorpsjonskapasiteten på henholdsvis MP'ene og PAH'ene.

Likevektstiden var henholdsvis 5 dager for fluoranten, 9 dager for fenantren ved 10 °C og 7 dager for fenantren ved 20 °C, uavhengig av polymertype og størrelse brukt i eksperimentene.

I dette studiet ble de ikke-lineære formene av fem vanlige isotermmodeller tilpasset de eksperimentelle dataene. Isotermmodellene inkluderte Dubinin-Ashtakhov, Freundlich, Langmuir, Dual Langmuir og Redlich-Peterson ligningene. Man kan bruke verdiene av R^2, SSE, K og B, beregnet ved å tilpasse de eksperimentelle dataene, og den visuelle tilpasningen, til å vurdere sorpsjonspotensialet PAH'er har til MP'er. Dubinin-Ashtkahov og Redlich-Peterson isotermene er nyttige når man undersøker sorptionsoppførselen til PAH'er på PE (10 µm) og PS (10 µm). Dette indikerer at disse to MP-typene har adsorpsjon som deres hoved sorpsjonsprosess. Resultatene viste at den lineære regresjonsmetoden er mer passende for å tilpasse de eksperimentelle sorpsjonsisotermene til PAH'er på PE (100 µm). Dette indikerer muligens at denne mikroplasten har absorpsjon som hoved sorpsjonsprosess.

Acknowledgements

I would like to thank the following persons:

My external supervisors, Andy Booth and Lisbet Sørensen, for letting me be able to take a part in such an exciting and environmentally important project. Lisbet has shown engagement in my thesis, been available 24/7 and shown a huge patience and helpfulness. You are very much appreciated. Andy has, throughout the project, had a positive attitude and been thankful for the work I've done. Lisbet and Andy have both helped me practically, theoretically and morally during this period.

My internal supervisor, Rudolf Schmid for input throughout the project. You accommodated my needs for the project, and always found a way of helping me.

Alexandros Asimakopoulos for putting me in contact with SINTEF in 2017.

The staff at SINTEF Sealab have been very welcoming and friendly, and interested in my work. I never hesitated to ask for their help when it came to laboratory procedures and helping me find the necessary equipment.

My boyfriend, for all the help with the programming and mathematical parts of the thesis.

My fellow students, for all the lunch-breaks and social events during this period.

Funding: JPI Oceans Plastox project and Norwegian Research Council Microfibre project (grant nr 268404).

List of publications

[1] Lisbet Sørensen, Emilie Rogers, Dag Altin, Andy M. Booth. Microplastic polymer and size influence the sorption and bioavailability of PAHs to *Acartia tonsa* and *Calanus finmarchicus.* Manuscript in preparation.

[2] Lisbet Sørensen, Emilie Rogers, Dag Altin, Marianne Unaas Rønsberg, Andy M. Booth. The role of microplastics size and type on PAH sorption and bioavailability to copepods. Poster presented at the 28th annual SETAC Europe meeting (Rome, Italy, 12-17th May 2018). See Appendix H for poster.

Table of contents

List of abbreviations

ARE	Average relative error
BFR	Brominated flame retardants
DAM	Dubinin-Ashtakhov isotherm model
DCM	Dichloromethane
DL	Dual Langmuir isotherm model
DLM	Dual Langmuir isotherm model
DMN	1,3-dimethylnaphthalene
EABS	Sum of absolute errors
FLA	Fluoranthene
FM	Freundlich isotherm model
GC-MS	Gas chromatography- mass spectrometry
HDPE	High-density polyethylene
HPLC	High performance liquid chromatography
LC-UC	Liquid chromatography- ultraviolet (detector)
LDPE	Low-density polyethylene
LM	Langmuir isotherm model
MeOH	Methanol
MP	Microplastic
MWSE	Mean weighed square error
OCP	Organochlorinated pesticides
PAH	Polycyclic aromatic hydrocarbon
PCB	Chlorinated biphenyls
PCDF	Polychlorinated dibenzofurans
PE	Polyethylene
PE-10	10 µm diameter polyethylene particles
PE-100	100 µm diameter polyethylene particles
PES	Polyester
PES-50	50 µm diameter polyester particles
PHE	Phenanthrene
POP	Persistent organic pollutant
PP	Polypropylene
PS	Polystyrene
PS-10	10 µm diameter polystyrene particles
PVC	Polyvinyl chloride
RIS	Recovery internal standard
RP	Redlich-Peterson isotherm model
RRF	Relative response factor
RSD	Relative standard deviation
SA	Surface area
SD	Standard deviation
SEM	Scanning electron microscopy
SIM	Selected ion monitoring
SIS	Surrogate internal standard
SSE	Sum squared error
SW	Seawater

1 Introduction

1.1 Plastic pollution

A world without plastic might seem unimaginable, but the large-scale production of plastic only dates back to around 1950. Plastic was invented in 1860 and developed for industry in the 1920s. The plastic production exploded in the 1940s. Since the 1950s global production of plastics has continued to rise. In 2013 299 million tons of plastic was generated, and in 2050 it is estimated to have risen to 33 billion tons (Gourmelon, 2015). China accounts for more than 49% of worldwide production. Plastic production surpasses most other man-made materials (except for steel and cement) (Geyer et al., 2017). The largest use of plastic is in packaging, and the growth accelerated during the global shift from reusable to single-use containers. As a result the share of plastics in solid waste, by mass, increased from less than 1 % in 1960 to more than 10 % by 2005 (Geyer et al., 2017).

Only about 10% of plastic waste is recycled (Barnes et al., 2009), indicating that most of the plastic ends up in landfills (Gourmelon, 2015), or the environment. Plastics began to enter the ocean in increasing quantities from the 1950s (GESAMP, 2015). In 2010 about 4 million to 12 million metric tons of plastic were estimated to have entered the marine environment. This is equivalent to 1,5 %-4,5 % of the world's total plastic production (Chen, 2015).

Man-made marine debris has increased substantially in the past hundred years (GESAMP, 2015). Galgani et al. (2010) defines marine debris, or litter, from non-natural sources as 'any persistent, manufactured or processed solid material discarded, disposed of or abandoned in the marine and coastal environment'. This solid material may consist of metal, glass, paper, fabric or plastic. According to Gregory and Ryan (1997) the plastics represent between 60% and 80% of the total quantity of debris in marine environments. Plastic forms non-degradable waste (Moore, 2008), and migrates to and accumulates in all marine habitats once discharged in the environment (Barboza et al., 2017, Setälä et al., 2014).

Accumulation of floating plastic debris in the open ocean is a rising concern. The magnitude and fate of this pollution, and the destiny of more than 99% of the oceans plastic debris, is still unknown (Cózar et al., 2014). Ingestion of plastics by biota has

shown to directly harm a wide range of marine organisms (Thompson et al., 2004) but there are many impacts on marine life that are still unclear.

1.2 Plastic polymers: types, composition and potential hazards

The term plastic is used here to define a class of products made of synthetic polymers. Polymers are long chain-like molecules made of units called monomers, and can have average molecular weights up to several million (GESAMP, 2015). The longer molecular chains allow for stronger Van der Waal attractive forces between them, obtaining properties as strength and fracture toughness, also making them little degradable (Andrady, 2017). Melting points also increase as the chain length increases. The chain length can influence certain physical properties of the polymer, such as the glass-transition temperature. Polymers can be categorized based on their glass transition temperature (T_g) as either rubber-like polymers or glass-like polymers (Hüffer and Hofmann, 2016). PE polymers are rubber-like (amorphous), having a high degree of flexibility and freedom and a lower T_g than for example PS polymers, which are glass-like. In the glassy state the polymer chains are relatively rigid (ten Hulscher and Cornelissen, 1996). The density of the polymer is directly connected with mass and packing. Amorphous polymers most commonly have a higher density relative to their glassy-states (Robertson, 1965).

The six most commonly mass-produced polymers are polyethylene (PE), high-density polyethylene (HDPE), polyvinyl chloride (PVC), low-density polyethylene (LDPE), polystyrene (PS) and polypropylene (PP) (Rochman et al., 2013, Andrady and Neal, 2009). Figure 1.1 shows a plot presenting the global production amount of these polymers in 2011.

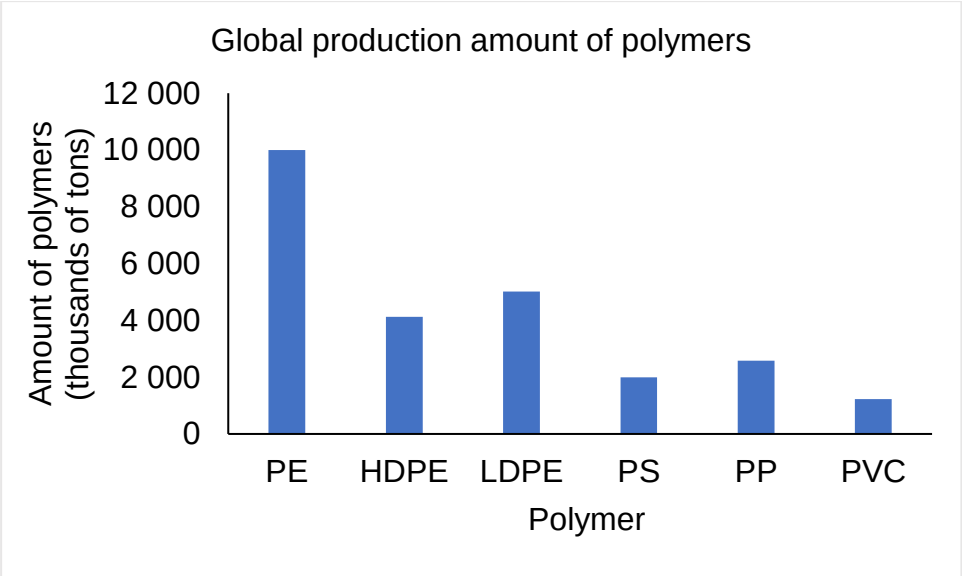

Figure 1.1. Global production of polymers (in thousands of tons) in 2011. PE: polyethylene (PE total, sum of LDPE and HDPE), HDPE: high-density polyethylene, LDPE: low-density polyethylene, PS: polystyrene, PP: polypropylene, PVC: polyvinyl chloride (Merrington, 2011).

Polymers are typically mixed with other chemicals, called additives, to enhance the product performance. Additives may include carbon or silica to reinforce the plastic material, thermal stabilizers, UV stabilizers to prevent degradation when exposed to sunlight and other additives with specific properties, such as fire retardants (Andrady and Neal, 2009). Plastics are cheap to produce, lightweight, and water and corrosion-resistant. They help us to avoid food waste, to save energy and to decrease CO_2 emissions (Gourmelon, 2015). All of these properties contribute to their many industrial and municipal applications (Wang and Wang, 2018b).

1.2.1 Polyethylene (PE)

The global production of polyethylene (PE) is about 80 million tons, making it the most widely used plastic (Merrington, 2011). PE is essentially a thermoplastic, meaning that it can be remade into a desired shape. It is therefore reusable and cost-effective. PE (*n*-alkanes) polymers include many different grades. They differ in molecular weight, strength and crystallinity, but they are all PE. Polyethylene comes as, among other types, low-density and high-density polyethylene (LDPE and HDPE, respectively). LDPE, with a density of 0,910-0,925 g/cm^3 and a molecular weight of 40 000 Dalton (Kurtz and Manley, 2009), is soft and ductile and is applied in milk carton lining, bowls,

buckets and squeezable bottles. HDPE, with a density of 0,959-0,965 g/cm^3 and a molecular weight of 100 to 250 000 Dalton (Kurtz and Manley, 2009), is applied in films for plastic bags. The different grades of PE differ in their susceptibility to weathering and fragmentation, and therefore their fate, behaviour and ecological impact in the marine environment will also differ (Andrady, 2017).

1.2.2 Polystyrene (PS)

PS is the most employed aromatic thermoplastic polymer (Lynwood, 2014), with a global production amount in 2011 of 1990 000 tons (Merrington, 2011). PS plastics are available as solid plastics and foam materials and are transparent. The solid plastics are mostly used in medical devices, and the foam materials as packing materials. Both PE and PS are non-polar MPs (Hüffer and Hofmann, 2016).

1.2.3 Polyester (PES)

PES is used mostly in textile industry, food packaging and the manufacturing of plastic bottles. Fibre products (e.g. textiles) do not experience significant recycling rates, increasing the probability of them ending up in the marine environment (Dris et al., 2017).

1.3 Microplastics (MPs)

1.3.1 Definition and sources of primary and secondary microplastics

Microplastics (MPs) are small pieces of plastic debris. They accumulate in the environment (Thompson, 2015). MPs are the dominant plastic pollution found in the marine environment, referring to their microscopic size (Cózar et al., 2014). Microplastics have typically been defined as any plastic particles with a size below 5mm. However, recent developments (e.g. GESAMP) are working towards a more detailed classification of mesoplastic (1-5 mm), microplastic (1 µm-1000 µm) and nanoplastic (<1 µm). MPs originate as a consequence of the fragmentation of larger items or the direct release of small particles (Thompson, 2015).

There are a variety of sources for MPs. These can be categorized as primary: the direct release of small particles, or secondary: fragmentation of larger items as a

consequence of physical and chemical effects in the environment (Zitko and Hanlon, 1991). Small particles from these sources can be transported with wastewater and through sewage treatment plants to enter aquatic habitats (Browne et al., 2007). Primary MPs are commonly used in facial cleansers and cosmetic products, in air-blasting (processes to remove rust and paint), and as resin pellets for further production of plastic products (Cole et al., 2011, Andrady, 2017). The fragmentation that leads to secondary MPs can come from physical, biological and chemical processes (Cole et al., 2011). Weathering breakdown of plastic litter in the beach environment is believed to be the dominant source of secondary MPs (Andrady, 2017). Clothes and textiles give off synthetic microfibres during use and washing (Browne, 2015, Gesamp, 2016). These fibres are also considered as secondary MPs, and can enter the marine environment e.g. through laundry (Browne et al., 2011). Polystyrene and polyethylene are of the most produced polymers and therefore expected to dominate microplastics in the environment (Andrady, 2017).

1.3.2 Abundance and fate of microplastics in the environment

There has been an increase in MP concentration over the last 30 years in the marine environment (Wright et al., 2013). Van Sebille et al. (2015) estimated that 15 to 51 trillion MP particles are present in the world's oceans, weighing between 93 and 236 thousand metric tons. Graca et al. (2017) observed that concentrations of MPs varied from 25 particles/kg at the open sea to 53 particles/kg at beaches of strongly urbanized bay. In bottom sediments the MPs concentrations were a lot less. Evidence has shown that the concentration of MPs in the marine environment increases with decreasing particle size (Andrady, 2011, Cózar et al., 2014). To fully understand the risk of plastic contamination to marine organisms, it is important to understand the amount, form and distribution of MPs in the marine environment.

A fraction of the plastics that enter the ocean are removed from the surface (Cózar et al., 2014). A likely route is through sinking due to their polymer density. Thompson et al. (2004) found similar types of polymers in the water column as in the sediments, suggesting that polymer density is not a major factor influencing distribution. Andrady (2017), on the other hand, concluded that the density determines where in the water column the MPs are most likely to reside, and thus the range of marine organisms they will encounter. Floating MPs accumulate, and their density can increase, causing them

to sink to the deep water. Also, marine organisms ingest MPs, acting as a major sink (Desforges et al., 2015, Long et al., 2015). Marine organisms may also influence the MPs vertical distribution in the water column through ingestion and transportation (Long et al., 2015).

Kooi et al. (2016) found that MP concentrations decrease with depth, and that MPs of 0.5-5 mm mainly occur in the upper 3 m of the water column. The lighter and smaller the particles are, the lower in the water column they can be distributed by vertical mixing. Some polymer types (e.g PE) are for example less dense than seawater and will float, while most (e.g PES, PS) are denser and will sink to the deep water or sediment. Additives may also play a part in the particles floating capability as they typically increase the density and can cause sinking (Andrady, 2015).

1.4 Conventional organic pollutants in the environment; persistent organic pollutants

Persistent organic pollutants (POPs) are synthetic organic compounds, mainly found spread on land and in aquatic environments (Rios et al., 2007). There are many classes of POP chemicals. The chlorinated biphenyls (PCBs), the brominated flame retardants (BFRs), the organochlorinated pesticides (OCPs), the polycyclic aromatic hydrocarbons (PAHs) and the dioxins (PCDF) are some of them (Casarett et al., 2013). The PCBs, for example, have been synthesised for industrial uses, others are accidental biproducts (PCDFs) (Jones and de Voogt, 1999, Breivik et al., 2004).

All classes of POPs are hydrophobic and lipophilic compounds, meaning ‘water-hating’ and ‘fat-loving’, respectively. In aquatic systems they partition strongly to solids, avoiding the aqueous phase, and in organisms they partition to lipids. This results in persistence. Metabolism is slow, and therefore POPs may accumulate both over time in organisms and in food chains (Jones and de Voogt, 1999). POPs have a lower solubility in seawater than in freshwater, altering the binding to surface plankton and other organic particulates, therefore often undergoing sedimentation (Basheer et al., 2005). POPs are persistent in the environment because of their chemical stability, having long half-lives in soils, sediments, air or biota (Jones and de Voogt, 1999).

POPs can enter the gas phase under environmental temperatures (10-30 °C). This gives them the chance to volatilise from water and soils into the atmosphere, and travel long distances before they re-deposite (Jones and de Voogt, 1999).

The presence of POPs in the environment has been a concern since the mid-1900s (Qing Li et al., 2006, Friedrich, 2016). The primary goal of the Stockholm Convention (2001) is to protect human health and the environment from these pollutants. The Convention consists of over ninety nations, all working together to eliminate the production and use of a number of POPs, prevent the release of certain POPs (those formed as by-products), and ensure safe disposal of these substances (Lallas, 2001).

1.4.1 Polycyclic aromatic hydrocarbons

Polycyclic aromatic hydrocarbons (PAHs) are a group within the POPs, of over 100 organic chemicals, that are formed during the incomplete burning of coal, oil, gas or garbage. PAHs are also found in organic materials, for example biomass. They are the most studied petroleum product. PAHS occur most often as a mixture of two or more compounds. Soot, for example, contains mostly PAHs. Some PAHs are also produced in many cases by anthropogenic activity (Rios et al., 2007).

The PAHs contain two or more fused benzene rings, and carbon and hydrogen are the only constituents (Casarett et al., 2013). The 4-, 5- and 6-ring PAHs seem to dominate the sediment samples, and the 2- and 3-ring species tend to dominate the constituents in the dissolved or vapor phases of air, precipitation and seawater (Latimer and Zheng, 2003). The PAHs are considered non-polar and semi-volatile (Casarett et al., 2013).

The PAHs can be separated into three categories based on their source: biogenic (from natural processes), petrogenic (derived from petroleum) and pyrogenic (formed as a result of incomplete combustion of fuel). The petrogenic PAHs consist mostly of low molecular mass PAHs with two to three rings (Zeng and Vista, 1997), as well as alkylated PAHs with one to a few methyl groups (Hong et al., 2016). The pyrogenic PAHs are often characterized by 4-6 aromatic rings. The ratios among parent PAHs and parent to alkyl homolog distributions of PAHs can determine the dominance of petrogenic vs. pyrogenic PAH sources (Latimer and Zheng, 2003). Parent compounds, not containing alkyl constituents, indicate pyrogenic sources, whereas compounds containing alkyl constituents indicate petrogenic sources (Latimer and Zheng, 2003, Neff, 2002).

The PAHs are resistant to biodegradation and thus remain in the environment for a long period of time (Casarett et al., 2013) and are of great environmental concern.

They are ubiquitous and have high mobility, giving long range transport. Many of them are also mutagens, teratogens and carcinogens (Casarett et al., 2013).

The US Environmental Protection Agency (EPA) have listed 16 PAHs on their priority pollutant list (Bojes and Pope, 2007), shown in Figure 1.2.

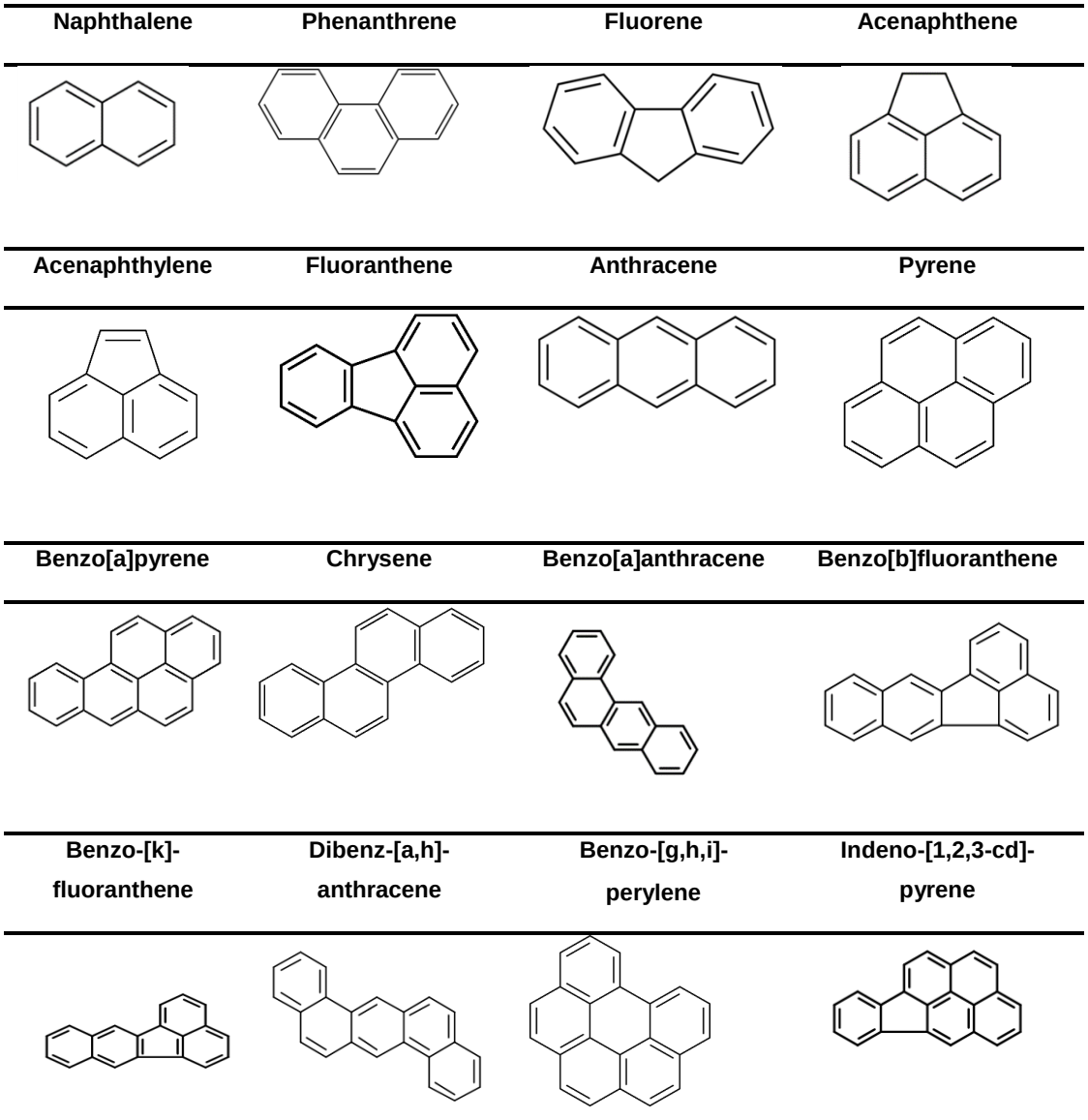

Figure 1.2. Chemical structure of 16 polycyclic aromatic hydrocarbons.

The lower the number of rings contained by the PAH, the lower their molecular weight and toxicity. The alkylated PAHs are more toxic than their parent compounds and are

present in seawater at higher concentrations. The 4-ring PAHs have higher molecular weight and occur at lower concentrations than the 2-3 ring PAHs, and the 5- and -ring PAHs generally occur at the lowest concentrations. The latter have low water solubility, giving them low bioavailability (Samanta et al., 2002).

Each year 43 000 metric tons of PAHs are discharged into the atmosphere, and 230 000 tons enter the marine environment, which are then distributed by physical transport and mechanical factors (Yim et al., 2007). According to the Norwegian environment agency (Green et al., 2016) there has been a significant increase in the emissions of PAHs to air and discharges to water. In Norway the emission to air in 2015 was 76 002 kg PAHs while it was 'only' 958 kg in 2014. The discharges to water were 4 853 kg PAHs in 2015 and 14 kg in 2014 (Green et al., 2016, Green et al., 2015).

PAHs are most concentrated in estuaries and coastal environments near urban centres. The major sources of PAHs to the marine environment include urban runoff, wastewater, industrial outfalls, atmospheric deposition, smelting industry and spills and leaks from production of fossil fuels (Latimer and Zheng, 2003). Phenanthrene enters the aquatic systems in large pulses mostly during storm events from e.g. fossil fuels and industrial processes (Teuten et al., 2007) because of washouts for example. The hydrophobicity of PAHs controls their distribution in the marine environment (Latimer and Zheng, 2003).

1.5 Interaction between microplastics, pollutants and organisms

1.5.1 Sorption

The process where a chemical (sorbate) becomes associated with a solid phase (sorbent) is called sorption (Pan and Xing, 2008). It is important to separate between adsorption and absorption processes. Adsorption is sorption onto the surface of a sorbent, and absorption is sorption into a condensed phase (Huffer, 2014).

K_d, the distribution coefficient, describes the sorption at equilibrium conditions in solid-water systems. K_d is given by the ratio:

$$K_{d} = \frac{c_S}{c_W} \qquad (1.1)$$

C_S is the equilibrium concentrations of the sorbate sorbed by the sorbent

C_W is the equilibrium concentration in water

Gibbs free energy, enthalpy and entropy are all thermodynamic quantities representing the sorption process (ten Hulscher and Cornelissen, 1996). A net sorption occurs when the free energy is negative (Hassett and Banwart, 1989). Both enthalpy- and entropy related forces play a role in the sorption process. The enthalpy affects the affinity of a chemical to the sorbent vs. the affinity of the chemical to the solvent, and the entropy describes the change in disorder of the system (Hassett and Banwart, 1989).

PAHs, being hydrophobic, have hydrophobic sorption as the main driving force behind the sorption process. London-Van der Waals interactions take place between solute and MP, and the entropy change resulting from the removal of sorbing chemical for the solution is large (ten Hulscher and Cornelissen, 1996).

It is stated that the effect of temperature on the sorption equilibrium is a direct indication of the strength of the sorption. Less influence of temperature is expected for weaker bonds, because of the lower equilibrium sorption enthalpy (ten Hulscher and Cornelissen, 1996).

1.5.2 Sorption models and mechanisms

The relationship between C_S and C_W is considered as sorption isotherms (Huffer, 2014), and the sorption isotherms are obtained by plotting C_{MP} versus C_{free}. An isotherm is a curve describing the retention of a substance on a solid. It is used to describe and predict the mobility of a substance in the environment (Limousin et al., 2007), and thus how pollutants interact with adsorbent materials. An accurate mathematical description of equilibrium adsorption capacity is necessary for reliable prediction of adsorption parameters and for comparing adsorption behaviour for different absorbents and materials (Gimbert et al., 2008). A linear sorption isotherm gives a constant K_d and is independent from the concentration range. A non-linear sorption isotherm implies that K_d is the sorption coefficient and depends on the C_{free} concentration (Huffer, 2014).

Both linear and non-linear regression methods have been compared in previous studies for selecting the optimum isotherm (Teuten et al., 2007). In the present master thesis, it is chosen to focus on the non-linear regression methods within each model. The non-linear methods have a uniform error distribution (explained in paragraph 1.5.2.6) for the whole range of experimental data, resulting in better isotherm

parameters for the given model (Kumar and Sivanesan, 2005). Five commonly used models, and the corresponding equation, are presented in Table 1.1 and discussed in the following.

Table 1.1. Sorption models used to fit sorption isotherms. Equations and explanations of parameters are also accompanied. For all models, C_{MP} is the sorbed PAH concentration on the MP (µg/kg), and C_{free} is the aqueous PAH concentration at equilibrium (µg/L) (Kah et al., 2011, Glomstad et al., 2017, Foo and Hameed, 2010, Hüffer and Hofmann, 2016, Kumar, 2007, Wang and Wang, 2018a, Redlich and Peterson, 1959, Gimbert et al., 2008).

Model	Equation	Parameters
Freundlich (FM)	$C_{MP} = K_f {C_{free}}^n$	K_f: Freundlich coefficient [L/µg] n: Freundlich exponent
Langmuir (LM)	$C_{MP} = \frac{Q^0 * K_L * C_{free}}{1 + (K_L * C_{free})}$	K_L: Langmuir affinity coefficient [L/µg]
Dual Langmuir (DLM)	$C_{MP} = \frac{Q_1^0 * K_{L1} * C_{free}}{1 + (K_{L1} * C_{free})} + \frac{Q_2^0 * K_{L2} * C_{free}}{1 + (K_{L2} * C_{free})}$	Similar to Langmuir model 1 and 2 refer to the two populations of sorption sites
Dubinin-Ashtakhov model (DAM)	$logC_{MP} = logQ^0 - (\frac{\mathcal{E}_{SW}}{E})^b$	$\mathcal{E}_{SW}$: Effective sorption potential, = RT ln (S_w/C_{free}) R: Universal gas constant (8,314 x 10^{-3} kJ/mol K) T: Absolute temperature (K) S_W: Aqueous solubility [µg/L] E: Correlating divisor b: Fitting parameter
Redlich-Peterson (RP)	$C_{MP} \frac{K_R * C_{free}}{1 + a_R C_{free}^B}$	K_R: Redlich Peterson coefficient [L/µg] a_R: Isoterm constant (L/µg) B: exponent between 0 and 1.

C_{MP}: Concentration adsorbed to MPs (µg/mg)
Q^0: Maximum adsorption capacity (µg/mg)
C_{free}: Equilibrium concentration in the water (µg/L

1.5.2.1 Linear absorption isotherm

The linear sorption model contains of the aqueous concentration [µg/L] plotted against the concentration of PAH on the MP [µg/mg]. The distribution coefficient (K_d) is then defined as the gradient (Teuten et al., 2007, Saha et al., 2017, Kumar, 2007, Gimbert et al., 2008, Wang and Wang, 2018a). The linear model follows linear regression (equation 1.2) and indicates that the dominating sorption mechanisms is absorption (Tang et al., 2018).

$$C_{MP} = K_d * C_{free} \quad (1.2)$$

1.5.2.2 Langmuir adsorption isotherm

The Langmuir model (LM) assumes monolayer adsorption of adsorbate over a homogeneous adsorbent surface. Once a site on the surface is occupied, no further adsorption can take place. Therefore the sorbent has a finale capacity for the adsorbate (Sreńscek-Nazzal et al., 2015).

1.5.2.3 Freundlich adsorption isotherm

It is assumed in the Freundlich model (FM) that there is no limited sorption capacity, and that each sorption site has different free-energy for interaction. The equation describes an adsorption on heterogeneous surfaces (Sreńscek-Nazzal et al., 2015), and is applicable to both monolayer and multilayer sorption (Wang and Wang, 2018a). When n=1, the sorption isotherm is linear, and the free-energy distribution of sorption sites is the same. When n<1, the sorption free-energy decreases with increasing chemical concentration. The curve will therefore have a concave shape. When n>1, the free-energy increases with increasing chemical concentration and the curve will have a convex shape (Pan and Xing, 2008).

1.5.2.4 Redlich-Peterson adsorption isotherm

The Redlich-Peterson (RP) isotherm model is known to give a good representation for moderate concentrations (Redlich and Peterson, 1959). The isotherm combines elements from both the Langmuir and Freundlich equations. Langmuir's equation is well confirmed for the lowest concentrations, as Freundlich's equation is for the higher

ones. The mechanism of adsorption for the Redlich-Peterson isotherm acts therefore as a hybrid (Gimbert et al., 2008), having both monolayer and multilayer adsorption as the main sorption mechanism. Redlich Peterson can represent adsorption equilibria over a wide concentration range. It approaches Freundlich isotherm model at high concentrations (B values close to zero) and the Langmuir isotherm at low concentrations (B values close to one) (Foo and Hameed, 2010). The exponent B is related to the degree of pore filling, the packing fraction of the surface (Chen and Yang, 1994, Gil and Grange, 1996).

1.5.2.5 Dubinin- Ashtakhov adsorption isotherm

The Dubinin-Ashtakhov isotherm model (DAM), and a similar model, Dubinin-Radushkevich, are both inbound in the Polanyi theory of micropore filling (Chen and Yang, 1994, Dubinin, 1975) that evaluates the parameters that characterize the microporous structure of the solid. The mechanism for adsorption in micropores is of pore-filling rather than layer-by-layer surface coverage (Hutson and Yang, 1997). The Dubinin- Radushkevich equation applies to solids with a uniform structure of micropores. The Dubinin-Ashtakhov equation, on the other hand, applies to solids with a non-homogeneous microporous structure (Gil and Grange, 1996), which in this case applies to the MPs used in this study. They both are temperature-dependent (Foo and Hameed, 2010).

1.5.2.6 Error functions for adsorption isotherms

An error function is required in single-component and non-linear isotherm studies. This is necessary for quantitatively comparing the applicability of different models in fitting data. The lower the value of the error function, the better fit the isotherm model has to the experimental data. The error function also obtains the best isotherm parameters which describes the adsorption process (Gimbert et al., 2008). There are many different error functions, including the average relative error (ARE), the sum of squared errors (SSE), the hybrid fractional error function (HYBRID), the mean weighed square error (MWSE) and the sum of absolute errors (EABS) (Gimbert et al., 2008, Kumar et al., 2008). It is important to know that the size of the error function alone is not a deciding factor in choosing the optimum isotherm. The theory behind the isotherm

model, the visual fit, and the R^2 (value closest to one) also has to be taken in to account (Kumar et al., 2008).

The mean weighed square error (MWSE) is calculated by

$$MWSE = \Sigma \left(\frac{1}{\upsilon} \frac{\left(C_{\mathrm{MP,measured}} - C_{\mathrm{MP,model}}\right)^2}{C_{\mathrm{MP,measured}}{}^2}\right) \quad (1.3)$$

where υ is the degree of freedom (FM, LM and DLM; υ= N-2, DAM and RP; υ=N-3, N is the number of experimental data points).

The sum of the squares of errors (SSE) is calculated by

$$SSE = \Sigma \left(C_{\mathrm{MP,model}} - C_{\mathrm{MP,measured}}\right)^2 \quad (1.4)$$

$C_{MP,\ measured}$ is the measured concentrations of sorbed sorbent.

$C_{MP,\ model}$ is the sorbed concentrations of the sorbent calculated by the model.

R^2 is calculated by

$$R^2 = 1 - \left(\mathrm{AVG}\left(C_{\mathrm{MP}} - f(x)\right)^2\right) \quad (1.5)$$

1.5.3 Sorption of environmental pollutants to microplastic

Polycyclic aromatic hydrocarbons are persistent and travel long distances. They tend to sorb to organic material such as organic matter, sediments and polymers. Thus, the MPs affect the global and local transport of PAHs in the marine environment (Thompson et al., 2004, Browne et al., 2011, Moore, 2008).

In both the marine and terrestrial environment, the sorption of hydrophobic contaminants to MPs is considered an important process (ten Hulscher and Cornelissen, 1996). The particle-water interactions are of the most important mechanisms controlling the distribution and movement of PAHs in marine environments. The partition/distribution coefficient is widely used (Zhou et al., 1999).

The occurrence of hydrophobic contaminants in marine plastic debris has widely been reported (Frias et al., 2010, Hüffer and Hofmann, 2016, Mato et al., 2001). MPs in the marine environment can carry persistent organic pollutants. Their composition and large surface area makes them prone to adhering pollutants (Cole et al., 2011).

The hydrophobic PAHs can be sorbed from surrounding seawater dependent on the affinity of the chemicals for the hydrophobic surface of the plastics. They can also be added during plastics manufacture (Teuten et al., 2009). According to Teuten et al. (2007) sorption of phenanthrene to polyethylene exceeds sorption to natural sediments, proving the potential occurrence of sorption of PAHs to MPs.

Knowledge of the sorption properties of MPs is of huge importance to our understanding of the possible impacts of MPs in aqueous environments. Experimental evidence and results from modelling studies show that the sorbent and sorbate properties, as well as polymer type, temperature, and weathering, influence the sorption capacity (Ziccardi et al., 2016).

1.5.3.1 The effect of polymer type and interactions on sorption

Polymer type and the interactions between the MP and polycyclic aromatic hydrocarbon effect the sorption.

Studies done in 2009 (Teuten et al.) and 2014 (Bakir et al.) showed that polyethylene accumulated more organic contaminants than other plastics. To the contrary, a study preformed in 2013 (Rochman et al.) documented that among all the six most commonly produced polymer types (HDPE, PS, PE, LDPE, PP, PVC), sorption of PAHs to polystyrene was the largest. Polyethylene came second. Non-expanded polystyrene pellets are glassy in state, so this result could be unexpected. Polyethylene is a rubbery polymer, suggesting a higher diffusivity than polystyrene. The polymeric backbone of polystyrene also has a benzene molecule where polyethylene has a hydrogen, restricting mobility within the polystyrene chains. In contrast, the benzene ring in polystyrene increases the distance between adjacent polymeric chains. This makes it easier for a chemical to diffuse into the polymer. A third study observed similar concentrations of PAHs in polystyrene and polyethylene (Rochman et al., 2013).

Hüffer and Hofmann (2016) performed a study of the sorption of organic compounds by MPs in aqueous solutions. The sorption was larger for polystyrene than for polyethylene. Aliphatic polyethylene can only undergo van-der Waals interactions with organic compounds, whereas aromatic polystyrene can also undergo π- π interactions (Hüffer and Hofmann, 2016). According to Velzeboer et al. (2014) hydrophobic and π -π interactions can explain the strong sorption of sorbents by polystyrene, compared

to that by polyethylene. This order doesn't reflect the particle sizes of the MPs. Polystyrene exhibited a much stronger sorption than similar-sized polyethylene particles, indicating the influence of additional factors on the sorption of the components than sorbent particle size and surface area.

1.5.3.2 The effect of temperature on sorption

Hulscher and Cornelissen (1996) studied the effect of temperature on sorption and sorption kinetics of micropollutants. For most compounds, equilibrium sorption decreased with increasing temperature. For others no effect of temperature on sorption equilibrium were found. Kees Booij (2003) concluded in his study that temperature, to a certain extent, isn't a key factor that controls sorption rates. There is rather little knowledge on the effect of temperature on the sorption of PAHs to MPs.

1.5.3.3 Adsorption or absorption

Endo et al. (2008) suggested a possible indicator for distinguishing between adsorption and absorption, using the ratio between the distribution coefficients of *n*-alkanes and their cyclic homologues (K_n/K_c). The ratio for the rubbery PE clearly indicates absorption to be the main sorption mode. Adsorption seemed to dominate sorption by glass- like polymers such as PS (Hüffer and Hofmann, 2016).

Hüffer and Hofmann (2016) fitted PE and PS sorption with the Freundlich isotherm model. Linear isotherms for PE suggested that the uptake of the component was due to absorption into the polymer. The Freundlich exponent (*n*) was approximately equal to 1. In contrast the isotherms for the sorption by glassy PS were non-linear. This suggests that the dominating sorption process for the tested compound and polymer was adsorption onto the polymer surface (Hüffer and Hofmann, 2016).

1.5.4 Microplastics as vectors for bioaccumulation of polycyclic aromatic hydrocarbons in marine organisms

Ingestion of different types of MPs in marine organisms is known (Setälä et al., 2014), and is of environmental concern as their small size makes them ingestible to a wide range of marine organisms (Cole et al., 2013). 83% of the studied lobsters in Norway, for example, were found to include MPs (Murray and Cowie, 2011). Ingested MPs can

disrupt feeding appendages and the alimentary canal, limit the food intake of an organism or be translocated into the circulatory system. (Cole et al., 2013).

The interaction between MPs and PAHs is of ecotoxicological relevance, as sorption to MPs can influence the fate and bioavailability of PAHs in aquatic environments. MPS may be important agents in the transfer of hydrophobic pollutants to organisms in the marine environment (Mato et al., 2001).

Polymers have large molecular sizes, prohibiting them to penetrate through cell membranes. They are therefore considered to be biochemically inert materials. The PAHs, however, can penetrate through the cell membranes of organisms and interact with the endocrine system. Studies by Teuten et al. (2007) have shown that plastics have a high capacity to sorb especially phenanthrene, and are therefore important agents for transporting contaminants to organisms. On the other hand, sorption of PAHs to MPs may lower the free aqueous concentration and therefore decrease the bioavailability of PAHs to the organisms (Lee et al., 2014).

Plastic resin pellets, a type of primary MPs, are widely distributed in the marine environment all over the world. These resin pellets are small granules 0,1-0,5 cm in diameter, and are commonly ingested by seabirds and other marine organisms (Mato et al., 2001). According to Andrady (2015) relatively low amounts of MPs can transport a disproportionately high dose of PAHs into an organism. Mato et al. (2001) documented that there was a positive correlation between the amount of ingested plastics and PCBs in fat tissue of certain organisms. The bioavailability is assumed to be high for small organisms, such as zooplanktons. The body burden of the PAHs that might be released into the organism can therefore be significant (Frias et al., 2014, Lima et al., 2014). These impacts may affect the entire food chain. The ingestion of plastics with sorbed pollutants has therefore been suggested as a possible exposure route for pollutants.

Endo et al. (2013), on the other hand, concluded that diffusion of hydrophobic organic contaminants (HOCs) in and out of MPs is slow, and only add a small contribution relative to already present PAHs. Based on results from studies done by Zarfl and Matthies (2010) it is agreed that MPs are not an efficient transport vector of contaminants, when compared to long range transport by ocean or atmosphere.

Ziccardi et al. (2016) concluded that the role of plastics in the transport of PAHs to organisms may be rather small compared with other pathways.

Control of exposure systems is necessary to ensure that the effects the contaminants might have on the organisms are derived from pollutants adsorbed to MP surfaces and not from desorption and dissolution into the aqueous media. Aquatic organisms are exposed to different sources of plastics, from various compartments, such as water, sediment, and food. Therefore, it is difficult to quantify the importance of MPs as a possible route of exposure. The exposure route must be considered in the context of other exposure routes (Barboza et al., 2017). It is also important to understand that the contaminants sorbed to the plastics are in equilibrium with other phases in the environment (Ziccardi et al., 2016). More data are needed to fully understand the extent to how the exposure to contaminants from MPs is compared with other exposure pathways. The potential importance of MPs as carriers of persistent organic pollutants into animals remains a strong theme in discussion on MPs.

1.6 Interactions between microplastics and copepods

Both *Acartia Tonsa* and *Calanus Finmarchicus* are filter feeding copepods and are food for many marine organisms. They are grazers, feeding on the primary producers, (Antonio Grassi, 2017), and their presence in the zooplankton in the marine environment is high, they can represent 55-95 % of the zooplankton (Blaxter et al., 1998). Their density is higher than the seawater, therefore giving them the tendency to sink when not swimming.

1.6.1 Acartia tonsa

Acartia tonsa has a length of 0,5-5 mm. They normally hatch in the sediments (Hjertholm and Gansel, 2016) and thrive at water temperatures of approximately 20 °C. Some copepods will filter-feed regardless of prey availability. *Acartia tonsa*, however, can limit their movement and filter-feeding to conserve energy when low food concentrations.

1.6.2 Calanus finnmarchicus

Calanus finmarchicus is a key zooplankton species in the North Atlantic Ocean (Rogne Halland et al., 2017), and has a length of 2,4-5 mm (Antonio Grassi, 2017). *Calanus finmarchicus* thrive at water temperatures of approximately 10 °C. The *Calanus* also has lipid storage, which means that they are likely to store persistent organic pollutants which are fat soluble.

Calanus finmarchicus has a prey size in the same size range as MPs. Therefore, it may feed on these particles.

1.6.3 Interactions between MPs and copepods

According to Kaposi et al. (2014) the filter feeding copepods are predicted to encounter the most MPs because these feeding modes are used to concentrate food from large volumes of water.

MPs have shown to be ingested by The *Acartia tonsa* (Hjertholm and Gansel, 2016, Cole et al., 2013). Rogne Halland et al. (2017) completed a study where the aim was to study the uptake and excretion rate on PS (10 µm) MPs in *Calanus finmarchicus.* It was proven that also these copepods ingest PS particles.

1.7 The aim of this study

This master thesis is part of The Joint Programming Initiative Healthy and Productive Seas and Oceans (JPI Oceans) research project ‘Plastox’- investigating direct and indirect ecotoxicological impacts of MPs on marine organisms. The main aim of the ‘Plastox’ project is to investigate the ingestion, food-web transfer and ecotoxicological impact of MPs, together with the persistent organic pollutants, metals and plastic additive chemicals associated with them, on key European marine species and ecosystems.

The aim of the present master’s thesis was to study the sorption behaviour of three polycyclic aromatic hydrocarbons (PAHs); phenanthrene, 1,3-dimethylnaphthalene and fluoranthene, to different microplastic (MP) polymers; polystyrene (PS), polyethylene (PE) and polyester (PES), at two different temperatures, 10 and 20 °C. Sorption equilibrium and isotherms were sought established for the different pairings

of MP and PAHs. Furthermore, the influence of MP bead size on sorption behaviour was studied.

1.7.1 Study microplastics

In this study the three polymer types applied were polyester (PES) fibres, polystyrene (PS) beads and polyethylene (PE) beads. Figure 1.3 shows their structure.

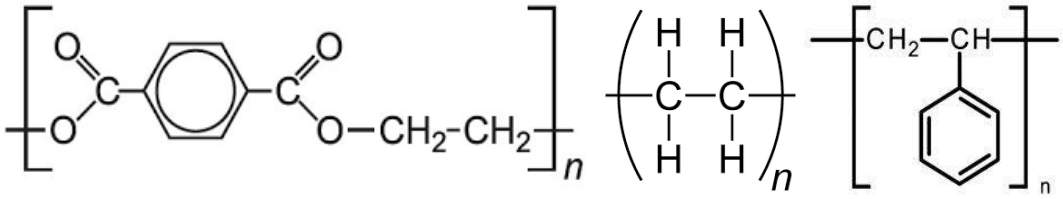

Figure 1.3. Structures of the polymer types used in this study. From the left: polyester, polyethylene and polystyrene.

The PS- and PE- polymers were chosen for this study because they are intensively used, and due to their sizes being relevant for uptake in organisms. We also know that these particles are the most frequently found MPs in the marine and terrestrial environment (Heo et al., 2013, Martins and Sobral, 2011). PES-fibres, on the other hand, there is little knowledge about. We also know little about the sorption regarding them.

1.7.2 Study PAHs

The PAHs phenanthrene ($C_{14}H_{10}$), 1,3-dimethylnaphthalene ($C_{12}H_{12}$) and fluoranthene ($C_{16}H_{10}$) were all applied in this study. Figure 1.4 shows their structure, and selected properties of the chemicals are listed in Table 1.2.

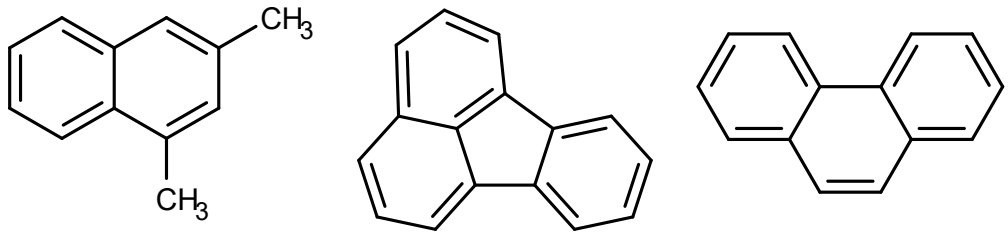

Figure 1.4. Structures of the PAHs used in this study. From left: 1,3-dimethylnaphthalene, fluoranthene, phenanthrene.

Table 1.2. Physicochemical properties of 1,3-dimethylnaphthalene (DMN), fluoranthene (FLA) and Phenanthrene (PHE).

Compound	Molecular weight (g/mol)	Boiling point (°C)	Melting point (°C)	Density (g/cm^3)	Solubility in seawater (mg/L)	Solubility in freshwater (mg/L), 25°C
DMN	156,22	267[2]	39,0[2]	0,982[2]	31,0 (25°C)[1]	8,00[3]
FLA	202,26	384[1]	110[1]	1,25[1]	0,100 (22°C) [1]	0,260[3]
PHE	178,23	338[1]	99,0[1]	1,18[1]	0,600 (22°C) [1]	1,29[3]

[1]PubChem (https://pubchem.ncbi.nlm.nih.gov/), which are based on different studies (Verschueren, 2001, Verschueren, 1983, Pearlman et al., 1984, Latimer and Zheng, 2003).
[2]Chemspider (US EPA, EPIsuite, version 4.1)
[3] Mackay and Shiu (1977).

There is a relatively large body of knowledge regarding PAHs persistence and toxicity, and their concentrations in the environment. 1,3-Dimethyllnaphthalene, phenanthrene and fluoranthene were specifically chosen for this study because they span a reasonably large area within the PAHs when it comes to water solubility and size. 1,3-Dimethyllnaphthalene, phenanthrene and fluoranthene are all present in the seas across the world (Savinov et al., 2003, Law et al., 1997). 1,3-dimethylnaphthalene is

expected to be present in larger quantities in seawater than sorbed to microplastics due to its relatively high water solubility (Latimer and Zheng, 2003).

2 Materials and methods

All experiments and laboratory work were performed at SINTEF Ocean Sealab in Trondheim, Norway, during the period January- April 2018. Prior to the project start-up, relevant MP types and sizes for uptake in *Acartia tonsa* and *Calanus finnmarchicus* were determined, as well as PAH solubilities in seawater.

2.1 Chemicals and materials

2.1.1 Chemicals

Ultrapure (MilliQ) water was supplied by a Millipore filtration system. Dichloromethane (DCM) was supplied by Rathburn, and *n*-hexane by Fluka analytical, with Emsure® quality. Acetonitrile (ACN) and methanol (MeOH) was supplied by Honeywell, Riedel-de Haen, with a purity of 99,9%. Hydrochloric acid (HCl) was supplied by Sigma Merck and diluted in MilliQ water to 15%.

1,3-Dimethylnaphthalene (DMN), fluoranthene (FLA) and phenanthrene (PHE) were purchased from Sigma-Aldrich, with >96 %, >98 % and >98% purity, respectively. Deuterated PAHs were supplied by Chiron AS.

Stock solutions of PAHs were prepared in both MeOH and DCM, and stored in the dark at 4-5 °C. For the LC-UV calibration the PAHs were prepared in MeOH, and for the preparation of experimental solutions, they were prepared in DCM. The concentrations of the stock solutions are listed in Table 2.1. For the amounts of PAHs weighed see Appendix A.

Table 2.1. Concentrations of 1,3-dimethylnaphthalene (DMN), fluoranthene (FLA) and phenanthrene (PHE) in methanol (MeOH) and dichloromethane (DCM) stock solutions.

Compound	Concentration in MeOH (µg/mL)	Concentration in DCM (mg/mL)
DMN	110	149
FLA	106	204
PHE	92,0	999

Surrogate internal standards (SIS) and recovery internal standards (RIS) were applied in this study. Table 2.2 presents the standards. The stock solutions and calibration standards were prepared in DCM.

Table 2.2. The surrogate (SIS) and recovery (RIS) internal standards, the chemicals they consist of, and their respective concentrations.

Standard ID	Chemicals	SIS A703 (µg/mL)	SIS A681 (µg/mL)
Surrogate internal standards (SIS)	naphtalene-d_8	25,1	251
	phenanthrene-d_{10}	5,00	50,0
	perylene-d_{12}	5,08	50,8
	chrysene-d_{12}	4,86	48,6
		RIS A705 (µg/mL)	**RIS A690 (µg/mL)**
Recovery internal standards (RIS)	acenaphtene-d_{10}	10,6	106
	fluorene-d_{10}	9,84	98,4

2.1.2 Microplastic particles

Polystyrene (PS) was purchased as an aqueous dispersion from Polysciences Europe Gmbh (www.polysciences.com). Polyethylene (PE) was purchased in powder form from Cospheric LLC (www.cospheric.com). The PES-particles were produced in-house from white polyester yarn (spun with 36 filaments of approximately 10 µm diameter each), kindly supplied by The Pierre Robert Group. The PES microfibres (50 µm) were prepared using Matt Coles (2016) method. Briefly, yarn was fixed in frozen glycol solution (Neg 50®) and cut to 50 µm using a HM 500 O microtome set to -20 °C. The fibres were isolated from the glycol solution by filtration (HAWP 0,45 µm filters), rinsed with MilliQ water, and allowed to air dry before use in experiments. Selected properties of the MPs used in this study are listed in Table 2.3.

Table 2.3. Nominal values of selected properties of MPs. PE-polyethylene: PS-polystyrene: PES-polyester.

	PE (10 µm)	PE (100 µm)	PS* (10 µm)	PE (200 µm)	PES (10 µm)
Diameter range (µm)	3,00- 16,0	90,0-106	10,0	180-212	10,0
Length (µm)	-	-	-	-	50,0
Theoretical average diameter (µm)	9,50**	98,0**	10,0	196**	10,0
Average particle volume (cm^3)	3,4E-10	3,7E-07	3,9E-10	3,0E-06	3,93E-09
Density (g/cm^3)	0,960***	0,960***	1,05***	0,960***	1,37****
Particle mass (mg)	3,2E-07	3,5E-04	4,1E-7	2,8E-03	5,4E-06
Particles/mg	3,1E+06	2818	2,4E+06	352	1,8E+05
Surface area (μm^2)	284	30172	314	120687	1728
Surface area (m^2)/mg	0,877	0,0850	0,833	0,0425	0,321

*PS was delivered as an aqueous solution with a concentration in suspension (w/v, %) of 2,6. The solution was shaken well before use.

** The theoretical average diameter (µm) of PE was calculated based on the range given by the manufacturer.

*** Value given by manufacturer

**** Polyester nominal density

High-density PE has density above ~0,94 g/cm^3, as mentioned in the introduction. The PE material in the present master thesis can therefore be classified as HDPE.

2.1.3 Laboratory equipment

All glass (except volumetric) was baked at 450 °C in a ceramic oven before use. Equipment that could not be baked was rinsed thoroughly with DCM (glass, metal and Teflon) or MilliQ-water (plastic) prior to use.

2.2 Experimental

2.2.1 Preparation of the test media

The study medium was sterile filtered (Sterivex cartridge filter, 0,22 µm) seawater sourced from the Trondheim fjord outside Trondheim harbor, from a depth of 80 meters below the thermocline. After filtration, the water was acclimatized to 10 or 20 °C overnight.

To achieve solutions with maximum seawater solubility of the test PAHs, a so-called 'Teflon-WAF' (WAF= water accommodated fraction) was prepared for each chemical. The PAHs, dissolved in DCM, were applied to Tetrafluoroethylene and ethylene polymer monofilament (Teflon grid) pads (4x8 cm) produced by Fluortex™, Sefar AG., in Heiden, Switzerland (Lofthus et al., 2016). The PAHs were applied with a 200 µL syringe, one drop at a time. For the volumes and concentrations applied see Table 2.4. The amount applied exceeded the theoretical solubility in the volume seawater they were applied in (10 L). The Teflon grid pads were set to dry for about 30 minutes before they were hung down in each glass bottle with 10 L of sterile filtered seawater without touching the bottom. The bottles were carefully stirred using a magnetic stirrer, at 10 or 20 °C. The equilibration time (pre-determined) was two (1,3-dimethylnaphthalene) or three days (fluoranthene and phenanthrene). The Teflon grid pads were then taken out of the bottles, and the stirring went on for 15 minutes before the bottles were left for another 30 minutes without stirring. The solutions were tapped through a small tap at the bottom of the bottles, to oven baked glass bottles (1 L and 2 L) and stored in the dark at 10 or 20 °C until they were used. For comparability reasons, only the solutions prepared at 10 °C were used in experiments, while the solutions prepared at 20 °C were used to determine seawater solubility of the PAHs at 20 °C. to verify the stability of the solutions.

The concentration in the un-used bottles was measured after one month of storage. See Appendix B for the calculated concentrations of the bottles at day 0 and after a month.

Table 2.4. Concentration of 1,3-dimethylnaphthalene (DMN), fluoranthene (FLA) and phenanthrene (PHE) in DCM and volume of the PAHs in DCM solution applied to the Teflon grid pads.

	DMN	FLA	PHE
Concentration of PAH in DCM (mg/mL)	149	2,04	9,99
Volume to be applied to Teflon grid pad (mL)	2,50	1,20	1,20

2.2.2 Sorption studies

To allow removal of sample solution at several time-points without disturbing the PAH-MP equilibrium, sample bottles (250 mL) were applied for the uptake kinetics experiment, while sample vials (22 mL) were used for the isotherm experiments. Teflon-lined caps were used for both types of flasks. There was about 10 % (by volume) headspace of air in each bottle or vial.

For experiments with 250 mL bottles, MPs were weighed in aluminium weighing boats and transferred to the bottles with a few droplets of sterile filtered seawater. For experiments with 22 mL vials, MPs were directly weighed in the vials. PE and PES MPs were weighed using a Mettler Toledo (XPE205) scale with an accuracy of 0,01 mg, routinely calibrated and verified daily before use. Polystyrene was transferred from dispersion (after shaking) using an Eppendorf ® pipette (100 µL).

Samples (in bottles or vials) were shaken on a Gerhardt shaking table, with a horizontal movement back and forth. The adjustments were optimized to hold the particles steadily in suspension, with a motor speed of 8 (8 of 10, ~2-3 Hz per second). During the experiment, the samples were kept in the dark (at 10 or 20 °C). The temperature was monitored during the experiments with an electronic, calibrated thermometer. The temperatures were 10 ±2 °C and 20 ± 1 °C throughout the sorption studies.

At each sampling point, the water samples were filtered to remove MPs from the water prior to analysis. The filtration set-up consisted of an empty glass SPE-column (2 mL) used as a sample reservoir, connected by luer-lock to a 13 mm 0,45 µm PTFE syringe filter. PTFE filters has previously proven suitable for PAH isolation from aqueous particle dispersions (Glomstad et al., 2017)). The samples were transferred to the SPE-column connected to the PTFE syringe filter using a glass pipette. The sample was pushed through the filter using the plunger from a BD Plastipak 2 mL syringe. To

saturate the filter, clean seawater and a small portion (~2 mL) of the sample solution was filtered through the filter first and discarded before collection of the sample.

2.3 The experiments

2.3.1 Uptake kinetics

The first aim of this study was to establish equilibration time for the different pairings of MP and PAH at 10 and 20 °C. To determine the uptake kinetics, it was necessary to execute three experiments to find the equilibration time.

For all three experiments the same concentration of each chemical was used. A sample from the chemical seawater solution was first analysed by LC-UV. See Appendix B for the concentrations from each seawater solution. To allow comparable experiments, 1,3-dimethylaphthalene, phenanthrene and fluoranthene were all diluted to 20 µg/L using temperature acclimatized, sterile filtered seawater. For the amounts of MP applied to the samples in the uptake kinetic experiments see Appendix E. The uptake kinetic samples were analysed by LC-UV as described later.

2.3.1.1 Kinetic experiment 1

In experiment 1, PE-10, PE-100, PS-10 and PES-50, each in combination with 1,3-dimethylnaphthalene, phenanthrene and fluoranthene were included. Control samples of each chemical without MP were also included to account for other losses than MP sorption.

In experiment 1, the concentrations of MPs added were kept constant on a surface area (SA) basis for each polymer type. The concentrations of the different MP particles are listed in Table 2.5.

Table 2.5. Weight, surface area and number basis of polyethylene 10 µm (PE-10), polyethylene 100 µm (PE-100), polystyrene 10 µm (PS-10) and polyester 50 µm (PES-50).

	PE 10 (µm)	PE 100 (µm)	PS 10 (µm)	PES 50 (µm)
mg/L	3,24	33,4	3,72	8,84
SA(µm²) /L	2,84E+09	2,84E+09	2,84E+09	2,84E+09
# particles/L	1,00E+07	9,40E+04	9,00E+06	3,60E+07

Samples were taken at five (phenanthrene and 1,3-dimethylnaphthalene) and six (fluoranthene) time points; day 1, 2, 3, 4 and 7 for phenanthrene and 1,3-dimethylnaphthalene, and day 1, 2, 3, 4, 7 and 9 for fluoranthene.

2.3.1.2 Kinetic experiment 2

In experiment 2, PE-10 in combination with 1,3-dimethylnaphthalene, phenanthrene and fluoranthene was included. Control samples (triplicate) of each chemical without MP were also included to account for other losses than MP sorption. In this experiment the relevant amount of MP was increased. The concentrations of PE-10 is given in Table 2.6.

Table 2.6. Concentration of polyethylene 10 µm (PE-10).

	PE 10 (µm)
mg/L	32,3
SA(µm^2)/L	2,83E+10
# particles/L	1,00E+08

Samples were taken at six time-points for phenanthrene, 1,3-dimehtylnaphthalene and fluoranthene, on day 0, 1, 2, 3, 4 and 7.

2.3.1.3 Kinetic experiment 3

In experiment 3, PE-10, PE-100, PE-200 and PS-10 in combination with phenanthrene and fluoranthene were included. Control samples (triplicate) of each chemical without MP were also included to account for loss not due to MP sorption.

The concentrations of MPs were kept constant on both a SA and mass basis for each polymer type. The concentrations of the different MPs used in the experiment are given in Table 2.7.

Table 2.7. Concentrations of PE-10, PE-100 and PE-200 concentration comparable to PE-10 by surface area (SA) or mass, PS 10 µm (PS-10) concentration comparable both by surface area (SA) and mass.

MP- type	mg/L	SA(µm^2) /L	#particles/L
PE-10	32,3	2,84E+10	1,00E+08
PE-100 SA	333	2,84E+10	9,40E+05
PE-100 mass	32,3	3,02E+12	1,00E+08
PE-200 SA	667	2,78E+10	2,30E+05
PE-200 mass	32,3	1,21E+13	1,00E+08
PS-10 SA/mass	37,2	2,83E+10	9,02E+07

Samples were taken at six (fluoranthene) and nine (phenanthrene) time-points respectively. Day 0, 1, 2, 3, 4, 7, 9, 11 and 14 for PHE, and day 0, 1, 2, 3, 4 and 7 for fluoranthene.

2.3.2 Range-finding study

Prior to the isotherm-study, a range-finding study was conducted to find the appropriate concentrations of MPs to sufficiently reduce the concentration of PAHs in solution by aiming for approximately 50% reduction- at the range of PAH concentrations intended to be applied in the isotherm-study.

Three different concentrations (100%, 21% and 5%) of fluoranthene and phenanthrene were utilized in the range-finding study. Fluoranthene and phenanthrene were taken directly from the stock solution and diluted with sterile filtered, acclimated seawater.

For the number of replicates of the different pairings of MPs with PAHs, and the concentrations of the different MPs for the fluoranthene and phenanthrene samples, see Table 2.8. In addition to these samples, three replicates of control samples for each concentration of PAH were also analysed. Appendix F shows the amount of MP in each sample and the concentration of PAH in each sample, for the range-finding study.

Table 2.8. Number of replicates of the different pairings of MP with PAHs, and concentrations of PE-10, PE-100 and PE-100, in the range-finding study.

		PAH concentration (%)			SA(µm²)/L	#particles/L
	MP type and amount (mg/L)	5	21	100		
FLA	PE-10 (7,50)	-	-	3	6,70E+09	2,30E+07
	PE-10 (15,0)	1	1	1	1,30E+10	4,07E+07
	PE-10 (30,0)	1	3	1	2,70E+10	9,40E+07
	PE-10 (45,0)	1	1	1	4,00E+10	1,40E+08
	PE-100 (150)	1	1	1	1,30E+10	4,30E+05
	PE-100 (300)	1	3	1	2,60E+10	8,60E+05
	PE-100 (450)	1	1	1	3,90E+10	1,30E+06
	PE-100 (600)	-	-	3	5,20E+10	1,70E+06
	PS-10 (11,5)	1	1	1	8,80E+09	2,80E+07
	PS-10 (36,5)	1	3	1	2,90E+10	9,10E+07
	PS-10 (109)	1	1	1	8,30E+10	2,70E+08
	PS-10 (328)	-	-	3	2,50E+11	8,00E+08
PHE	PE-10 (15,0)	1	1	1	1,30E+10	4,07E+07
	PE-10 (30,0)	1	1	3	2,70E+10	9,40E+07
	PE-10 (45,0)	1	1	1	4,00E+10	1,40E+08
	PE-100 (150)	1	1	1	1,30E+10	4,30E+05
	PE-100 (300)	1	1	3	2,60E+10	8,60E+05
	PE-100 (450)	1	1	1	3,90E+10	1,30E+06
	PE-100 (600)	-	-	3	5,20E+10	1,70E+06
	PS-10 (11,5)	1	1	1	8,80E+09	2,80E+07
	PS-10 (36,5)	1	1	1	2,90E+10	9,10E+07
	PS-10 (109)	1	1	3	8,30E+10	2,70E+08

All the fluoranthene samples were shaken at 10 °C and sampled after 5 days. The phenanthrene samples were shaken at 20 °C and sampled after 6 days.

The phenanthrene samples with 21 % and 100 % concentration were analysed directly with LC-UV, and the phenanthrene samples with 5 % concentration, and all the fluoranthene samples, were extracted then analysed by GC-MS.

2.3.3 Sorption isotherms

The final experiment in this study was conducted to establish sorption isotherms for the different pairings of MPs and PAHs at 10 and 20 °C. The PAH concentration varied, seven levels over two orders of magnitude (5, 8, 13, 21, 36, 60 and 100 % of solubility at 10 °C, corresponding a spacing factor of 1.67 between concentrations).

The methodologies applied within sorption isotherms are many, but common for them all is the determination of the concentration of PAHs in the aqueous solution and/or on the MPs. The method applied is dependent on the resources the laboratory has available, and the materials one is working with. The method used in the sorption isotherms in the present master thesis follows the same principle as Zindler et al. (2016) but is adapted to seawater and MPs.

Each sample was made up in 22 mL vials, with 20 mL PAH solution and the appropriate MP amount (Table G.1 and G2 in Appendix G). There were three replicates of each sample, and they were shaken for the equilibration time determined in the kinetics experiments 1-3. Sampling of fluoranthene was done after 5 days, and sampling of phenanthrene was done after 7 (20 °C) and 9 days (10 °C).

Upon sampling and filtration, HCl (100 µL 15 % solution in MilliQ-water) was applied to the filtered samples to lower the sample pH to avoid bacterial growth, which could then be stored (dark at 4-5 °C) for up to two weeks.

The concentrations of the different MPs for the fluoranthene and phenanthrene samples are listed in Table 2.9.

Table 2.9. Concentrations of PE-10, PE-100 and PS-10 particles in isotherm experiments with fluoranthene (FLA) and phenanthrene (PHE).

MP-type		mg/L	SA(µm^2) /L	#particles/L
FLA	**PE-10**	15,0	1,30E+10	4,70E+07
	PE-100	450	3,90E+10	1,30E+06
	PS-10	109	8,30E+10	2,70E+08
PHE	**PE-10**	30,0	2,70E+10	9,40E+07
	PE-100	450	3,90E+10	1,30E+06
	PS-10	109	8,30E+10	2,70E+08

For the fluoranthene samples there were, for each concentration of each MP three replicates, together with three control samples from each concentration. The fluoranthene samples were extracted and analysed with GC-MS. For the phenanthrene samples there was, for each concentration of each MP three replicates, together with three control samples from each concentration. The phenanthrene samples with the two lowest concentrations were extracted and analysed by GC-MS. The remaining samples had concentrations high enough to be analysed by LC-UV. The isotherm study was conducted both at 10 and 20 °C.

2.4 Extraction methods

2.4.1 Extraction of water samples

In the isotherm and range-finding study, concentrations of fluoranthene and the two lowest concentrations of phenanthrene were too low for LC-UV analysis. Therefore, extraction and concentration of the samples was necessary. The filtered samples (2 mL) were transferred to Kimax® tubes (12 mL) with an Eppendorf pipette. The SIS-A703 standard (10 µL) was applied to each Kimax® tube. The solvent (50 % DCM in *n*-hexane, 1 mL) was applied to the tubes with a glass pipette, and the tube closed with a Teflon-lined screw-cap.

The samples were vortexed with an IKA MS 3 basic vortex for 30 seconds, then centrifuged for two minutes with a 5804 R Centrifuge set to 2000 rpm and 20 °C. The top (organic) phase was transferred to a conical tube. If water was accidentally transferred, a ‘drying unit’ was prepared by adding baked Bilsom cotton to a glass pipette, with baked sodium sulfate (50 mg) on top. The organic phase with water was pipetted through the salt and Bilsom to remove water.

The extraction and the transfer of organic phase to the conical tube was repeated three times. Short vortex (five seconds) was used for the repeated extractions.

The combined organic phases (three extractions) were concentrated to 100 µL using a SBH13OD/3 block heater (Stuart), at 40 °C, under a gentle flow of N_2 gas. The concentrated sample was transferred to a GC-vial with a conical insert (250 µL) using a glass pipette. The Kimax® tube was then rinsed three times with DCM (50 µL), which was also transferred to the GC glass with insert. The solution in the GC-vial was concentrated to 90 µL and the RIS A705- standard (10 µL) was applied to each glass.

For each set of samples, a laboratory blank (MilliQ water) was included, which was treated the same way as the real samples. This extraction procedure was done for all the samples to be analysed by GC-MS.

2.5 Chemical analysis

2.5.1 LC-UV analysis

The liquid chromatography analysis with ultraviolet detection (LC-UV) was performed on an Agilent series 1200 HPLC system. LC-UV has previously proven suitable for analysis of PAHs (Glomstad et al., 2017, Zindler et al., 2016). Acetonitrile (70 %)- H_2O (30 %) was used as the mobile phase with a flow rate of 1,5 mL/min. The injection volume was 30 µL, and separation achieved using a Supelco Supelcosil LC-PAH column (10cm x 3mm), with a particle size of 3 µm. The detection was accomplished with UV-detection (diode array detector (Agilent 1260 Infinity II DAD) or variable wavelength detector (Agilent 1260 Infinity VWD), depending on availability. The wavelengths for detection were 250 nm for phenanthrene, 230 nm for fluoranthene and 220 nm for 1,3-dimethylnaphthalene. Chemstation software was used to monitor, record and integrate the chromatograms.

2.5.1.1 Quantification of results from LC-UV

Quantification for LC-UV was achieved using external standard calibration. For the calibration calculations for LC-UV see Tables D.1-D.4 in Appendix D. For the LC-UV a six-point calibration was performed (0,0001 µg/mL, 0,001 µg/mL, 0,01 µg/mL, 0,1 µg/mL, 1 µg/mL and 10 µg/mL PAH in MeOH and seawater). The standards for calibration were freshly prepared by dilution in sterile seawater before every analysis, using the stock solutions in methanol (Table 2.1).

After initial trials, preparation method of seawater calibration solutions for LC-UV was changed for a more efficient and precise one. From the stock solutions in methanol (Table 2.1) four stock solutions for each chemical were prepared (10 µg/mL, 1 µg/mL, 0,1 µg/mL and 0,01 µg/mL). These stock solutions were stored dark and at 4-5 °C. The solutions were used to make a freshly prepared nine-point calibration (0,0001 µg/mL, 0,0005 µg/mL, 0,001 µg/mL, 0,005 µg/mL, 0,01 µg/mL, 0,05 µg/mL, 0,1 µg/mL, 0,5 µg/mL and 1 µg/mL PAH in seawater) immediately prior to every analysis.

The concentration of target analytes was determined using Equation 2.1.

$$C_a = \frac{A_t - intercept}{Slope} \cdot \frac{1000}{\frac{\%\, recovered}{100}} \qquad (2.1)$$

A_t is the total area of quantification ion for the target chemical in the standard

2.5.2 GC-MS analysis

For experiments with PAH concentrations too low for LC-UV analysis, extracts of water samples were analysed by gas chromatography coupled to mass spectrometry (GC-MS). The GC-MS system comprised a gas chromatography Agilent 7890A GC equipped with an Agilent 5975 C Merck Sharp & Dohme (MSD) and an Agilent 7693 autosampler. The inlet was set to 250 °C, the transfer line to 300 °C, the ion source to 230 °C and the quadrupole to 150 °C. The carrier gas (mobile phase) was helium, at a constant flow of 1 mL/min. 1 µL of sample was injected using pulsed splitless injection. Preliminary analysis was done using ZB-1 column (30 meters long, with a thickness of 0,25 µm and 0,25 mm I.D.

The temperature program was 40 °C for the first minute, then 15 °C/min until 315 °C, and then a hold at 315 °C for five minutes. The solvent delay was seven minutes. The acquisition mode was Selected Ion Monitoring (SIM), and the method was set with five SIM windows. The start time for them was 7, 9, 12, 14 and 16 minutes, with two (134 and 136 m/z), five (141, 156, 162, 164 and 176 m/z), four (176, 178, 184 and 188 m/z), six (201, 202, 236, 240 and 264 m/z) and three (236, 240 and 264 m/z) number of ions, respectively.

Samples from the isotherm study were analysed using a DB5-MS ultra-inert column (30 meters long, with a film thickness of 0,25 µm and 0,25 mm ID). The temperature program was 40 °C for the first minute, then 40 °C/min until 120 °C, 15 °C/min until 300 °C, 40 °C/min until 320 °C, and then a hold at 320 °C for seven minutes. The solvent delay was six minutes. The acquisition mode was SIM, and the method was set with four SIM windows. The start time for them was 6, 9.5, 12 and 14 minutes, with seven (136, 141, 156, 162, 164, 174, 176 m/z), four (177, 178, 184, 188 m/z), two (201, 202 m/z) and three (236, 240 and 264 m/z) number of ions, respectively. The dwell time for both methods was optimized so that the number of cycles per second was five.

Chemstation MSD software was used to monitor, record and integrate the chromatograms.

2.5.2.1 Quantification of results from GC-MS

Quantification of GC-MS was achieved using internal standard calibration. For the relative response factors and their relative standard deviations see Table D.5 in Appendix D. For the GC-MS data an eight-point calibration was performed (0,001 µg/mL, 0,01 µg/mL, 0,025 µg/mL, 0,05 µg/mL, 0,10 µg/mL, 0,5 µg/mL, 1,0 µg/mL and 2,5 µg/mL). The standards for calibration were prepared once, using a stock solution containing a mix of the three chemicals (PAH mix), SIS A681- standard (100 µL) and RIS A690- standard (100 µL).

The relative response factors (RRF) for each level in the calibration curve were calculated using Equation 2.3.

$$RRF = \frac{A_t \cdot C_i}{A_i \cdot C_t} \qquad (2.3)$$

A_t is the total area of quantification ion for the target chemical in the standard

A_i is the total area of quantification ion for the recovery internal standard (fluorene-d_{10}) in the standard

C_t is the concentration of target chemical in the standard

C_i is the concentration of internal standard (fluorene-d_{10}) in the standard

The concentration of target analytes is determined using Equation 2.4.

$$C_a = \frac{A_a \cdot Amt_i}{A_i \cdot RRF_i \cdot REC \cdot V_a} \qquad (2.4)$$

C_a is the concentration of target analyte

A_a is the total area of quantification ion for the target analyte, calculated by A_t/A_i

Amt_i is the amount of internal standard (fluorene-d_{10}) added to the sample, calculated by C_i x V_i, where V_i is the volume of internal standard added to the sample

A_i is the total area of quantification ion for the internal standard

The recovery (REC) was calculated as the percentage recovery of the surrogate internal standard (phenanthrene- *d*10) compared to the added amount.

RRF_i is the average RRF for the analyte, determined from initial calibration

V_a is the sample volume

2.6 Calculations and statistical treatment

All sorting of data, calculations and model fits were performed in Microsoft Excel (version 2017).

2.6.1 Standard deviation

Standard deviation was determined using Equation 2.5.

$$\sigma = \sqrt{\frac{1}{N-1}\sum_{i=1}^{N}(x_i - \overline{x})^2}. \qquad (2.5)$$

σ is the standard deviation of the target analyte

X are the observed values of the sample items

$\bar{x}$ is the mean value of the observations

N is the number of observations in the sample

2.6.2 Filtration recovery

The percentage filtration recovery was applied for quantification of results from both LC-UV and GC-MS and was determined using Equation 2.2.

$$\%\, recovered = \frac{CTR_{filt}}{CTR_{unfilt}} \cdot 100 \qquad (2.2)$$

CTR_{filt} is the concentration of the filtered control sample

CTR_{ufilt} is the concentration of the unfiltered control sample

2.6.3 PAHs sorbed to MPs

The concentration of PAHs in the MPs was determined using Equation 2.7.

$$C_{mp} = \left(\overline{C_{PAH}} - C_{free}\right) \cdot \frac{V_s}{m_{MP}} \qquad (2.7)$$

C_{mp} is the concentration of PAH sorbed to the MPs (µg PAH/mg MP)

$\overline{C_{PAH}}$ is the average concentration of PAH in the control sample (µg/L)

C_{free} is the concentration of the PAH in the aqueous phase (µg/L) after the equilibrium

V_s is the sample volume

m_{MP} is the mass of the MP in the sample

2.6.4 Fit of isotherms

Sorption parameters were calculated, and the fitted curves for sorption isotherms were preformed, using Microsoft's spreadsheet, Excel 2017. The isotherm parameters were also determined in Excel, by a trial and error procedure, minimising the error function across a concentration range studied when using the solver add-in (Wang and Wang, 2018b, Gimbert et al., 2008, Saha et al., 2017, Kumar and Sivanesan, 2005).

3 Results and discussion

Missing data, clearly erroneous data and clear outliers is not presented in the following. Data are presented as average of replicates with standard deviation. See Appendixes D-G for all raw data, and calibration data for LC-UV and GC-MS measurements.

3.1 Concerning experimental setup

3.1.1 Achieved solubility in seawater

The achieved average solubility at 10 and 20 °C measured in the seawater solutions with 1,3-dimethylnaphthalene, fluoranthene (prepared twice) and phenanthrene are shown in Table 3.1.

Table 3.1. Average solubility (µg/L) measured in the seawater solutions ('Teflon-WAF') with 1,3-dimethylnaphthalene (DMN), fluoranthene (FLA) and phenanthrene (PHE) with standard deviation.

Compound	Average solubility (µg/L)	
	10 °C	**20 °C**
DMN	3123±78	na
FLA	21,6±0,4	83,6±0,6
	26,1 ±0,7	
PHE	159±1	414±5

na: not analysed

The concentration in the stored bottles of phenanthrene seawater solution was verified after a month because of potential degradation. The average concentration was found to be 156 ±2 µg/L, a difference of ~4 µg/L from the first measurement (table 3.1), proving the solutions were un-degraded. The solutions were therefore used for further experiments. See Tables B.1 and B.2 in Appendix B for the verification concentrations and the corresponding calibration calculations for phenanthrene.

3.1.2 Recovery of PAHs during filtration

Tables 3.2 and 3.3 show the percentage recovery of PAHs in the uptake kinetics and the sorption isotherm studies, respectively, after filtration. For the concentrations of the control samples before and after filtration, see Appendix C.

Table 3.2. Filtration recovery (%) of fluoranthene, phenanthrene and 1,3-dimethylnaphthalene in the uptake kinetics study.

PAH	Temperature (°C)	Recovery (%)
FLA	10	52
	20	64
PHE	10	72
	20	72
DMN	10	62
	20	48

Table 3.3. Recovery (%) of fluoranthene and phenanthrene in the sorption isotherm study.

PAH	Temperature (°C)	Recovery (%)
FLA	10	47
	20	47
PHE	10	63
	20	62

Of the two studies the percentage recovery of PAH was the lowest for the kinetics study. This is assumed to be because of smaller filtered volume in the kinetics study. In the sorption isotherm study the whole sample volume (~20 mL) was filtered, while in the kinetics study only a sub-sample (~1 mL) was filtered. A higher relative recovery in the primary scenario is explained by a higher saturation of the PTFE filter with PAHs, which is known to retain a certain amount of PAHs (Glomstad et al., 2017). Glass fibre filters could have provided less filtration loss but were a more expensive option.

3.2 Sorption kinetics

3.2.1 Sorption kinetics experiment 1

Figure 3.1 shows the evolution of 1,3-dimethylnaphthalene, fluoranthene and phenanthrene concentration in water samples with MPs and controls (no MPs) with time, 10 and 20 °C.

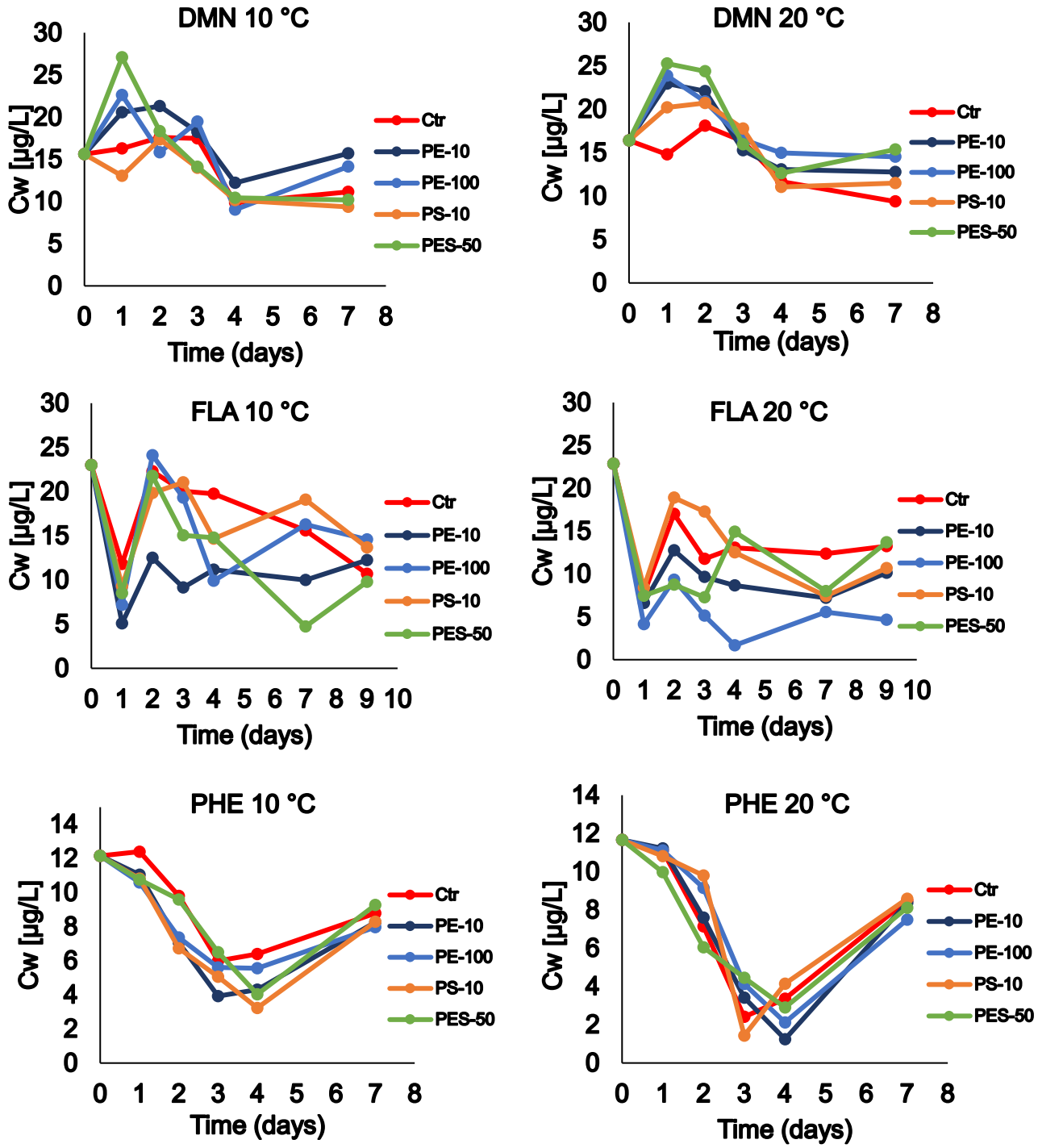

Figure 3.1. Sorption kinetics experiment 1. Concentration [µg/L] of 1,3-dimethylnaphthalene, fluoranthene and phenanthrene in samples with polyethylene (PE-10 and PE-100), polystyrene (PS-10) and polyester (PES-50) relative to the control sample.

There wasn’t a significant difference in concentration of PAH in the samples compared to the control sample, which suggests that the MP: PAH ratio was too low to observe considerable PAH depletion of the water phase. Because of the small difference in concentration between the two values the uptake of PAHs to the MPs couldn’t be calculated properly.

The depletion of PAHs in the control samples can be explained by sorption to the glass walls of the sample bottles. The loss in MP samples must therefore be viewed relative to the loss in the controls.

A dip in concentration after three-four days was observed consistently in the phenanthrene samples. There is great uncertainty to what has caused these dips but it can be related to the system coming to equilibrium. This process can include the sorption of the PAHs to the glass walls. A readily amount of the phenanthrene adsorbs to the glass walls at the start and is then slowly released back into the water phase as the whole system approaches a true equilibrium. Another possible reason for the dips in the phenanthrene samples may be that the day 7 samples had some form of instrumental error which has caused them to be higher than the day 3 and 4 samples.

3.2.2 Sorption kinetics experiment 2

In sorption kinetics experiment 2 the concentration of MP was increased ten-fold on a mass basis, with PE-10 as the test MP. Figure 3.2 shows the concentration of 1,3-dimethylnaphthalene, fluoranthene and phenanthrene in the samples with PE-10 and control samples (triplicate) as a function of time, at 10 °C and 20 °C.

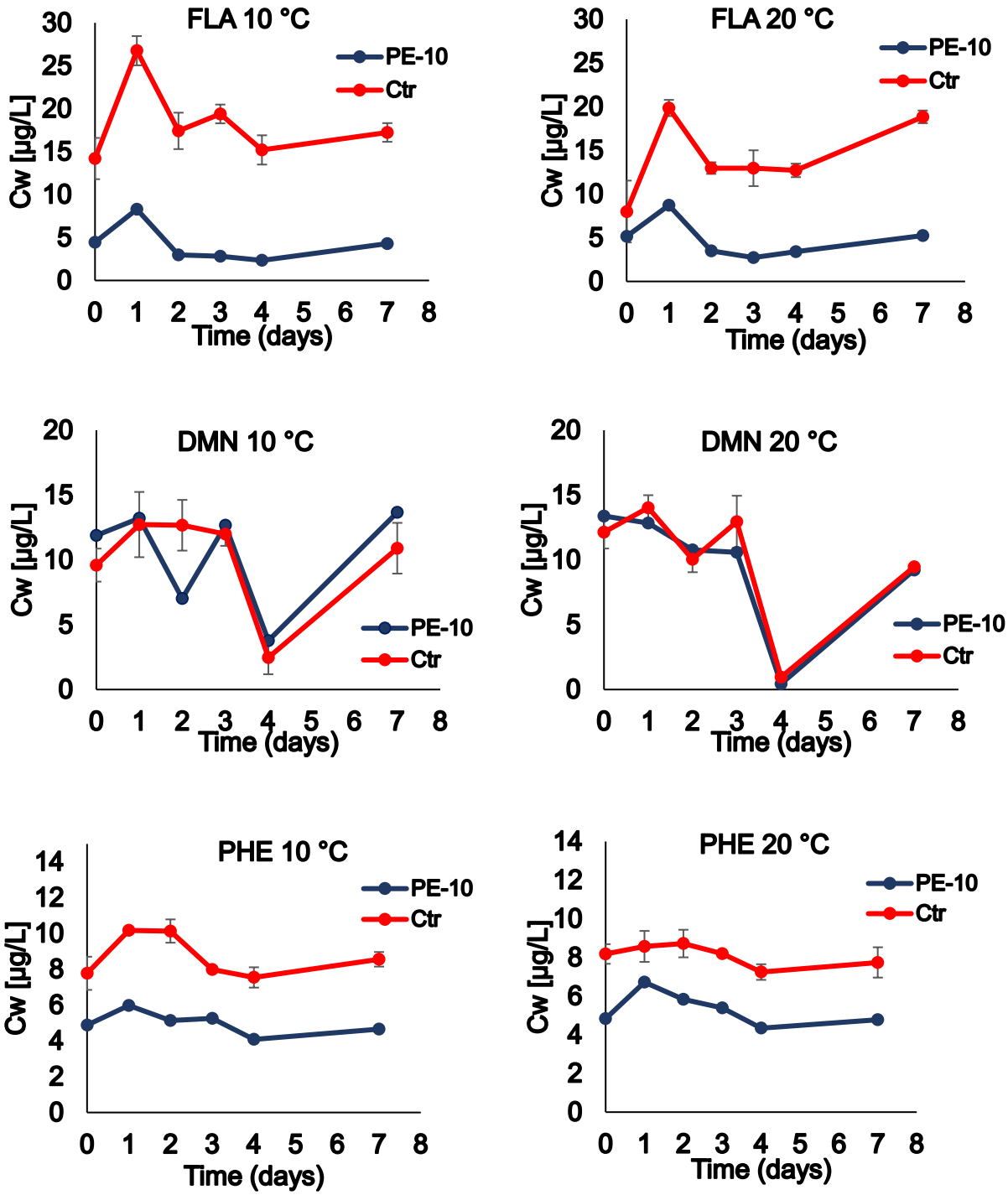

Figure 3.2. Sorption kinetics experiment 2. Concentration [µg/L] of 1,3-dimethylnaphthalene, fluoranthene and phenanthrene in samples with PE-10 relative to the control sample. Error bars represent the standard deviation.

In sorption kinetics experiment 2 there was a significant difference in concentration of PAH in the samples compared to the control sample. The concentration of fluoranthene and phenanthrene in the samples with PE was less than the concentration in the control sample, indicating sorption. For 1,3-dimethylnaphthalene, on the other hand, it

was not observed any considerable difference between depletion in controls and PE-10 solutions with increasing the MP concentration 10-fold between the two experiments. Thus, indicating that the partitioning of this compound to MPs will be negligible, or at least too low to measure with the experimental design used in the current study.

The time-dependent uptake (CPE, µg/mg) of fluoranthene and phenanthrene to PE-10, at 10 and 20 °C, are shown in Figure 3.3. Uptake of 1,3-dimethylnaphthalene to PE showed negligible or negative values, meaning no sorption. It was therefore not plotted. It was concluded that increasing the amount of PE for the sorption effects of 1,3-dimethylnaphthalene gave no useful results and this compound was therefore omitted from the further experiments.

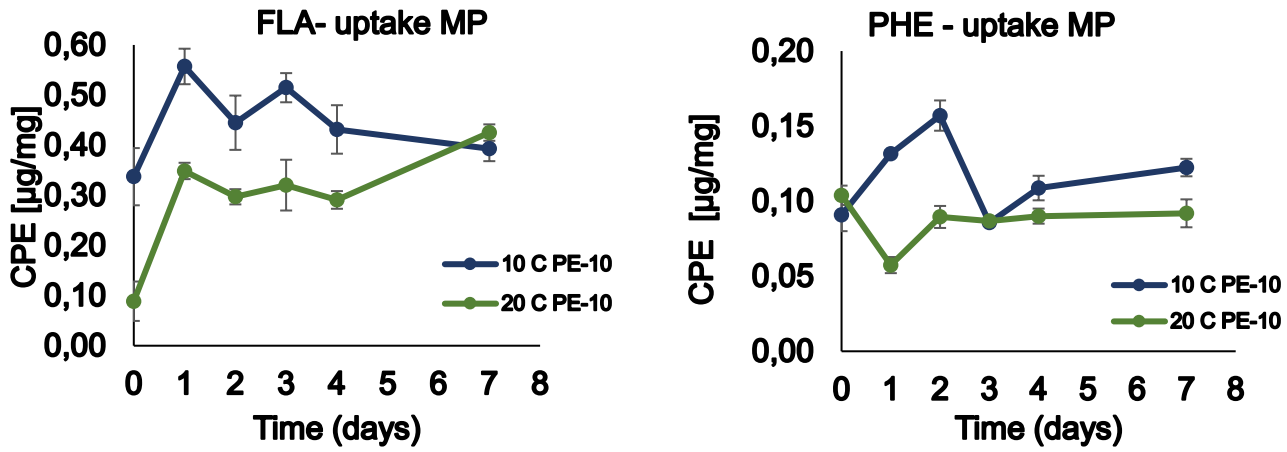

Figure 3.3. Uptake [µg/mg] of fluoranthene and phenanthrene to PE-10 at 10 and 20 °C. Error bars represent the standard deviation.

Looking at the graphs in figure 3.3, the degree of sorption for both fluoranthene and phenanthrene to PE was higher at 10 °C, about 0,20 µg/mg for fluoranthene and 0,15 µg/mg for phenanthrene, than at 20 °C.

The uptake of PAHs to MPs stabilize after 5-6 days, indicating sorption equilibrium has been reached. Sorption and desorption occur side by side, until equilibrium is reached.

3.2.3 Sorption kinetics experiment 3

Sorption kinetic experiment 2 showed sorption of phenanthrene and fluoranthene to PE-10. In this experiment different sizes of PE (100 µm and 200 µm) in addition to PS-10 was included. The concentration of MP added of each was increased compared to experiment 1, reflecting the observed increase of sorption with a ten-fold increase of PE-10 concentration in experiment 2. Using PE-10 as a reference, the amounts of PE-100 and PE-200 were varied to keep either MP mass or surface area constant in the exposure solutions with different MPs. This was done to investigate whether mass or surface area is the domination metric for PAH sorption to MPs. Figure 3.4 shows the time-dependent concentration of fluoranthene and phenanthrene in the samples with the MP relative to the control sample, at 10 and 20 °C.

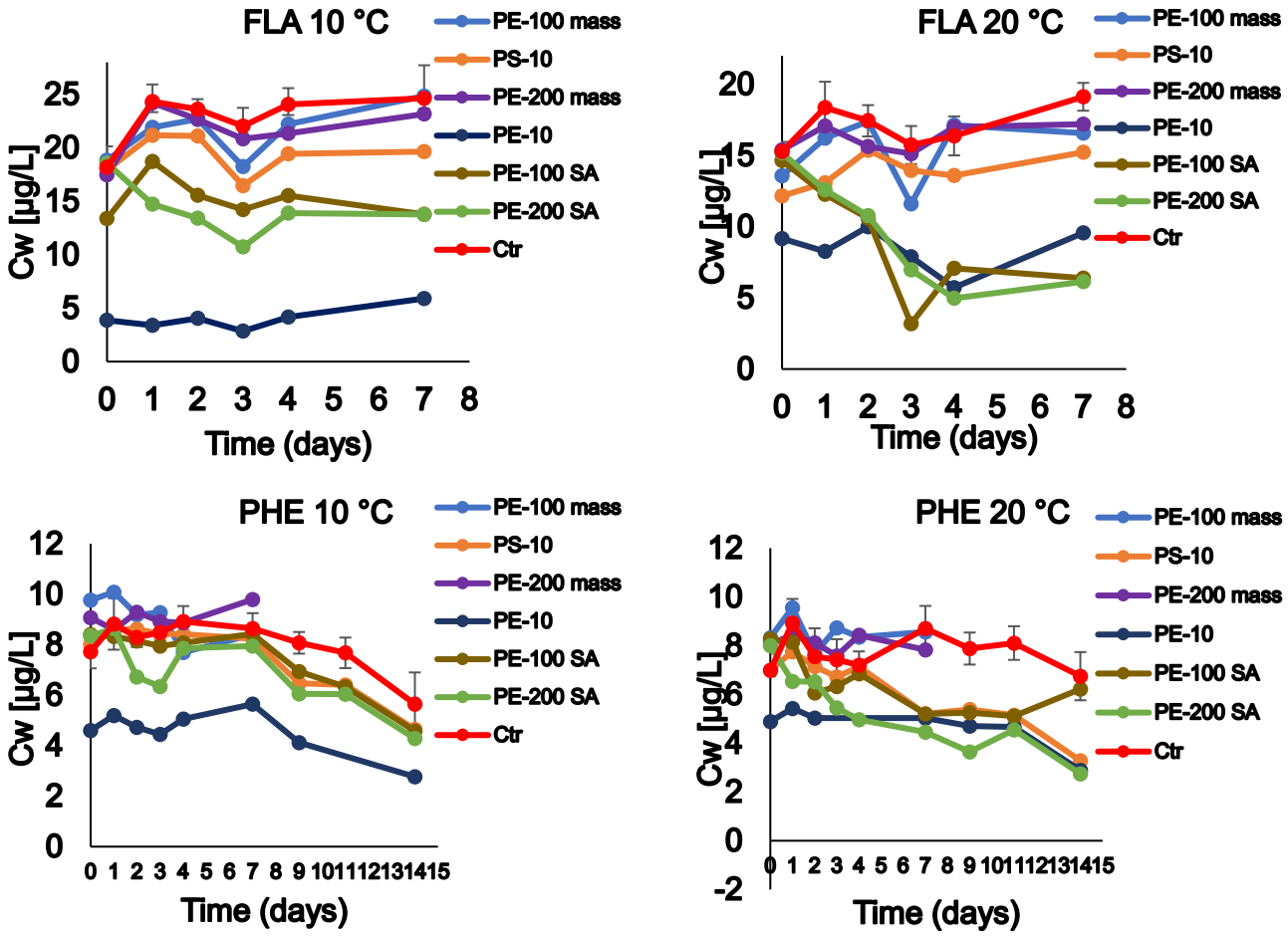

Figure 3.4. Sorption kinetics experiment 3. Concentration [µg/L] of fluoranthene and phenanthrene in samples with polyethylene (PE-10, PE-100 and PE-200) and polystyrene (PS-10) relative to the control sample. PE-100 and PE-200 mass means the mass added is comparable to that of PS-10 and PS-10. PE-100 and PE-200 SA means the surface area added is comparable to that of PE-10 and PS-10. Error bars represent the standard deviation.

There was a significant difference between depletion in controls and PS-10 and PE-10 solutions, comparable by mass, and PE-100 and PE-200 solutions, comparable by surface area. This applied for both fluoranthene and phenanthrene and suggests sorption of fluoranthene and phenanthrene to the respective MPs.

There was little difference in the fluoranthene and phenanthrene concentrations in solution with each MP at 10 and 20 °C. The fluoranthene concentration in all the MP samples were lower than the control sample. For phenanthrene, on the other hand, all the MP samples with PAH showed depletion except for the PE-200 and PE-100 solutions comparable by mass. Therefore, the uptake of phenanthrene to PE-100 and PE-200, in the mass-normalized solutions, wasn't calculated. The time-dependent uptake (CPE, µg/mg) of fluoranthene and phenanthrene to the different MPs, concentration comparable to mass, at 10 and 20 °C, are shown in Figure 3.5.

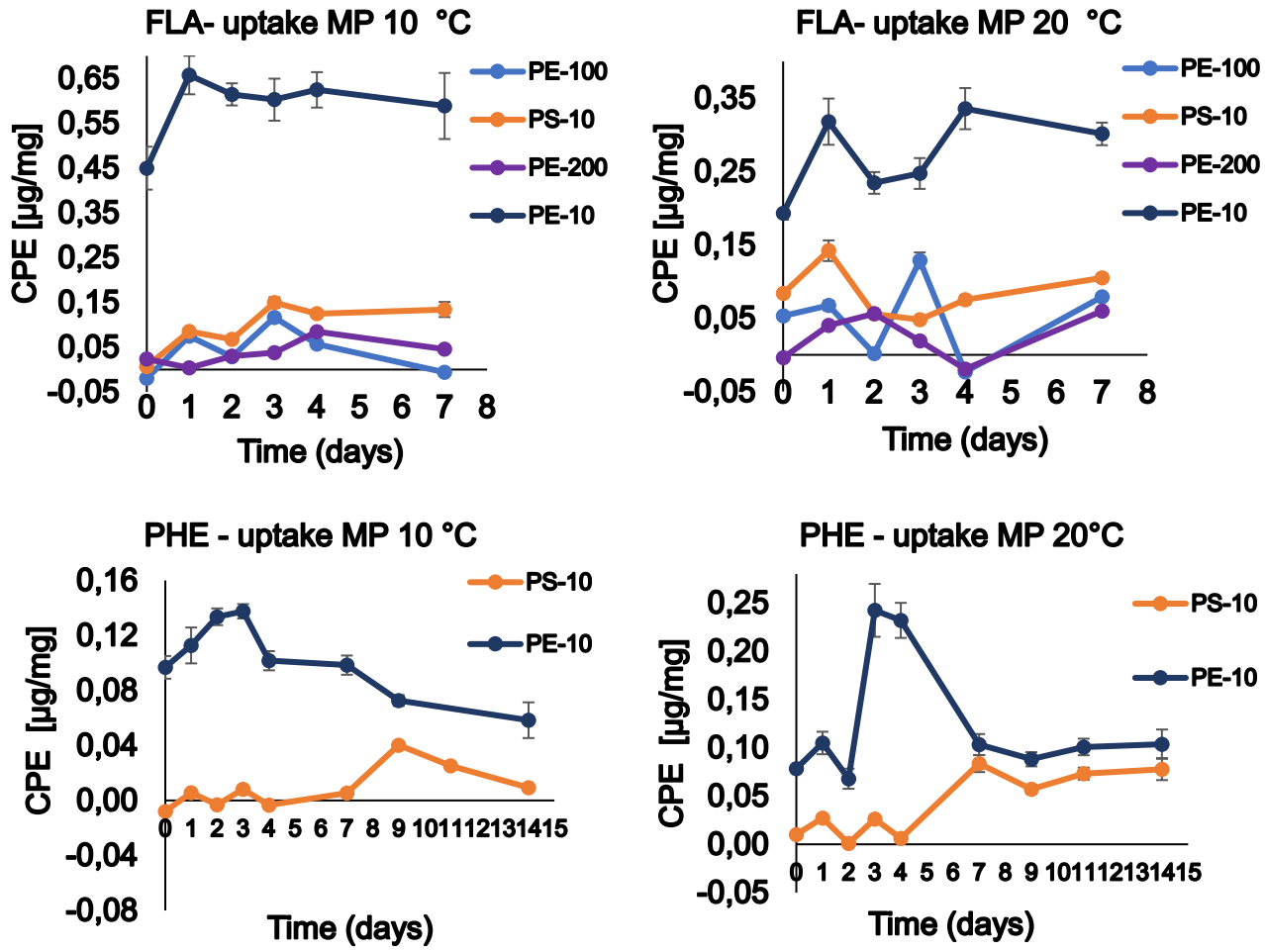

Figure 3.5. Uptake [µg/mg] of fluoranthene and phenanthrene to polyethylene (PE-10, PE-100, and PE-200) and polystyrene (PS-10), concentration comparable by mass, at 10 and 20°C. Error bars represent the standard deviation.

A clear result, at both temperatures, with concentrations comparable to mass, was the sorption of fluoranthene to PE-10 (Figure 3.5), being significantly higher than the sorption to PS-10, PE-100 and PE-200. PS-10, PE-100 and PE-200 had similar sorption levels amongst them, with PS-10 showing a slightly higher sorption. The sorption of phenanthrene to PE-10 was significantly higher than the sorption to PS-10.

Fluoranthene showed an overall higher sorption to PE-10 than did phenanthrene, and the sorption to the MP was higher at 10 °C for fluoranthene and about the same at 10 and 20 °C for phenanthrene (Figure 3.5). The other MPs showed similar sorption capacities at the two temperatures.

The time-dependent uptake (CPE, µg/mg) of fluoranthene and phenanthrene to the different MPs, concentration comparable to surface area, at 10 and 20 °C, are shown in Figure 3.6.

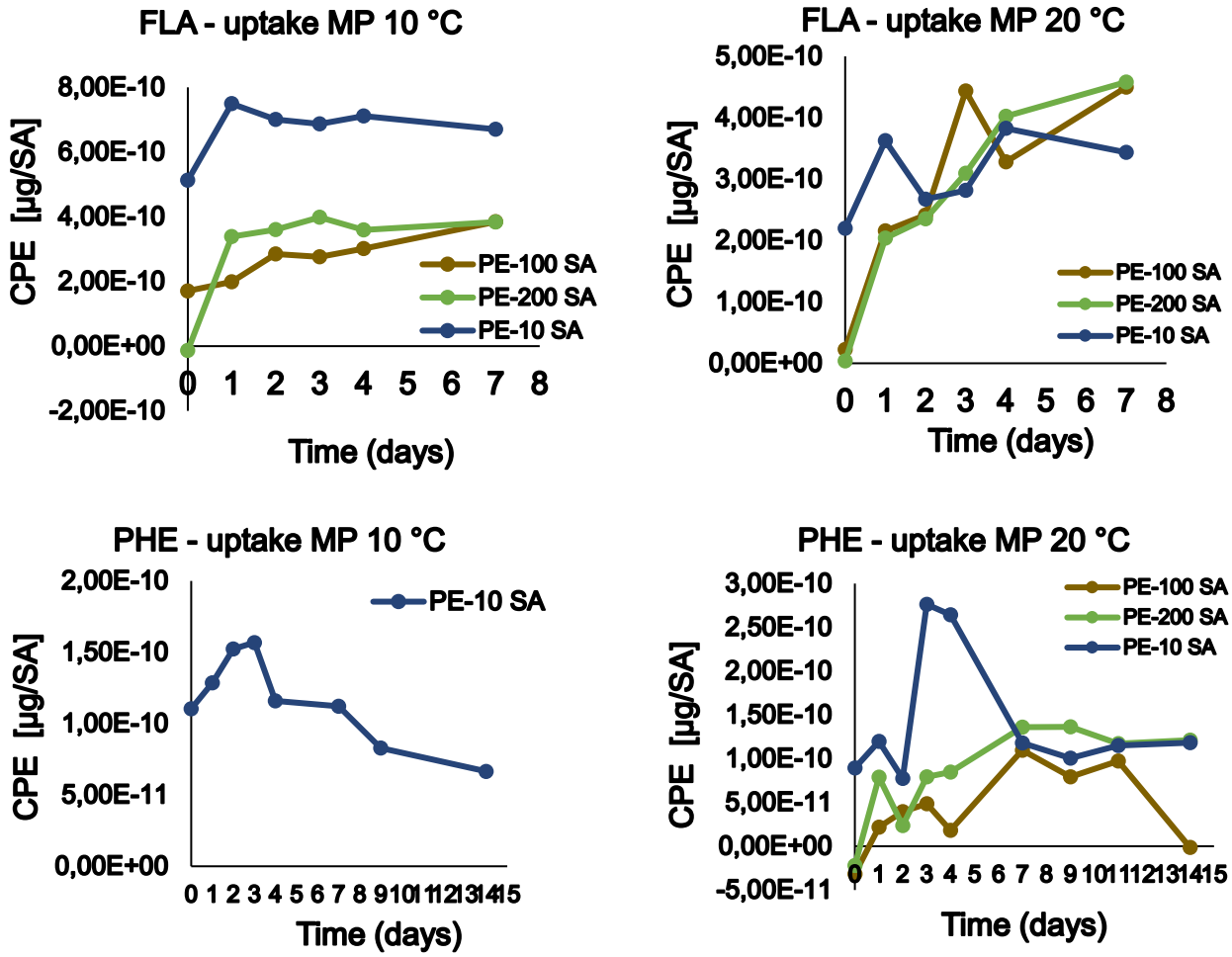

Figure 3.6. Uptake [µg/mg] of fluoranthene and phenanthrene to polyethylene (PE-10, PE-100, and PE-200) and polystyrene (PS-10), concentration comparable by surface area, SA, at 10 and 20°C.

PE-100 and PE-200, with concentrations comparable by surface area, had similar sorption patterns for both fluoranthene and phenanthrene at 20 °C (Figure 3.6). At 10 °C, the uptake of phenanthrene to PE-100 and PE-200, concentration comparable to surface area, showed negligible or negative values, meaning no significant/observable sorption. They were therefore not plotted in Figure 3.6.

At 10 °C fluoranthene and phenanthrene had a clearly higher sorption to PE-10, concentration comparable to surface area, than to PE-100 and PE-200 (Figure 3.6). At 20 °C, on the other hand, the sorption levels were almost identical for all three microplastics, except for PE-10 having a slightly higher sorption at the start. The overall sorption to PE-10, with concentration comparable by surface area, was higher for fluoranthene than for phenanthrene.

Based on the set of kinetics experiments, the equilibration times between MP and PAH in seawater determined for phenanthrene were 9 days at 10 °C and 7 days at 20 °C. Fluoranthene had an equilibration time of 5 days at both temperatures. The equilibration times were used as sampling points for the range-finding and isotherm studies.

It has previously been found that equilibration time generally increases with increasing hydrophobicity (Kim and Kwon, 2010). Fluoranthene, with a solubility in seawater of ~0,1 µg/L, has a lower water solubility than phenanthrene, having ~0,6 µg/L, therefore a higher hydrophobicity, meaning a higher affinity for the MPs. This can be the possible reason for fluoranthene having a shorter equilibration time than phenanthrene. Fluoranthene also has higher distribution coefficient values (explained in paragraph 3.4.2), explaining the lower equilibrium sorption times than for phenanthrene.

The sorption of phenanthrene at 10 °C had a longer equilibration time than at 20 °C. In line with this observation, it has previously been shown that sorption equilibrium time shortens at higher temperatures (Haftka et al., 2010). However, in the current study, the equilibration time for fluoranthene at the two temperatures was found to be the same.

3.3 Concentration-dependent sorption

3.3.1 Range-finding study

The range-finding study was conducted to find the appropriate concentration of MP to sufficiently reduce the concentration of PAHs in solution by approximately 50 %, at the range of PAH concentrations intended to be applied in the isotherm-study.

Table 3.4. Depletion of PAH relative to control sample (%) for fluoranthene (FLA) and phenanthrene (PHE) with the MPs of different concentrations. Where there were three replicates of the sample the average loss with its standard deviation is stated. For mass of each MP and concentration of fluoranthene and phenanthrene measured in each sample, see Appendix F.

Sample ID (MP concentration (mg/L))	PAH in sample	Loss of PAH relative to control sample (%)		
		100 % PAH	21 % PAH	5 % PAH
PE-10 (15)	PHE	17	*	3,0
PE-10 (30)	PHE	54±3	42	31
PE-10 (45)	PHE	59	66	45
PE-100 (150)	PHE	27	15	9,0
PE-100 (300)	PHE	27±8	53	15
PE-100 (450)	PHE	41	41	28
PE-100 (600)	PHE	43±4	na	na
PS-10 (11,5)	PHE	4,0	10	17
PS-10 (36,5)	PHE	19	15	27
PS-10 (109)	PHE	51±5	65	61
PE-10 (7,5)	FLA	87±22	na	na
PE-10 (15)	FLA	68	67	46
PE-10 (30)	FLA	81	74±2	64
PE-10 (45)	FLA	90	83	71
PE-100 (150)	FLA	37	17	*
PE-100 (300)	FLA	33	31±8	23
PE-100 (450)	FLA	33	30	27
PE-100 (600)	FLA	84±28	na	na
PS-10 (11,5)	FLA	16	*	*
PS-10 (36,5)	FLA	40	18	16
PS-10 (109)	FLA	41	52±15	*
PS-10 (328)	FLA	90±18	na	na

* The relative uptake was too low to be calculated.
na: not analysed.

A tendency (shown in Table 3.4) is a decrease in percentage sorbed fluoranthene and phenanthrene from the highest concentrations (100 %) of the PAHs to the lowest (5 %), and from the highest concentrations of the MPs to the lowest. The higher concentrations show a higher percentage of sorbed PAH to the MPs. The reason for

this may be that there is less percentage loss of PAHs to the glass walls when higher concentrations of PAHs. The glass walls become saturated. Sorption is not linearly dependent on PAH concentration.

PE-10 (15 mg/L), PE-100 (450 mg/L) and PS-10 (109 mg/L) all sufficiently reduce the concentration of fluoranthene in solution by approximately 50 % (Table 3.4) For phenanthrene PE-10 (30 mg/L) was necessary to obtain the desired depletion, while the same amounts of PE-100 and PS-10 as for fluoranthene were sufficient. These MP concentrations were thus applied in the isotherm study. The corresponding concentrations comparable by surface area were PE-10 (1,3E+10 μm^2/L), PE-100 (3,9E+10 μm^2/L) and PS-10 (8,3E+10 μm^2/L) for fluoranthene. For phenanthrene PE-10 (2,7E+10 μm^2/L) was applied, and the same amounts of PE-100 and PS-10 as for fluoranthene (Table 2.9). The ratio between the concentrations of PE-10, when comparable by surface area, were similar to the ratio when comparable by mass. Overall, there was a smaller difference in the concentrations when the concentrations were comparable by surface area.

3.3.2 Sorption isoterms

The experimentally determined solubility of PAHs was applied for the calculations of the isotherm equations, see Table 3.1. For mass of each MP and concentrations of fluoranthene and phenanthrene measured in each sample, see Appendix G.

Based on previous sorption mechanisms for polymer sorption (Hüffer and Hofmann, 2016, Bakir et al., 2012, Kah et al., 2011, Velzeboer et al., 2014, Teuten et al., 2007, Wang and Wang, 2018a, Wang and Wang, 2018b, Foo and Hameed, 2010), the sorption models chosen to fit the sorption isotherms in this study were Dubinin-Ashtakhov, Freundlich, Langmuir, Dual Langmuir and Redlich-Peterson. A multitude of other sorption models are available.

The Redlich-Peterson was specifically chosen because it is a hybrid between the Langmuir and the Freundlich model, fitting both the experimental data with lower and higher concentrations well, resulting in a possibly better fit than Langmuir and Freundlich separately.

Two error functions: mean weighed square error (MWSE) and the sum of square or errors (SSE), are proven to give good results (Shahmohammadi-Kalalagh and

Babazadeh, 2014, Sreńscek-Nazzal et al., 2015). The two studies show that the mentioned error functions result in the parameter set that produces the best overall isotherm fits. They are also found to be a better option to minimize the error distribution between the experimental data and the predicted model data. MWSE and SSE were therefore tested in the present master thesis.

The criteria for evaluating the goodness of fit are R^2, the error function and the visual fit between the calculated values and the experimental data. All in all, SSE gave the best results in the present master thesis. In general, the R^2 values were higher, the SSE was closer to zero, and the models fitted the experimental data better, fitting both the lower and higher concentrations. For further discussions SSE was therefore applied. See Table G.3 in Appendix G for values of MWSE and the corresponding fitting parameters for the various isotherm models.

Tables 3.5 and 3.6 show the fitted parameters and error of the chosen models for sorption isotherms of phenanthrene and fluoranthene to PE-10, PE-100 and PS-10 at 10 and 20 °C.

Table 3.5. Fitted parameters of the Freundlich, Langmuir, Dual Langmuir, Dubinin-Ashtakhov and Redlich-Peterson models for adsorption isotherms of fluoranthene to three types of MPs at 10 and 20 °C.

Freundlich

MP	*Kf* *([µg/mg]/[µg/L]^n)*	*n*	R^2	*SSE*
PE-10 10 °C	0,0290	1,97	0,9968	0,3570
PE-10 20 °C	0,106	1,11	0,9999	0,0877
PE-100 10 °C	2,0E-03	0,934	1,0000	3,999E-05
PE-100 20 °C	4,0E-03	0,821	0,9999	9,33E-05
PS-10 10 °C	0,0120	0,557	0,9999	0,0024
PS-10 20 °C	0,0120	0,757	0,9999	0,0071

Langmuir

MP	Q^0 [µg/mg]	K_L [L/µg]	R^2	*SSE*
PE-10 10 °C	2317	7,02E-05	0,9996	0,607
PE-10 20 °C	840	1,00E-04	0,9995	0,222
PE-100 10 °C	0,204	6,90E-03	1,000	3,99E-05
PE-100 20 °C	0,259	0,0120	0,9999	6,77E-05
PS-10 10 °C	0,0979	0,0941	0,9999	2,20E-03
PS-10 20 °C	0,185	0,0863	0,9999	5,50E-03

Dual Langmuir

MP	Q^0 [µg/mg]		K_L [L/µg]		R^2	*SSE*
	1	*2*	*1*	*2*		
PE-10 10 °C	2462	2465	3,48	3,13E-05	0,9996	0,607
PE-10 20 °C	1190	58961	0,000	1,91E-06	0,9991	0,254
PE-100 10 °C	7,00E-03	35,63	0,0560	2,92E-05	1,0000	3,98E-05
PE-100 20 °C	4,00E-04	0,260	0,000	0,0120	0,9999	6,77E-05
PS-10 10 °C	0,0680	0,0300	0,094	0,0930	0,9999	0,00220
PS-10 20 °C	48,7	3,0E-03	2,0E-04	262	0,9999	0,0133

Dubinin-Ashtakhov

MP	*Log Q^0 [µg/mg]*	*E (kJ/mol)*	*b*	R^2	*SSE*
PE-10 10 °C	24058	0,0220	0,288	0,9233	0,276
PE-10 20 °C	730	0,767	0,512	0,9946	0,0836
PE-100 10 °C	0,0335	5,83	1,03	0,9831	3,992E-05
PE-100 20 °C	0,172	6,43	1,08	0,9885	7,31E-05
PS-10 10 °C	0,0683	8,24	1,56	0,9720	2,40E-03
PS-10 20 °C	3,18	2,32	0,571	0,9773	0,0149

Redlich-Peterson

MP	a_r	K_R [L/µg]	B	R^2	*SSE*
PE-10 10 °C	0,0007	0,163	11,3	0,9996	0,607
PE-10 20 °C	0,000	0,133	2,32	0,9990	0,130
PE-100 10 °C	9,3E-03	1,3E-03	33,7	0,9999	4,26E-05
PE-100 20 °C	0,0128	2,7E-03	13,5	0,9999	8,07E-05
PS-10 10 °C	0,0410	5,2E-03	11,8	0,9999	9,00E-04
PS-10 20 °C	0,0526	9,9E-03	7,67	0,9999	1,40E-03

Table 3.6. Fitted parameters of the Freundlich, Langmuir, Dual Langmuir, Dubinin-Ashtakhov and Redlich-Peterson models for adsorption isotherms of phenanthrene to three types of MPs at 10 and 20 °C.

Freundlich

MP	*Kf* *([µg/mg]/[µg/L]^n)*	*n*	R^2	*SSE*
PE-10 10 °C	5,0E-03	1,27	0,9989	0,365
PE-10 20 °C	0,0370	0,686	0,9999	0,0420
PE-100 10 °C	2,0E-03	0,825	0,9999	5,00E-04
PE-100 20 °C	2,0E-03	0,721	0,9999	4,00E-04
PS-10 10 °C	0,0250	0,492	0,9999	0,0147
PS-10 20 °C	0,0300	0,552	0,9999	0,0114

Langmuir

MP	Q^0 [µg/mg]	K_L [L/µg]	R^2	*SSE*
PE-10 10 °C	161	9,92E-05	0,9999	0,459
PE-10 20 °C	1,31	0,0150	0,9999	0,0364
PE-100 10 °C	0,160	5,00E-03	0,9999	5,00E-04
PE-100 20 °C	185	4,00E-06	0,9999	8,00E-04
PS-10 10 °C	0,316	0,0310	0,9999	0,0136
PS-10 20 °C	0,412	0,0360	1,0000	6,7E-03

Dual Langmuir

MP	Q^0 [µg/mg]		K_L [L/µg]		R^2	*SSE*
	1	*2*	*1*	*2*		
PE-10 10 °C	5688	0,1	2,48E-06	2549	0,9971	0,584
PE-10 20 °C	1,31	0,000	0,015	2,90	0,9999	0,0364
PE-100 10 °C	5,0E-03	136	5039	3,22E-06	1,0000	6,00E-04
PE-100 20 °C	0,101	0,000	0,0130	1,00E-04	0,9999	3,00E-04
PS-10 10 °C	0,0240	0,337	5127	0,0180	1,0000	0,0124
PS-10 20 °C	0,000	0,412	12,0E+06	0,0360	1,0000	0,00670

Dubinin-Ashtakhov

MP	Log Q^0 [µg/mg]	*E (kJ/mol)*	*b*	R^2	*SSE*
PE-10 10 °C	44848	1,46E-07	0,0960	0,9713	1,63
PE-10 20 °C	1,12	10,2	1,76	0,9793	0,0363
PE-100 10 °C	0,0650	6,69	1,23	0,9631	5,00E-04
PE-100 20 °C	0,0650	10,0	2,34	0,9507	3,00E-04
PS-10 10 °C	0,262	9,95	1,50	0,9833	0,0131
PS-10 20 °C	0,359	12,0	2,39	0,9870	0,00690

Redlich-Peterson

MP	a_r	K_L [L/µg]	B	R^2	*SSE*
PE-10 10 °C	7,00E-04	0,0319	0,000	0,9999	0,455
PE-10 20 °C	0,0162	0,0205	0,937	0,9999	0,0364
PE-100 10 °C	9,3E-03	6,00E-04	33,7	0,9999	4,00E-04
PE-100 20 °C	0,0128	9,00E-04	13,5	0,9999	2,00E-04
PS-10 10 °C	0,0135	0,00630	1,79	0,9999	0,0131
PS-10 20 °C	0,0222	0,0117	1,45	0,9999	5,9E-03

Adsorption of phenanthrene and fluoranthene to PE-10, PE-100 and PS-10 at 10 and 20 °C and the fitted isotherm curves for the model best representing the data for each PAH+MP combination, are presented in Figures 3.7-3.9. C_{MP} is the adsorbed concentration and C_{free} is the equilibrium water phase concentration. Fitted curves of all the tested isotherm models are available in Figures G.1-G.10 in Appendix G.

3.3.2.1 Adsorption isotherms for PE-10 and PS-10

Of the tested isotherm models, the Redlich-Peterson equation gave the best fit for PS-10 (20 °C) for fluoranthene and phenanthrene (Figure 3.7). As shown in Tables 3.5 and 3.6 the Redlich Peterson didn't necessarily give the lowest SSE-values, but it had high R^2 values (>0,99) and a satisfactory fit between the calculated values and experimental data in all cases. The equation also included the lowest experimental data concentrations.

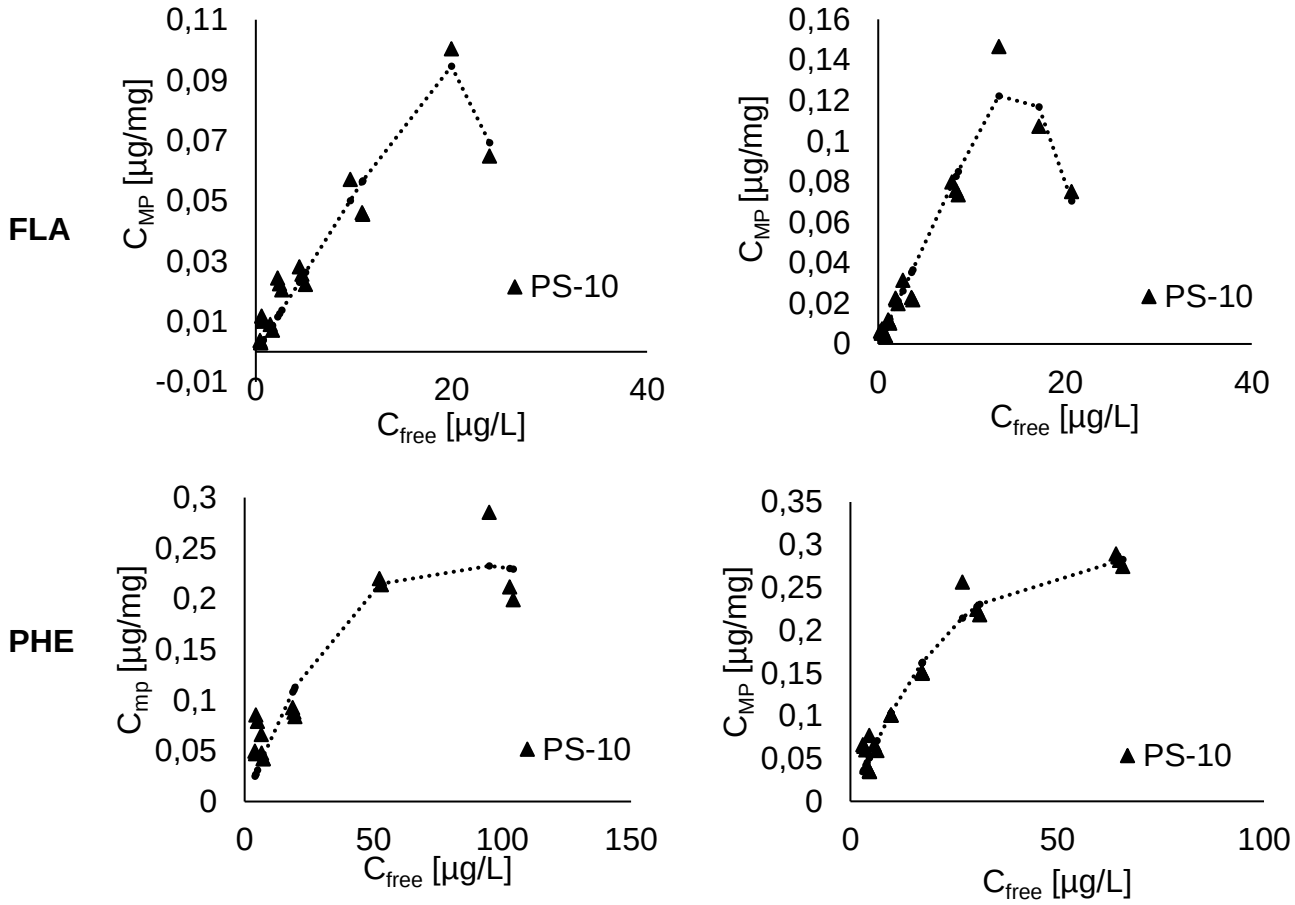

Figure 3.7. Adsorption isotherms of PS-10 at 10 °C (left) and 20 °C (right) to fluoranthene and phenanthrene, plotted as individual replicates. The dotted lines represent the fitting of the Redlich-Peterson model to the experimental data, with some "overfitting" for fluoranthene.

For PE-10 and PS-10, at 10 °C, the Dual Langmuir (Appendix G, Figure G.7), Freundlich (Appendix G, Figure G.5) and Redlich-Peterson (Figure 3.7) isotherm models gave a decent fit, with both fluoranthene and phenanthrene. The majority of the models showed R^2 values >0,99, the SSE values were similar within each MP type (~ 0,015 for PS-10 and ~0,6 for PE-10) and the fit between the calculated values and experimental data was good (Figures 3.7 and 3.8). The Redlich-Peterson equation showed a slightly lower SSE value though, hence most likely being the model giving the best fit. It can therefore be concluded that Redlich-Peterson was the appropriate model for the sorption to PS-10 (at both temperatures) and PE-10 (10 °C), and that a mixture of monolayer and multilayer adsorption might therefore be the dominant mechanism in the uptake of phenanthrene and fluoranthene by the two kinds of MPs at the given temperatures.

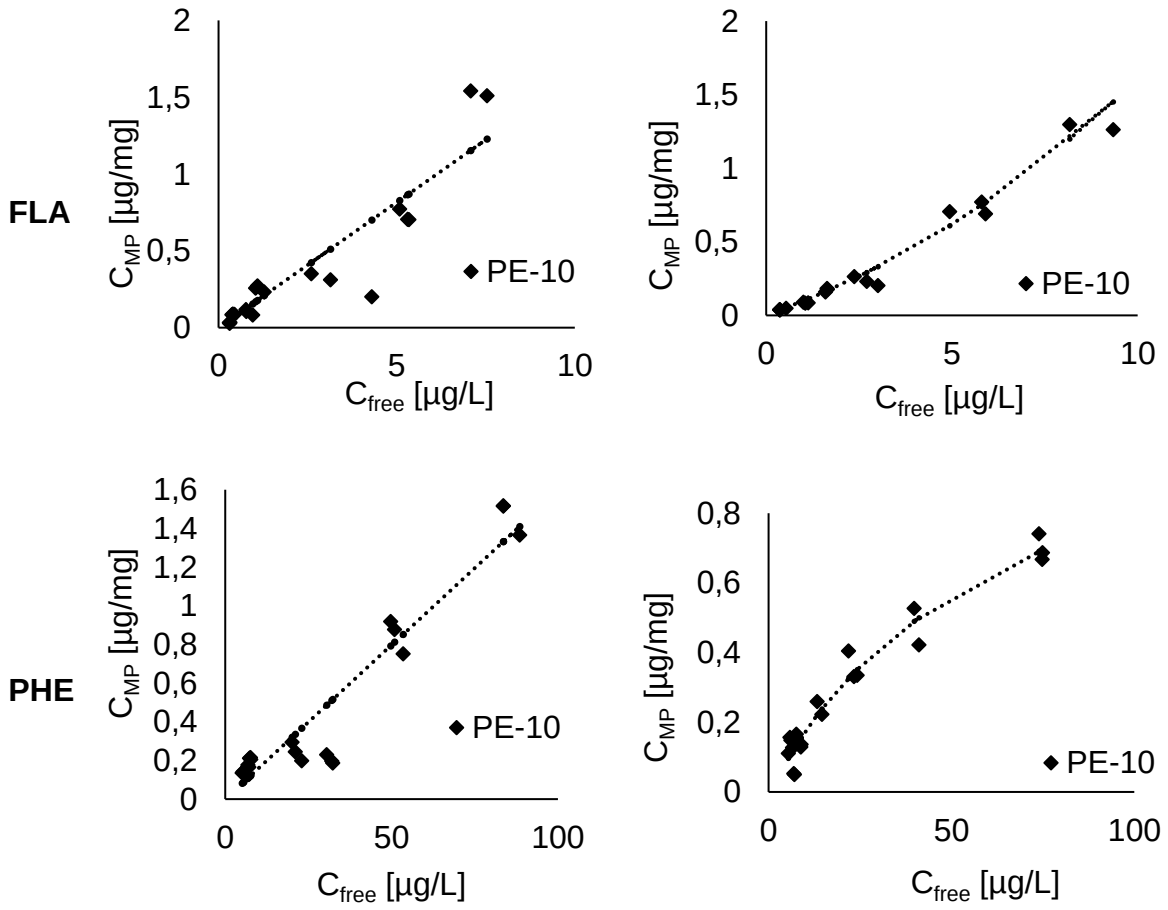

Figure 3.8. Sorption isotherms of PE-10 at 10 °C (left) to fluoranthene and phenanthrene, plotted as individual replicates. The dotted lines represent the fitting of the Redlich-Peterson model to the experimental data. Sorption isotherms of PE-10 at 20 °C (right), to fluoranthene and phenanthrene, plotted as individual replicates. The dotted lines represent the Dubinin-Ashtakhov fitted curves.

The higher B values (exponent related to the degree of pore filling), seen for PS-10 with fluoranthene (20 °C) and PS-10 and PE-10 with fluoranthene (10 °C) (Table 3.5), indicate that Redlich-Peterson model is approaching the Langmuir isotherm at low concentrations. The lower B values, seen for PS-10 with phenanthrene (20 °C) and PS-10 and PE-10 with phenanthrene (10 °C) (Table 3.6), indicate that Redlich-Peterson model is approaching the Freundlich isotherm at high concentrations. This is supported by the fact that the equation is a hybrid between Langmuir and Freundlich (Gimbert et al., 2008, Foo and Hameed, 2010).

The Dubinin-Ashtakhov model gave the best fit for PE-10 at 20 °C (Figure 3.8). It didn't give the highest R^2 values, but it gave the lowest SSE-values (Table 3.5 and 3.6) and a good fit between the calculated values and experimental data. Dubinin-Ashtakhov was therefore the most appropriate model for the PE-10 (20 °C), indicating that adsorption in to the micropores might be the dominant mechanism in the uptake of fluoranthene and phenanthrene by PE-10 at 20 °C (Hutson and Yang, 1997). PE-10 might therefore have a possible difference in properties at the two temperatures, being softer and more receptive and vulnerable at 20 °C. It is speculated that at 10 °C PE-10 might be 'harder', with less chance of sorption into surface micropores being the dominant mechanism in the uptake of fluoranthene and phenanthrene.

A trend seen throughout all the non-linear isotherm models was that PE-10 exhibited an overall higher adsorption capacity than PS-10 (~ 1,5 µg/mg), see graphs in Figure 3.7 and 3.8.

It was observed no significant differences in the sorption capacity of phenanthrene and fluoranthene to PS-10 at 10 and 20 °C (Figure 3.7). As for PE-10 a similar trend for sorption capacity at the two temperatures was observed for fluoranthene. For phenanthrene the sorption capacity increased at 10 °C. It is difficult to know the actual cause for the difference in sorption capacity at the two temperatures, whether it being the use of two different models, or if it is because of the water solubility being lower at 10 °C, therefore leading to a larger amount of phenanthrene being sorbed to PE-10.

There was no significant trend in the difference of sorption capacity at 10 and 20 °C for the isotherm models in general (Figures G.1-G.10 and Appendix G).

3.3.2.2 Adsorption isotherms for PE-100

From the basis of the initial, non-linear, isotherm fits (Figures G.1-G.10 in Appendix G) for PE-100 using the above-discussed models, it was observed that the sorption of fluoranthene and phenanthrene to the MP had a linear tendency. Therefore, the linear sorption isotherm was tested for this MP. It turned out that the linear sorption isotherm gave lower SSE-values than the other isotherms tested for this MP, and high R^2 values (>0,99). See Table 3.7 for the fitted parameters of the linear model for sorption isotherms of phenanthrene and fluoranthene to PE-100 at 10 °C and 20 °C.

Table 3.7. Fitted parameters of the linear model for sorption isotherms of phenanthrene and fluoranthene to polyethylene (PE, 100 µm) at 10 and 20 °C.

Linear model				
MP	**PAH**	***K [L/µg]***	***R^2***	***SSE***
PE-100 10 °C	**FLA**	1,3E-04	0,9999	4,26E-05
PE-100 20 °C	**FLA**	0,000	0,9999	8,07E-05
PE-100 10 °C	**PHE**	5,00E-04	0,9999	6,00E-04
PE-100 20 °C	**PHE**	7,00E-04	0,9999	8,00E-04

The linear isotherm equation also fitted the lowest experimental data concentrations and gave the best fit between the calculated values and experimental data for PE-100 at both temperatures, for both fluoranthene and phenanthrene. The linear isotherm model was therefore observed to give the best fit for PE-100 at both temperatures, and for both pollutants. This is consistent with a previous review on sorption to polyethylene (10-180 µm) conducted by Velzeboer et al. (2014), where also here the linear isotherm model fitted the experimental data best. According to another review though, the Langmuir isotherm fitted the experimental data for sorption to PE (100-150 µm) best (Wang and Wang, 2018b).

See Figure 3.9 for the linear sorption isotherms of phenanthrene and fluoranthene to PE-100 at 10 °C and 20 °C, and the isotherm fitted curves. There has been conducted little research regarding the kind of sorption of PAHs to PE-100, but a possible sorption mechanism, observed in the present study, of fluoranthene and phenanthrene to PE-100 may be absorption due to the linear sorption isotherm giving a good fit.

Based on the results in the present study, the main sorption mechanism of fluoranthene and phenanthrene to PE-10 was indicated to be monolayer and multilayer adsorption, and adsorption in to the surface micropores. For PE-100, the main mechanism appears to be absorption. The reason for this difference might be the difference in size between the two particles. PE-100, having higher molecular weight, might be softer, having larger pore sizes, leading to possible absorption of fluoranthene and phenanthrene in to the polymer.

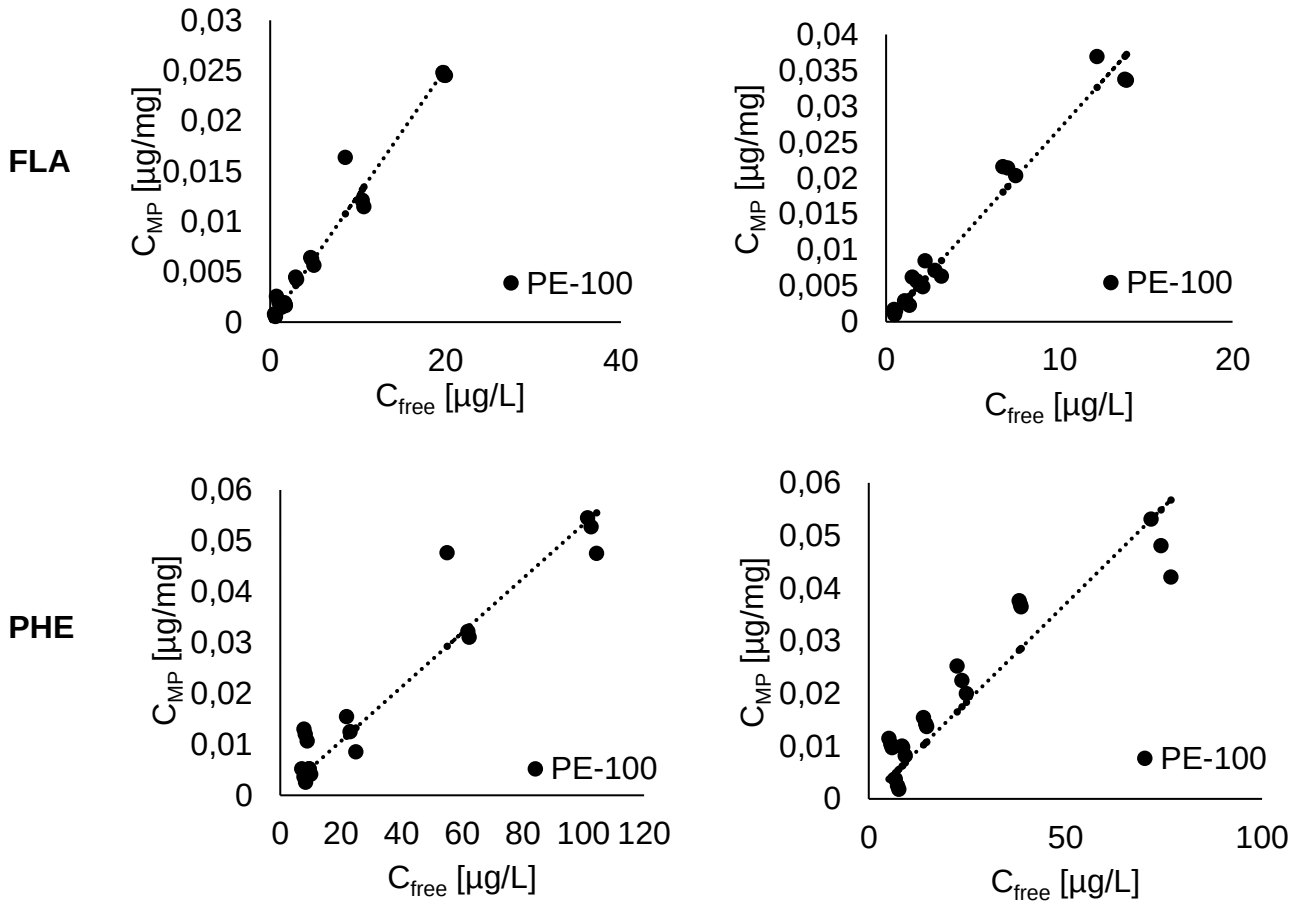

Figure 3.9. Adsorption isotherms of PE-100 at 10 °C (left) and 20 °C (right) to fluoranthene and phenanthrene, plotted as individual replicates. The dotted lines represent the fitting of the linear model to the experimental data.

3.4 General discussion of the results as a whole

3.4.1 Mass vs surface area (SA)

In environmental studies with anthropogenic particles a common question is what metric is best used to describe their behaviour when it comes to toxicity and interaction with other components in a dispersion (Syberg et al., 2015, Rushton et al., 2010). In the current study, the metrics mass and surface area for describing sorption of PAHs to MPs was investigated using different sizes and concentrations of PE-particles. Different sizes of PE (100 µm and 200 µm) in addition to PS-10 was included. Using PE-10 as a reference, the amounts of PE-100 and PE-200 were varied to keep either MP mass or surface area constant in the exposure solutions with different MPs.

Figures 3.5 and 3.6 show the uptake of fluoranthene and phenanthrene to PE (10, 100 and 200 µm) and PS (10µm), with concentrations comparable to mass, and the uptake of fluoranthene and phenanthrene to polyethylene (10, 100 and 200 µm), with concentrations comparable to surface area. The sorption of PAHs increased in the order PE-10>PS-10>PE-100/PE-200 per mass and PE-10>PE-100/200 per surface area of the polymers. The results are coherent: for both mass and surface area PE-10 show the highest sorption. PE-10 has the smallest mass of all the MPs, but the largest surface area (Table 2.3). Thus, both surface area and mass are important factors for the sorption of PAHs to MPs. PS-10 has the second largest surface area and mass (Table 2.3), coming also second in the sorption capacity.

Whether talking about adsorption or absorption an important point is that the PAHs are only available to the MPs at the surface of the MPs. A bigger surface area results in higher adsorption of the PAHs to MPs and an increased availability of the PAHs to absorb in to the MP. With a larger mass (volume) a larger amount of PAH can also penetrate into the MP. Both the mass and surface area therefore play important roles on the sorption of PAHs to MPs.

In sorption kinetics experiment 3 the concentrations of fluoranthene and phenanthrene in the samples with the MPs, with concentrations both comparable by mass and surface area (Figure 3.4), are lower than the concentrations in the control samples. However, the samples with PE-100 and PE-200, concentrations compared by surface area, showed a lower concentration of PAH than did the samples with concentrations comparable by mass. This can indicate that the surface area plays a slight larger role

in the sorption of PAHs to MPs. Another case is the linear sorption isotherm giving a good fit for the sorption of PAHs to PE-100 (Figure 3.9). This possibly indicating absorption as the main sorption mechanism, and potentially meaning that mass plays a larger role in the sorption of PAHs to PE-100 than surface area. A bigger mass gives a bigger volume for the PAHs to absorb into the MP.

3.4.2 Polymer type

In the current study, two MPs of similar size, but different polymer composition, was included (PE-10 and PS-10). A trend seen throughout the experiments was that PE-10 had higher sorption capacity than PS-10, independent of temperature, PAH and the concentrations of the MPs being comparable to surface area or mass.

Of all the polymer types PE and PS have shown to have the highest sorption capacities of PAHs (Teuten et al., 2007, Rochman et al., 2013, Bakir et al., 2014, Wang and Wang, 2018b). These studies involve size ranges of polymers that are larger than the MPs applied in the present study but can still give a good indication of the sorption capacities of the different polymers. A study based specifically on the sorption to micro-sized plastic particles, however, show that PS and PE showed similar sorption capacities, PS having slightly higher values (Hüffer and Hofmann (2016)). In the latter study the polymers applied were smaller than 250 µm, thus, larger than the MPs used in this study, and the findings didn't reflect the particle sizes of the MPs. In the present study the trend for uptake of phenanthrene and fluoranthene to PE-10 and PS-10 showed higher sorption to PE-10. This order, however, can reflect the particle sizes, PE-10 being larger than PS-10.

Figure 3.10 shows scanning electron microscopy (SEM) images of pristine PS and PE, 10 µm. The two MPs show a clear difference in shape and morphology. There is a large variation in shape of the PE-10 particles. In contrast the PS-10 particles are smoother and more spherical. Looking at the images one can imagine a higher sorption capacity to PE-10 because of the possible ability to change form and therefore be more receptive to the PAHs.

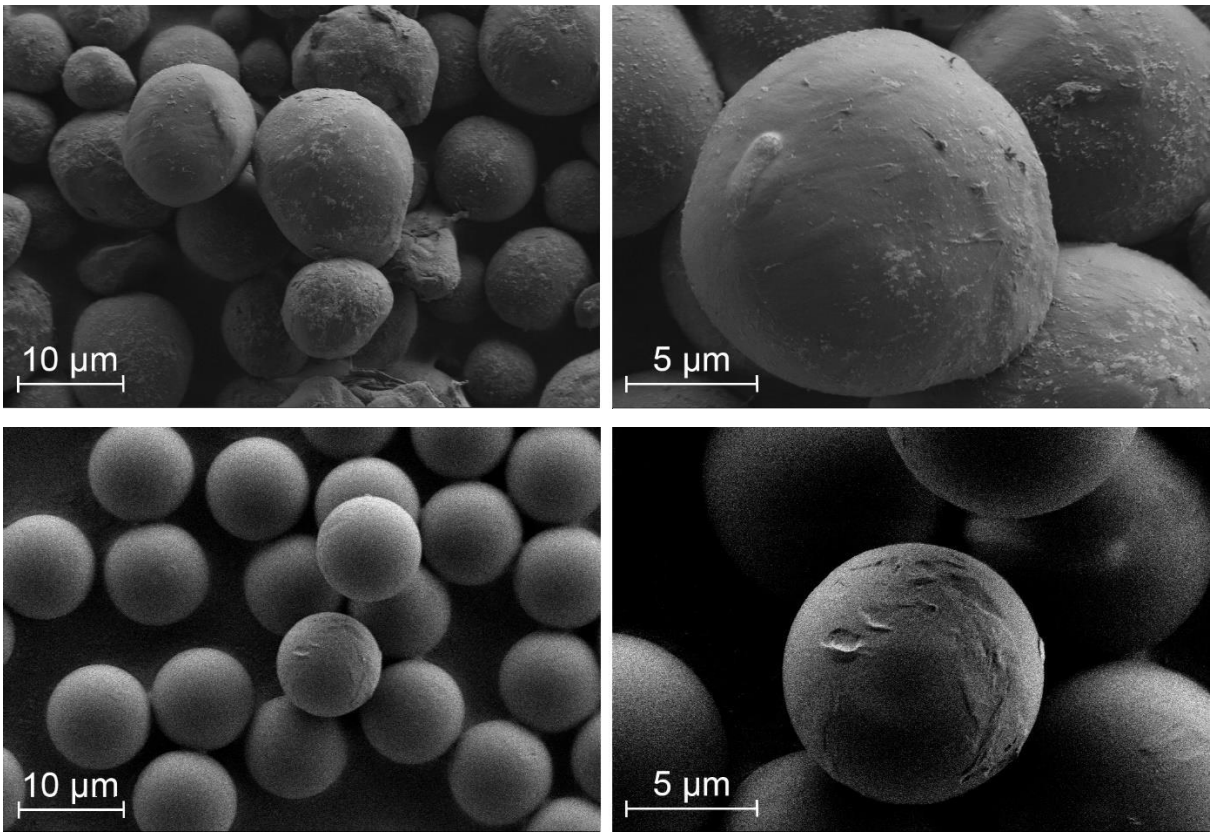

Figure 3.10. Top: SEM images of pristine polyethylene (10 µm), bottom: SEM images of pristine polystyrene (10 µm). Images taken with at 2000x (left) and 5000x (right) magnification. Image by: Marion Olsen Hepsø (2016).

Another explanation for why PE-10 showed an overall higher sorption capacity than PS-10 in the present study is the distribution coefficients (K_d-values). The K_d-value is the distribution (or partitioning) coefficient between the seawater and the MPs. Lee et al. (2014) measured partition coefficients (K_{MPSW}) between PE and seawater for eight PAHs, phenanthrene and fluoranthene being two of them. Temperature details were not mentioned. The partition coefficients for phenanthrene, fluoranthene and seawater were found to be high, implying high sorption capacity of MPs. Looking at Table 3.5 and 3.6 PE-10 had the highest distribution coefficients (>0,1500 µg/L) when comparing the distribution coefficients (K_d-values) for PS-10 and PE-10 fitted to the Redlich-Peterson isotherm. This indicates a possibly higher sorption capacity for the latter MP. In addition Voice et al. (1983) have shown that there is an increase in partitioning as solids concentration decreases. PS had a higher concentration than PE (Table 2.9), supporting the findings in the latter study.

There has not been conducted a lot of research within the sorption of PAHs to polyester (PES). Unfortunately, rather little can be concluded from the results given in this study.

PES, like PE and PS, gave no difference in the concentration of PAH in the sample relative to the control sample in sorption kinetic experiment 1 (Figure 3.1) and was not applied in the further experiments.

3.4.3 PAH

Based on available literature and physicochemical properties, it is expected that the degree of sorption of the three PAHs included in the study may differ. Fluoranthene, phenanthrene and 1,3-dimethylnaphthalene have different water solubilities, indicating different degrees of sorption to the MPs.

In the present study it was observed a significant uptake of fluoranthene and phenanthrene to MPs (Figures 3.3, 3.5 and 3.6). 1,3-Dimethylnaphthalene has a higher water solubility than fluoranthene and phenanthrene (table 1.2), indicating in general that a higher amount of the chemical remains in the seawater, and that the sorption on to the MP is minimal. 1,3-Dimethylnaphthalene has in other words a higher affinity to the seawater. The lower the water solubility, which is the case for phenanthrene and fluoranthene, the higher the possibility of sorption to the MPs.

In general, fluoranthene showed a higher sorption capacity to the MPs then did phenanthrene. For example, in uptake kinetics experiment nr 3, fluoranthene showed a higher sorption to PE-10 than did phenanthrene; 0,10 µg/mg for phenanthrene and 0,45 (10 °C) and 0,20 (20 °C) for fluoranthene (Figure 3.5).

For the linear sorption of fluoranthene and phenanthrene to PE-100 at 10 °C the K_d-values are higher for fluoranthene (Table 3.7), resulting in fluoranthene absorbing more readily to PE-100 than phenanthrene.

3.4.4 Temperature

Previous literature has shown little research on the impact temperature has on the sorption of PAHs to MPs. We do however know that the water solubilities of PAHs differ at the different temperatures, possibly altering the sorption capacity of the given PAH to the MP. An overall trend in the sorption at the two temperatures, 10 and 20 °C, was observed. The uptake at 10 °C exceeded the uptake at 20 °C.

In the sorption kinetic experiments, both fluoranthene and phenanthrene had the highest sorption at 10 °C (Figures 3.3, 3.5 and 3.6). The water solubility of fluoranthene and phenanthrene is lower at 10 °C (Table 3.1), resulting in a larger amount of the PAHs being sorbed to the MPs at 10 °C. Also, the equilibrium sorption decreases with increased temperature, minimalizing the sorption capacity at higher temperatures (ten Hulscher and Cornelissen, 1996).

The isotherm models fitted to the experimental data (Figures 3.7-3.9), on the other hand, showed a minimal difference in uptake between the two temperatures. A possible reason is that all the samplings took place at 20 °C, giving the PAHS in the samples at 10 °C the opportunity to show slight changes in their sorption activity, approaching the sorption capacity of 20 °C.

Temperature can have a significant effect on the distribution/partitioning coefficient (K_d-values) (Tremblay et al., 2005), effecting the sorption capacities. The K_d-value generally increases with decreasing temperature, altering the sorption capacity (Lüers and Ten Hulscher, 1996). In this study the K_d-values, determined from the Redlich-Peterson equation for PS-10 and 10 and 20 °C, were higher at 20 °C (Tables 3.5 and 3.6), not corresponding to the findings elsewhere in this research area. Also, the K_d values, determined from the linear regression method for PE-100 at 10 and 20 °C, were higher at 20 °C (Table 3.7). The influence of temperature on the distribution/partition coefficient seems to be dependent on the kind of solution which is partitioned and on the polymer concentration. PAHs have lower aqueous solubilities at 10 °C, a fraction of fluoranthene and phenanthrene may therefore have been present as crystals, resulting in an overestimation of aqueous concentrations, giving lower K_d-values and therefore lower sorption capacities than at 20 °C (Muijs and Jonker, 2009).

3.5 Implications of results

In this study fluoranthene and phenanthrene have shown to sorb on to MPs, altering, among other things, the concentrations and transport of PAHs in the water phase, and also the bioavailability of PAHs to marine organisms. The results in the present master thesis therefore suggest important roles of MPs debris in the marine environment.

MPs are released in the oceans of the world, leading to the possible sorption of polycyclic aromatic hydrocarbons. These MPs can then be taken up/ingested by

marine organisms from the surrounding aqueous environment, transferring the PAHs to the organisms. The PAHs can potentially become bioavailable to the organisms, interfering with processes and mechanisms in the body. The marine organism can die from hunger from the microplastics themselves or from the toxicity the PAHs imply on the body.

High sorption capacity of PAHs to microplastics can also affect the transport of PAHs in the marine environment. Where desorption is available the PAHs can instead be sorbed and easily transported in to organisms. The sorption to MPs can retard its transport.

Looking at it differently the MPs can also actually ‘’save’’ the organism from the toxicity the PAH can inflict, putting aside the fact that the MPs themselves can interfere with the organisms. The bioavailability of the PAHs, and their dissolved concentration, can be decreased due to the MPs. A possible solution can be to investigate the possibilities of capturing the MPs in the ocean, with the PAHs sorbed to them, thus, reducing the potential toxicity the PAHs, and the damage the MPs themselves, can inflict on the marine organisms.

4 Conclusions and recommendations for future work

4.1 Conclusions

The objective of this study was to study sorption behaviour of three polycyclic aromatic hydrocarbons (PAHs); 1,3-dimethylnaphthalene, fluoranthene and phenanthrene to different microplastics (MPs) polymers; polyethylene (PE), polystyrene (PS) and polyester (PES). The study took place at 10 and 20 °C, two realistic environmentally temperatures. Sorption equilibration times and isotherms were determined for the different pairings.

The equilibration times were found to be 5 days for fluoranthene, 9 days for phenanthrene at 10 °C and 7 days for phenanthrene at 20 °C, irrespective of polymer type and size used in the current experiments.

Sorption of phenanthrene and fluoranthene to the MPs were found to be highly polymer and PAH specific. It was shown that fluoranthene and phenanthrene sorb on to MPs. The partitioning of 1,3-dimethylnaphthalene to the MPs showed negligible or negative values, and sorption could therefore not be observed. PE-10 and fluoranthene had the largest sorption capacities of the MPs and the PAHS, respectively.

Non-linear isotherm models were fitted to the microplastics, and the best fit was based on the lowest values of the error function, SSE, the R^2 value and how the calculated data fitted the experimental data. These parameters were evaluated together. The Redlich-Peterson equation gave the best fit for PE-10 at 10 °C, and PS-10 at 10 and 20 °C. The Dubinin-Ashtakhov equation gave the best fit for PE-10 at 20 °C. PE-10 and PS-10 had therefore adsorption as their main sorption process, the Redlich-Peterson being a hybrid between the Langmuir and Freundlich equation, implying both monolayer and multilayer sorption, and the Dubinin-Ashtakhov, indicating that adsorption in to the micropores might be the dominant mechanism in the uptake of fluoranthene and phenanthrene.

It was observed that PE-100, at both temperatures had sorption isotherms that could be described by linear regression. The linear model gave the best fit, thus indicating PE-100 having absorption of PAHs as the possible main sorption process.

The lowest concentrations of fluoranthene and phenanthrene used in this study are relevant for the amounts of the PAHs present in seawater, as the water masses in the ocean are huge compared to the amount of PAH present. As for the microplastics, on

the other hand, the concentrations applied in this study are much larger than the amount actually present in the marine environment per litre. However, this study still gives a realistic picture of the sorption mechanisms between PAHs and MPs.

4.2 Recommendations for future work

In laboratory-based experiments, as the present master thesis was, complex marine situations are simplified and represented by a constant solution environment in terms of salinity and temperature. The advantages are that the conditions can be modified to study the influence of various parameters. On the other hand, laboratory-based experiments can fail to simulate the dynamic and complex marine environment realistically. For example, not all the PAHs in the solution may sorb only to MPs, but to other organic materials as well, and there are varying concentrations of MPs in the environment. MPs are also transported between locations with varying PAH concentrations and varying and fluctuating temperatures. The results achieved must therefore be used with caution.

In this study two analysis methods, GC-MS and LC-UV, were applied in the sorption isotherms study. This was necessary due to the different concentrations of fluoranthene and phenanthrene needed to be analysed. It is questioned if the use of two methods within the same study should be avoided in future studies, giving slightly non-corresponding results.

4.3 Future work

In the present master thesis, polymers in the form of beads and fibres were investigated. Also, in this study only three polymer types were applied. Polymers in the form of flakes, and polymer types other than PE, PS and PES, might have different sorption behaviours, thus playing a different role in the marine environment. More investigation can easily be implemented to this field.

This study includes only the sorption of PAHs to MPs at 10 and 20 °C, in seawater. Different temperatures may alter the effects on the sorption of PAHs to MPs. Seawater has a significantly higher salinity than freshwater, also altering the sorption capacities to MPs. There can be done more research in this field.

Polyester also demands closer research. It is known that the mentioned MP can end up in the marine environment, but their sorption processes to MPs and other organic material is yet rather unknown.

The partition/distribution coefficients (K_d-values) of the sorption of PAHs to the different MPs can also with advantage be investigated to a further extent. This will be helpful for a wider understanding, and for monitoring, the global and local distribution of PAHs using MPs as samplers. Desorption of solutes from sorbents is not studied in the present master thesis but plays an important role in the bioavailability of PAHs to marine organisms, and thus needs further investigation.

Little research is done on the bioavailability of the PAHs to the marine organisms. We do know that the PAHs sorb on to MPs, and that the organisms ingest the MPs, but there is conducted little research on whether the PAHs are released to the organism's stomach and intestines or not.

5 References

ANDRADY, A. L. 2011. Microplastics in the marine environment. *Marine Pollution Bulletin,* 62**,** 1596-1605.

ANDRADY, A. L. 2015. Persistence of plastic litter in the oceans. *Marine anthropogenic litter.* Springer.

ANDRADY, A. L. 2017. The plastic in microplastics: A review. *Marine Pollution Bulletin,* 119**,** 12-22.

ANDRADY, A. L. & NEAL, M. A. 2009. Applications and societal benefits of plastics. *Philosophical Transactions of the Royal Society B: Biological Sciences,* 364**,** 1977-1984.

ANTONIO GRASSI, P. 2017. *Effects of light intensity on motility three species of copepods: Acartia tonsa, Calanus Finmarchicus and Temora Longicornis.* Master, University of OSlo

BAKIR, A., ROWLAND, S. J. & THOMPSON, R. C. 2012. Competitive sorption of persistent organic pollutants onto microplastics in the marine environment. *Marine Pollution Bulletin,* 64**,** 2782-2789.

BAKIR, A., ROWLAND, S. J. & THOMPSON, R. C. 2014. Enhanced desorption of persistent organic pollutants from microplastics under simulated physiological conditions. *Environmental Pollution,* 185**,** 16-23.

BARBOZA, L. G. A., FRIAS, J., P.G.I, BOOTH, A. M., VIEIRA, L. R., MASURA, J., BAKER, J., FOSTER, G. & GUILHERMINO, L. 2017. Marine pollution by microplastics: Environmental contamination, biological effects, and research challenges. *World seas, an environmental evaluation.*

BARNES, D. K., GALGANI, F., THOMPSON, R. C. & BARLAZ, M. 2009. Accumulation and fragmentation of plastic debris in global environments. *Philosophical Transactions of the Royal Society B: Biological Sciences,* 364**,** 1985-1998.

BASHEER, C., OBBARD, J. P. & LEE, H. K. 2005. Analysis of persistent organic pollutants in marine sediments using a novel microwave assisted solvent extraction and liquid-phase microextraction technique. *Journal of Chromatography A,* 1068**,** 221-228.

BLAXTER, J. H., DOUGLAS, B., TYLER, P. A. & MAUCHLINE, J. 1998. *The biology of calanoid copepods*, Academic Press.

BOJES, H. K. & POPE, P. G. 2007. Characterization of EPA's 16 priority pollutant polycyclic aromatic hydrocarbons (PAHs) in tank bottom solids and associated contaminated soils at oil exploration and production sites in Texas. *Regulatory Toxicology and Pharmacology,* 47**,** 288-295.

BOOIJ, K., HOFMANS, H. E., FISCHER, C. V. & VAN WEERLEE, E. M. 2003. Temperature-dependent uptake rates of nonpolar organic compounds by semipermeable membrane devices and low-density polyethylene membranes. *Environmental Science & Technology,* 37**,** 361-366.

BREIVIK, K., ALCOCK, R., LI, Y.-F., BAILEY, R. E., FIEDLER, H. & PACYNA, J. M. 2004. Primary sources of selected POPs: regional and global scale emission inventories. *Environmental Pollution,* 128**,** 3-16.

BROWNE, M. A. 2015. Sources and pathways of microplastics to habitats. *Marine anthropogenic litter.* Springer.

BROWNE, M. A., CRUMP, P., NIVEN, S. J., TEUTEN, E., TONKIN, A., GALLOWAY, T. & THOMPSON, R. 2011. Accumulation of microplastic on shorelines woldwide: sources and sinks. *Environmental science & technology,* 45**,** 9175-9179.

BROWNE, M. A., GALLOWAY, T. & THOMPSON, R. 2007. Microplastic—an emerging contaminant of potential concern? *Integrated environmental assessment and Management,* 3**,** 559-561.

CASARETT, L. J., DOULL, J. & KLAASSEN, C. D. 2013. *Casarett and Doull's Toxicology: the basic science of poisons* New York McGraw-Hill Medical

CHEN, A. 2015. *Here's how much plastic enters the ocean each year* [Online]. Science [Accessed].

CHEN, S. & YANG, R. 1994. Theoretical basis for the potential theory adsorption isotherms. The Dubinin-Radushkevich and Dubinin-Astakhov equations. *Langmuir,* 10**,** 4244-4249.

COLE, M. 2016. A novel method for preparing microplastic fibers. *Scientific reports,* 6**,** 34519.

COLE, M., LINDEQUE, P., FILEMAN, E., HALSBAND, C., GOODHEAD, R., MOGER, J. & GALLOWAY, T. S. 2013. Microplastic ingestion by zooplankton. *Environmental science & technology,* 47**,** 6646-6655.

COLE, M., LINDEQUE, P., HALSBAND, C. & GALLOWAY, T. S. 2011. Microplastics as contaminants in the marine environment: A review. *Marine Pollution Bulletin,* 62**,** 2588-2597.

CÓZAR, A., ECHEVARRÍA, F., GONZÁLEZ-GORDILLO, J. I., IRIGOIEN, X., ÚBEDA, B., HERNÁNDEZ-LEÓN, S., PALMA, Á. T., NAVARRO, S., GARCÍA-DE-LOMAS, J. & RUIZ, A. 2014. Plastic debris in the open ocean. *Proceedings of the National Academy of Sciences,* 111**,** 10239-10244.

DESFORGES, J.-P. W., GALBRAITH, M. & ROSS, P. S. 2015. Ingestion of microplastics by zooplankton in the Northeast Pacific Ocean. *Archives of environmental contamination and toxicology,* 69**,** 320-330.

DRIS, R., GASPERI, J., MIRANDE, C., MANDIN, C., GUERROUACHE, M., LANGLOIS, V. & TASSIN, B. 2017. A first overview of textile fibers, including microplastics, in indoor and outdoor environments. *Environmental Pollution,* 221**,** 453-458.

DUBININ, M. I. 1975. Physical adsorption of gases and vapors in micropores. *Progress in surface and membrane science.* Elsevier.

ENDO, S., GRATHWOHL, P. & SCHMIDT, T. C. 2008. Absorption or adsorption? Insights from molecular probes n-alkanes and cycloalkanes into modes of sorption by environmental solid matrices. *Environmental science & technology,* 42**,** 3989-3995.

ENDO, S., YUYAMA, M. & TAKADA, H. 2013. Desorption kinetics of hydrophobic organic contaminants from marine plastic pellets. *Marine pollution bulletin,* 74**,** 125-131.

FOO, K. Y. & HAMEED, B. H. 2010. Insights into the modeling of adsorption isotherm systems. *Chemical Engineering Journal,* 156**,** 2-10.

FRIAS, J., OTERO, V. & SOBRAL, P. 2014. Evidence of microplastics in samples of zooplankton from Portuguese coastal waters. *Marine Environmental Research,* 95**,** 89-95.

FRIAS, J., SOBRAL, P. & FERREIRA, A. 2010. Organic pollutants in microplastics from two beaches of the Portuguese coast. *Marine Pollution Bulletin,* 60**,** 1988-1992.

FRIEDRICH, D. 2016. The problems won't go away: Persistent Organic Pollutants (POPs) in the Arctic

GALGANI, F., FLEET, D., VAN FRANEKER, J., KATSANEVAKIS, S., MAES, T., MOUAT, J., OOSTERBAAN, L., POITOU, I., HANKE, G. & THOMPSON, R. 2010. *Marine Strategy Framework directive-Task Group 10 Report marine litter do not cause harm to the coastal and marine environment. Report on the identification of descriptors for the Good Environmental Status of European Seas regarding marine litter under the Marine Strategy Framework Directive*, Office for Official Publications of the European Communities.

GESAMP 2015. Sources, fate and effects of microplastics in the marine environment: a global assessment. *In:* KERSHAW, P. J., ED. (ed.). London: IMO/FAO/UNESCO-IOC/UNIDO/WMO/IAEA/UN/UNEP/UNDP Joint group of Experts on the Scientific Aspects of Marine Enrionmental Protection.

GESAMP 2016. Sources, fate and effects of microplastics in the marine environment: part two of a global assessment. . *In:* KERSHAW, P. J., ED. (ed.). London: IMO/FAO/UNESCO-IOC/UNIDO/WMO/IAEA/UN/UNEP/UNDP Joint group of experts on the Scientific aspects of marine environmental protection.

GEYER, R., JAMBECK, J. R. & LAW, K. L. 2017. Production, use, and fate of all plastics ever made. *Science advances,* 3**,** e1700782.

GIL, A. & GRANGE, P. 1996. Application of the Dubinin-Radushkevich and Dubinin-Astakhov equations in the characterization of microporous solids. *Colloids and Surfaces A: Physicochemical and Engineering Aspects,* 113**,** 39-50.

GIMBERT, F., MORIN-CRINI, N., RENAULT, F., BADOT, P.-M. & CRINI, G. 2008. Adsorption isotherm models for dye removal by cationized starch-based material in a single component system: Error analysis. *Journal of Hazardous Materials,* 157**,** 34-46.

GLOMSTAD, B., SØRENSEN, L., LIU, J., SHEN, M., ZINDLER, F., JENSSEN, B. M. & BOOTH, A. M. 2017. Evaluation of methods to determine adsorption of polycyclic aromatic hydrocarbons to

dispersed carbon nanotubes. *Environmental Science and Pollution Research,* 24**,** 23015-23025.
GOURMELON, G. 2015. Global plastic production rises, recycling lags. *New Worldwatch Institute analysis explores trends in global plastic consumption and recycling. Recuperado de http://www. worldwatch. org*.
GRACA, B., SZEWC, K., ZAKRZEWSKA, D., DOŁĘGA, A. & SZCZERBOWSKA-BORUCHOWSKA, M. 2017. Sources and fate of microplastics in marine and beach sediments of the Southern Baltic Sea—a preliminary study. *Environmental Science and Pollution Research,* 24**,** 7650-7661.
GREEN, N. W., SCHØYEN, M., ØXNEVAD, S., RUUS, A., ALLAN, I., HJERMANN, D. Ø., HØGÅSEN, T., BEYLICH, B., HÅVARDSTUN, J. & LUND, E. 2015. Contaminants in coastal waters of Norway 2014.
GREEN, N. W., SCHØYEN, M., ØXNEVAD, S., RUUS, A., ALLAN, I., HJERMANN, D. Ø., HØGÅSEN, T., BEYLICH, B., HÅVARDSTUN, J. & LUND, E. 2016. Contaminants in coastal waters of Norway 2015.
GREGORY, M. R. & RYAN, P. G. 1997. Pelagic plastics and other seaborne persistent synthetic debris: a review of Southern Hemisphere perspectives. *Marine Debris.* Springer.
HAFTKA, J. J., GOVERS, H. A. & PARSONS, J. R. 2010. Influence of temperature and origin of dissolved organic matter on the partitioning behavior of polycyclic aromatic hydrocarbons. *Environmental Science and Pollution Research,* 17**,** 1070-1079.
HASSETT, J. J. & BANWART, W. L. 1989. The sorption of nonpolar organics by soils and sediments. *Reactions and movement of organic chemicals in soils***,** 31-44.
HEO, N. W., HONG, S. H., HAN, G. M., HONG, S., LEE, J., SONG, Y. K., JANG, M. & SHIM, W. J. 2013. Distribution of small plastic debris in cross-section and high strandline on Heungnam beach, South Korea. *Ocean Science Journal,* 48**,** 225-233.
HJERTHOLM, E. & GANSEL, L. 2016. *Opptak av mikroplast i hoppekrepsen Acartia Tonsa.* Bachelor, NTNU.
HONG, W.-J., JIA, H., LI, Y.-F., SUN, Y., LIU, X. & WANG, L. 2016. Polycyclic aromatic hydrocarbons (PAHs) and alkylated PAHs in the coastal seawater, surface sediment and oyster from Dalian, Northeast China. *Ecotoxicology and Environmental Safety,* 128**,** 11-20.
HUFFER, T. 2014. *Sorption of non-ionic organic compounds by carbon-based nanomaterials-systematic characterization. modeling, and application.* Duisburg-Essen.
HUTSON, N. D. & YANG, R. T. 1997. Theoretical basis for the Dubinin-Radushkevitch (D-R) adsorption isotherm equation. *Adsorption,* 3**,** 189-195.
HÜFFER, T. & HOFMANN, T. 2016. Sorption of non-polar organic compounds by micro-sized plastic particles in aqueous solution. *Environmental Pollution,* 214**,** 194-201.
JONES, K. C. & DE VOOGT, P. 1999. Persistent organic pollutants (POPs): state of the science. *Environmental Pollution,* 100**,** 209-221.
KAH, M., ZHANG, X., JONKER, M. T. & HOFMANN, T. 2011. Measuring and modeling adsorption of PAHs to carbon nanotubes over a six order of magnitude wide concentration range. *Environmental science & technology,* 45**,** 6011-6017.
KAPOSI, K. L., MOS, B., KELAHER, B. P. & DWORJANYN, S. A. 2014. Ingestion of microplastic has limited impact on a marine larva. *Environmental science & technology,* 48**,** 1638-1645.
KIM, S. J. & KWON, J. H. 2010. Determination of partition coefficients for selected PAHs between water and dissolved organic matter. *CLEAN–Soil, Air, Water,* 38**,** 797-802.
KOOI, M., REISSER, J., SLAT, B., FERRARI, F. F., SCHMID, M. S., CUNSOLO, S., BRAMBINI, R., NOBLE, K., SIRKS, L.-A. & LINDERS, T. E. 2016. The effect of particle properties on the depth profile of buoyant plastics in the ocean. *Scientific reports,* 6**,** 33882.
KUMAR, K. V. 2007. Optimum sorption isotherm by linear and non-linear methods for malachite green onto lemon peel. *Dyes and Pigments,* 74**,** 595-597.
KUMAR, K. V., PORKODI, K. & ROCHA, F. 2008. Comparison of various error functions in predicting the optimum isotherm by linear and non-linear regression analysis for the sorption of basic red 9 by activated carbon. *Journal of hazardous materials,* 150**,** 158-165.

KUMAR, K. V. & SIVANESAN, S. 2005. Prediction of optimum sorption isotherm: Comparison of linear and non-linear method. *Journal of hazardous materials,* 126**,** 198-201.
KURTZ, S. & MANLEY, M. 2009. CHAPTER 61 - Cross-Linked Polyethylene A2 - by, Edited. *In:* HOZACK, W. J., PARVIZI, J. & BENDER, B. (eds.) *Surgical Treatment of Hip Arthritis.* Philadelphia: W.B. Saunders.
LALLAS, P. L. 2001. The Stockholm Convention on persistent organic pollutants. *American Journal of International Law,* 95**,** 692-708.
LATIMER, J. S. & ZHENG, J. 2003. and Fate of PAHs in the Marine Environment. *PAHs: an ecotoxicological perspective***,** 9.
LAW, R. J., DAWES, V. J., WOODHEAD, R. J. & MATTHIESSEN, P. 1997. Polycyclic aromatic hydrocarbons (PAH) in seawater around England and Wales. *Marine Pollution Bulletin,* 34**,** 306-322.
LEE, H., SHIM, W. J. & KWON, J.-H. 2014. Sorption capacity of plastic debris for hydrophobic organic chemicals. *Science of the Total Environment,* 470**,** 1545-1552.
LIMA, A., COSTA, M. & BARLETTA, M. 2014. Distribution patterns of microplastics within the plankton of a tropical estuary. *Environmental Research,* 132**,** 146-155.
LIMOUSIN, G., GAUDET, J. P., CHARLET, L., SZENKNECT, S., BARTHÈS, V. & KRIMISSA, M. 2007. Sorption isotherms: A review on physical bases, modeling and measurement. *Applied Geochemistry,* 22**,** 249-275.
LOFTHUS, S., ALMÅS, I. K., EVANS, P., PELZ, O. & BRAKSTAD, O. G. 2016. Biotransformation of potentially persistent alkylphenols in natural seawater. *Chemosphere,* 156**,** 191-194.
LONG, M., MORICEAU, B., GALLINARI, M., LAMBERT, C., HUVET, A., RAFFRAY, J. & SOUDANT, P. 2015. Interactions between microplastics and phytoplankton aggregates: Impact on their respective fates. *Marine Chemistry,* 175**,** 39-46.
LÜERS, F. & TEN HULSCHER, T. E. 1996. Temperature effect on the partitioning of polycyclic aromatic hydrocarbons between natural organic carbon and water. *Chemosphere,* 33**,** 643-657.
LYNWOOD, C. 2014. *Polystyrene: synthesis, characteristics, and applications,* New York, Nova Science Publishers, Inc. .
MACKAY, D. & SHIU, W. Y. 1977. Aqueous solubility of polynuclear aromatic hydrocarbons. *Journal of Chemical and Engineering Data,* 22**,** 399-402.
MARTINS, J. & SOBRAL, P. 2011. Plastic marine debris on the Portuguese coastline: a matter of size? *Marine pollution bulletin,* 62**,** 2649-2653.
MATO, Y., ISOBE, T., TAKADA, H., KANEHIRO, H., OHTAKE, C. & KAMINUMA, T. 2001. Plastic resin pellets as a transport medium for toxic chemicals in the marine environment. *Environmental science & technology,* 35**,** 318-324.
MERRINGTON, A. 2011. Recycling of plastics. *Applied Plastics Engineering Handbook.* Elsevier.
MOORE, C. J. 2008. Synthetic polymers in the marine environment: A rapidly increasing, long-term threat. *Environmental Research,* 108**,** 131-139.
MUIJS, B. & JONKER, M. T. 2009. Temperature-dependent bioaccumulation of polycyclic aromatic hydrocarbons. *Environmental science & technology,* 43**,** 4517-4523.
MURRAY, F. & COWIE, P. R. 2011. Plastic contamination in the decapod crustacean Nephrops norvegicus (Linnaeus, 1758). *Marine pollution bulletin,* 62**,** 1207-1217.
NEFF, J. M. 2002. *Bioaccumulation in marine organisms: effect of contaminants from oil well produced water*, Elsevier.
PAN, B. & XING, B. 2008. Adsorption mechanisms of organic chemicals on carbon nanotubes. *Environmental science & technology,* 42**,** 9005-9013.
PEARLMAN, R. S., YALKOWSKY, S. H. & BANERJEE, S. 1984. Water solubilities of polynuclear aromatic and heteroaromatic compounds. *Journal of physical and chemical reference data,* 13**,** 555-562.
QING LI, Q., LOGANATH, A., SENG CHONG, Y., TAN, J. & PHILIP OBBARD, J. 2006. Persistent organic pollutants and adverse health effects in humans. *Journal of Toxicology and Environmental Health, Part A,* 69**,** 1987-2005.

REDLICH, O. & PETERSON, D. L. 1959. A useful adsorption isotherm. *Journal of Physical Chemistry,* 63**,** 1024-1024.

RIOS, L. M., MOORE, C. & JONES, P. R. 2007. Persistent organic pollutants carried by synthetic polymers in the ocean environment. *Marine Pollution Bulletin,* 54**,** 1230-1237.

ROBERTSON, R. E. 1965. Polymer order and polymer density. *The Journal of Physical Chemistry,* 69**,** 1575-1578.

ROCHMAN, C. M., MANZANO, C., HENTSCHEL, B. T., SIMONICH, S. L. M. & HOH, E. 2013. Polystyrene plastic: a source and sink for polycyclic aromatic hydrocarbons in the marine environment. *Environmental science & technology,* 47**,** 13976-13984.

ROGNE HALLAND, G., ALTIN, D., HENRIK HANSEN, B., M. BOOTH, A., J.OLSEN, A. & SALABERRIA, L. 2017. Uptake and excretion of polystyrene microplastics in the marine copepod Calanus Finmarchicus. Biotrix and Sintef ocean, Trondheim, Norway Norwegian University of Science and TEchnology (NTNU)

RUSHTON, E. K., JIANG, J., LEONARD, S. S., EBERLY, S., CASTRANOVA, V., BISWAS, P., ELDER, A., HAN, X., GELEIN, R. & FINKELSTEIN, J. 2010. Concept of assessing nanoparticle hazards considering nanoparticle dosemetric and chemical/biological response metrics. *Journal of Toxicology and Environmental Health, Part A,* 73**,** 445-461.

SAHA, A., BHADURI, D., PIPARIYA, A. & KUMAR GHOSH, R. 2017. Linear and nonlinear sorption modelling for adsorption of atrazine onto activated peanut husk. *Environmental Progress & Sustainable Energy,* 36**,** 348-358.

SAMANTA, S. K., SINGH, O. V. & JAIN, R. K. 2002. Polycyclic aromatic hydrocarbons: environmental pollution and bioremediation. *TRENDS in Biotechnology,* 20**,** 243-248.

SAVINOV, V. M., SAVINOVA, T. N., MATISHOV, G. G., DAHLE, S. & NÆS, K. 2003. Polycyclic aromatic hydrocarbons (PAHs) and organochlorines (OCs) in bottom sediments of the Guba Pechenga, Barents Sea, Russia. *Science of The Total Environment,* 306**,** 39-56.

SETÄLÄ, O., FLEMING-LEHTINEN, V. & LEHTINIEMI, M. 2014. Ingestion and transfer of microplastics in the planktonic food web. *Environmental pollution,* 185**,** 77-83.

SHAHMOHAMMADI-KALALAGH, S. & BABAZADEH, H. 2014. Isotherms for the sorption of zinc and copper onto kaolinite: comparison of various error functions. *International Journal of Environmental Science and Technology,* 11**,** 111-118.

SREŃSCEK-NAZZAL, J., NARKIEWICZ, U., MORAWSKI, A. W., WRÓBEL, R. J. & MICHALKIEWICZ, B. 2015. Comparison of optimized isotherm models and error functions for carbon dioxide adsorption on activated carbon. *Journal of Chemical & Engineering Data,* 60**,** 3148-3158.

SYBERG, K., KHAN, F. R., SELCK, H., PALMQVIST, A., BANTA, G. T., DALEY, J., SANO, L. & DUHAIME, M. B. 2015. Microplastics: addressing ecological risk through lessons learned. *Environmental toxicology and chemistry,* 34**,** 945-953.

TANG, X., KONG, D. & YAN, X. 2018. *Multiple regression analysis of a woven fabric sound absorber*.

TEN HULSCHER, T. E. M. & CORNELISSEN, G. 1996. Effect of temperature on sorption equilibrium and sorption kinetics of organic micropollutants - a review. *Chemosphere,* 32**,** 609-626.

TEUTEN, E. L., ROWLAND, S. J., GALLOWAY, T. S. & THOMPSON, R. C. 2007. Potential for plastics to transport hydrophobic contaminants. *Environmental science & technology,* 41**,** 7759-7764.

TEUTEN, E. L., SAQUING, J. M., KNAPPE, D. R., BARLAZ, M. A., JONSSON, S., BJÖRN, A., ROWLAND, S. J., THOMPSON, R. C., GALLOWAY, T. S. & YAMASHITA, R. 2009. Transport and release of chemicals from plastics to the environment and to wildlife. *Philosophical Transactions of the Royal Society of London B: Biological Sciences,* 364**,** 2027-2045.

THOMPSON, R. C. 2015. Microplastics in the marine environment: Sources, consequences and solutions. *Marine anthropogenic litter.* Springer.

THOMPSON, R. C., OLSEN, Y., MITCHELL, R. P., DAVIS, A., ROWLAND, S. J., JOHN, A. W., MCGONIGLE, D. & RUSSELL, A. E. 2004. Lost at sea: where is all the plastic? *Science,* 304**,** 838-838.

TREMBLAY, L., KOHL, S. D., RICE, J. A. & GAGNÉ, J.-P. 2005. Effects of temperature, salinity, and dissolved humic substances on the sorption of polycyclic aromatic hydrocarbons to estuarine particles. *Marine Chemistry,* 96**,** 21-34.

VAN SEBILLE, E., WILCOX, C., LEBRETON, L., MAXIMENKO, N., HARDESTY, B. D., VAN FRANEKER, J. A., ERIKSEN, M., SIEGEL, D., GALGANI, F. & LAW, K. L. 2015. A global inventory of small floating plastic debris. *Environmental Research Letters,* 10**,** 124006.

VELZEBOER, I., KWADIJK, C. & KOELMANS, A. 2014. Strong sorption of PCBs to nanoplastics, microplastics, carbon nanotubes, and fullerenes. *Environmental science & technology,* 48**,** 4869-4876.

VERSCHUEREN, K. 1983. Handbook of environmental data on organic compounds. Van Nostrand Reinhold: New York.

VERSCHUEREN, K. 2001. *Handbook of environmental data on organic chemicals: Vol. 1*, John Wiley and Sons, Inc.

VOICE, T. C., RICE, C. P. & WEBER, W. J. 1983. Effect of solids concentration on the sorptive partitioning of hydrophobic pollutants in aquatic systems. *Environmental science & technology,* 17**,** 513-518.

WANG, W. & WANG, J. 2018a. Comparative evaluation of sorption kinetics and isotherms of pyrene onto microplastics. *Chemosphere,* 193**,** 567-573.

WANG, W. & WANG, J. 2018b. Different partition of polycyclic aromatic hydrocarbon on environmental particulates in freshwater: Microplastics in comparison to natural sediment. *Ecotoxicology and environmental safety,* 147**,** 648-655.

WRIGHT, S. L., THOMPSON, R. C. & GALLOWAY, T. S. 2013. The physical impacts of microplastics on marine organisms: a review. *Environmental Pollution,* 178**,** 483-492.

YIM, U. H., HONG, S. H. & SHIM, W. J. 2007. Distribution and characteristics of PAHs in sediments from the marine environment of Korea. *Chemosphere,* 68**,** 85-92.

ZARFL, C. & MATTHIES, M. 2010. Are marine plastic particles transport vectors for organic pollutants to the Arctic? *Marine Pollution Bulletin,* 60**,** 1810-1814.

ZENG, E. Y. & VISTA, C. L. 1997. Organic pollutants in the coastal environment off San Diego, California. 1. Source identification and assessment by compositional indices of polycyclic aromatic hydrocarbons. *Environmental toxicology and Chemistry,* 16**,** 179-188.

ZHOU, J., FILEMAN, T., EVANS, S., DONKIN, P., READMAN, J., MANTOURA, R. F. C. & ROWLAND, S. 1999. *The partition of fluoranthene and pyrene between suspended particles and dissolved phase in the Humber Estuary: A study of the controlling factors*.

ZICCARDI, L. M., EDGINGTON, A., HENTZ, K., KULACKI, K. J. & KANE DRISCOLL, S. 2016. Microplastics as vectors for bioaccumulation of hydrophobic organic chemicals in the marine environment: A state-of-the-science review. *Environmental toxicology and chemistry,* 35**,** 1667-1676.

ZINDLER, F., GLOMSTAD, B., ALTIN, D., LIU, J., JENSSEN, B. M. & BOOTH, A. M. 2016. Phenanthrene bioavailability and toxicity to Daphnia magna in the presence of carbon nanotubes with different physicochemical properties. *Environmental science & technology,* 50**,** 12446-12454.

ZITKO, V. & HANLON, M. 1991. Another source of pollution by plastics: skin cleaners with plastic scrubbers. *Marine Pollution Bulletin,* 22**,** 41-42.

Appendix

Appendix A: PAH stock solutions

Table A.1. Amounts (mg) of 1,3-dimethylnahpthalene, fluoranthene and phenanthrene weighed in for the stock solutions.

PAH	PAH (mg) in methanol (MeOH)	PAH (mg) in dichloromethane (DCM)
DMN	2,740	1492
FLA	2,640	20,42
PHE	2,310	99,91

Appendix B: Teflon-WAF solubilities

Solubilities and the corresponding calibration calculations of the Teflon-WAF bottles for phenanthrene (PHE), fluoranthene (FLA) and 1,3-dimethylnaphthalene (DMN) at 10 and 20 °C.

Table B.1. Calibration calculation for the Teflon-WAF solubilities at 10 °C.

	PHE	FLA		DMN
	WAF-bottle	WAF-bottle 1	WAF-bottle 2	
Slope (a)	718,6	133,8	188,5	381,5
Intercept (b)	-26,76	1,742	-0,2378	-8,530
R^2	0,9994	1,000	0,9989	0,9997

Table B.2. The solubilities of the Teflon- WAF bottles at 10 °C.

	Concentration [µg/L]				
WAF-bottle	**PHE**		**FLA**		**DMN**
	WAF-bottle	**Verification WAF-bottle**	**WAF-bottle 1**	**WAF-bottle 2**	
1	158,5	155,1	21,98	24,72	3102
2	159,7	158,1	21,67	26,72	3108
3	159,5	155,0	21,04	26,31	3256
4	158,1	157,6	21,35	26,01	3099
5	157,3	153,6	22,12	26,62	3049
Average	158,6	155,9	21,63	26,08	3123

Table B.3. Calibration calculation for the Teflon-WAF solubilities at 20 °C.

	PHE	FLA
Slope (a)	331,1	144,2
Intercept (b)	-1,09	0,7720
R^2	0,9999	0,9496

Table B.4. The solubilities of the Teflon- WAF bottles at 20 °C.

WAF-bottle	PHE	FLA
1	410,4	84,05
2	420,0	82,92
3	412,0	83,95
Average	414,1	83,64

Appendix C: Filtration recovery

Concentrations and the corresponding calibration calculation for the filtered and unfiltered control samples of the PAHS; phenanthrene (PHE), fluoranthene (FLA) and 1,3-dimethylnaphthalene (DMN).

Table C.1. The concentrations of the PAHs.

PAH	Temperature (°C)	Control samples					
		Unfiltered replicates			Filtered replicates		
		1	2	3	1	2	3
PHE	**10**	12,16	12,03	12,25	8,557	9,670	8,119
	20	11,67	11,49	11,83	7,147	8,868	9,248
FLA	**10**	22,43	23,15	23,37	11,06	12,96	11,64
	20	23,12	22,47	22,97	14,15	13,99	15,84
DMN	**10**	15,48	14,76	16,62	9,113	9,450	10,50
	20	16,63	16,91	15,69	5,615	7,155	10,99

Table C.2. Calibration calculation for the control samples of the PAHs.

	PHE	FLA	DMN
Slope (a)	744,4	188,3	319,9
Intercept (b)	0,7240	-0,04600	0,5530
R^2	0,9762	0,9942	0,9398

Appendix D: Calibration

Table D.1. Calibration calculations for the LC-UV, sorption kinetics, experiment nr.1.

Days	PHE			FLA			DMN		
	Slope (a)	Intercept (b)	R^2	Slope (a)	Intercept (b)	R^2	Slope (a)	Intercept (b)	R^2
1	744,4	0,7243	0,9762	188,3	-0,0465	0,9942	319,9	0,5530	0,9398
2	754,9	1,419	0,8862	179,0	-0,1274	0,9941	385,7	-0,6122	0,8995
3	641,1	3,074	0,9949	130,6	0,1932	1,000	347,3	0,03860	0,9101
4	668,7	2,769	0,9993	106,8	0,4346	0,9992	369,2	0,1262	0,9996
7	672,4	0,7613	0,9989	180,8	-0,0201	0,9911	354,8	0,2197	0,9995
9	-	-	-	180,7	0,0801	1,000	-	-	-

Table D.2. Calibration calculations for LC-UV, sorption kinetics, experiment 2.

Days	PHE			FLA			DMN		
	Slope (a)	Intercept (b)	R^2	Slope (a)	Intercept (b)	R^2	Slope (a)	Intercept (b)	R^2
0	672,0	0,9173	0,9989	180,8	-0,02010	0,9911	354,8	0,2197	0,9995
1	801,7	-0,01550	0,9996	125,3	-0,3109	0,9202	364,1	0,05190	0,9183
2	778,2	0,02150	0,9970	180,7	0,08010	1,0000	369,6	0,1769	0,9999
3	830,2	0,5066	0,9999	199,4	0,1251	0,9998	400,4	0,04730	1,0000
4	873,4	0,8540	0,9989	203,2	0,2039	0,9992	429,9	2,284	0,9908
7	745,1	1,261	0,9980	199,8	0,1131	1,0000	391,1	0,1772	0,9999

Table D.3. Calibration calculations for LC-UV, sorption kinetics, experiment 3.

Days	PHE			FLA		
	Slope (a)	Intercept (b)	R^2	Slope (a)	Intercept (b)	R^2
0	745,1	1,261	0,9980	199,8	0,1131	1,0000
1	825,9	0,4525	1,0000	197,9	-0,0301	0,9977
2	873,5	0,6839	0,9998	200,7	0,1072	0,9992
3	833,6	0,8065	0,9994	202,7	0,1614	0,9999
4	874,1	0,3447	0,9997	200,6	-0,0855	0,9995
7	855,6	0,1390	0,9986	188,5	-0,2378	0,9989
9	832,7	0,7575	0,9987	-	-	-
11	868,5	0,5974	0,9998	-	-	-
14	863,2	1,351	0,9985	-	-	-

Table D.4. Calibration calculations for LC-UV, isotherm studies.

Day	PHE		
	Slope (a)	Intercept (b)	R^2
1	946,7	0,01340	0,9988
2	806,1	-2,871	0,9767

Table D.5. Relative response factors (RRFs) and their relative standard deviation (RSD) for the GC-MS analysis of fluoranthene and phenanthrene.

	RRF	RSD (%)
Calibration nr 1		
PHE	1,773	11,10
FLA	1,515	18,86
Calibration nr 2		
PHE	1,793	8,650
FLA	1,491	20,15
Calibration nr 3		
PHE	1,865	17,12
FLA	1,712	12,93

Appendix E: Sorption kinetics

Tables E.1-E.3 present sample ID, polycyclic aromatic hydrocarbon (PAH) in sample, amount of microplastic (MP) weighed (mg), and concentration of PAH in solution for the kinetic uptake experiments. The MPs are polyethylene (PE), polyester (PES) and polystyrene (PS).

Table E.1. Sorption kinetics experiment 1.

Sample ID		PAH in sample	MP (mg)	Concentration of chemical in solution [µg/L]						
Temperature (°C)	MP			Day 0	Day 1	Day 2	Day 3	Day 4	Day 7	Day 9
10 °C	**Ctr**	PHE	-	12,1	12,4	9,80	5,99	6,39	8,78	na
10 °C	**PE-10**	PHE	0,840	na*	11,0	7,06	3,93	4,30	8,25	na
10 °C	**PE-100**	PHE	8,35	na*	10,6	7,36	5,60	5,56	7,96	na
10 °C	**PS-10**	PHE	0,930	na*	10,8	6,72	5,05	3,23	8,29	na
10 °C	**PES-50**	PHE	1,94	na*	10,8	9,59	6,49	4,04	9,28	na
20 °C	**Ctr**	PHE	-	11,7	11,1	7,15	2,41	3,36	8,49	na
20 °C	**PE-10**	PHE	0,8200	na*	11,2	7,60	3,42	1,25	8,37	na
20 °C	**PE-100**	PHE	8,36	na*	11,1	9,15	4,13	2,12	7,49	na
20 °C	**PS-10**	PHE	0,930	na*	10,8	9,80	1,44	4,15	8,59	na
20 °C	**PES-50**	PHE	1,94	na*	9,98	6,06	4,45	2,90	8,12	na
10 °C	**Ctr**	FLA	-	23,0	11,8	22,3	20,1	19,8	15,6	10,7

10 °C	**PE-10**	FLA	0,780	na*	5,09	12,5	9,15	11,2	10,0	12,2
10 °C	**PE-100**	FLA	8,34	na*	7,17	24,1	19,3	9,89	16,2	14,6
10 °C	**PS-10**	FLA	0,930	na*	9,29	19,8	21,0	14,7	19,1	13,7
10 °C	**PES-50**	FLA	1,94	na*	8,50	21,8	15,0	14,8	4,74	9,78
20 °C	**Ctr**	FLA	-	22,9	7,69	17,0	11,8	13,1	12,4	13,3
20 °C	**PE-10**	FLA	0,840	na*	6,60	12,8	9,65	8,66	7,21	10,1
20 °C	**PE-100**	FLA	8,33	na*	4,14	9,34	5,14	1,67	5,56	4,66
20 °C	**PS-10**	FLA	0,930	na*	8,38	18,9	17,3	12,5	7,42	10,7
20 °C	**PES-50**	FLA	1,93	na*	7,47	8,76	7,27	14,9	7,99	13,7
10 °C	**Ctr**	DMN	-	15,6	16,3	17,6	17,5	9,84	11,1	na
10 °C	**PE-10**	DMN	0,790	na*	20,6	21,3	18,3	12,2	15,7	na
10 °C	**PE-100**	DMN	8,37	na*	22,6	15,8	19,5	9,02	14,1	na
10 °C	**PS-10**	DMN	0,930	na*	13,1	17,4	14,0	10,2	9,36	na
10 °C	**PES-50**	DMN	1,96	na*	27,1	18,3	14,1	10,4	10,2	na
20 °C	**Ctr**	DMN	-	16,4	14,8	18,1	16,3	11,7	9,37	na
20 °C	**PE-10**	DMN	0,820	na*	23,0	22,1	15,3	13,1	12,8	na
20 °C	**PE-100**	DMN	8,33	na*	23,9	20,9	16,5	15,0	14,5	na
20 °C	**PS-10**	DMN	0,930	na*	20,2	20,7	17,8	11,1	11,5	na
20 °C	**PES-50**	DMN	1,93	na*	25,3	24,4	16,0	12,6	15,4	na

na: not analysed

na*: Concentration on day 0 were only measured in the control samples. It is assumed that the concentration is the same in the samples.

Table E.2. Sorption kinetics experiment 2.

Sample ID		PAH in sample	MP (mg)	Concentration of chemical in solution [ug/L]					
Temperature (°C)	MP			Day 0	Day 1	Day 2	Day 3	Day 4	Day 7
		PHE	-	8,27	10,2	10,4	8,14	8,18	8,26
10 °C	Ctr	PHE	-	6,71	9,99	9,39	7,93	7,09	8,38
		PHE	-	8,35	10,3	10,6	7,90	7,37	9,02
10 °C	Ctr	PHE	7,99	4,88	5,98	5,14	5,26	4,08	4,66
		PHE	-	8,19	8,85	9,23	8,17	7,65	8,26
20 °C	Ctr	PHE	-	8,69	7,76	8,22	8,27	7,24	8,13
		PHE	-	7,67	9,20	Sl	8,14	6,85	6,84
20 °C	PE-10	PHE	8,06	4,83	6,72	5,84	5,40	4,34	4,78
		FLA	-	17,1	24,6	16,6	18,9	17,8	16,0
10 °C	Ctr	FLA	-	12,5	25,6	15,4	18,3	16,0	16,4
		FLA	-	15,9	27,9	19,5	20,4	14,4	18,0
10 °C	PE-10	FLA	7,96	4,45	8,29	2,97	2,82	2,34	4,30
		FLA	-	4,50	18,8	12,6	11,0	12,5	18,7
20 °C	Ctr	FLA	-	11,6	20,1	13,5	12,8	12,1	18,2
		FLA	-	7,91	20,6	12,8	15,1	13,6	19,6
20 °C	PE-10	FLA	7,98	5,16	8,72	3,49	2,73	3,42	5,26
		DMN	-	8,70	11,4	10,7	12,3	2,11	9,96

10 °C	**Ctr**	DMN	-	10,5	15,6	14,6	12,7	3,89	13,2
		DMN	-	Sl	11,1	12,7	11,0	1,39	9,59
10 °C	**PE-10**	DMN	8,02	11,9	13,2	7,03	12,7	3,77	13,7
		DMN	-	13,4	12,9	8,96	12,0	1,05	9,55
20 °C	**Ctr**	DMN	-	10,9	14,7	10,2	15,3	0,73	9,34
		DMN	-	12,0	14,5	10,9	11,6	1,08	9,47
20 °C	**PE-10**	DMN	8,05	13,4	12,8	10,8	10,6	0,44	9,22

sl: sample lost

Table E.3. Uptake kinetics experiment 3.

Sample ID		PAH in sample	MP (mg)	Concentration of chemical in solution (ug/L)								
Temperature (°C)	MP			Day 0	Day 1	Day 2	Day 3	Day 4	Day 7	Day 9	Day 11	Day 14
		PHE	-	8,47	9,47	8,55	8,54	9,56	8,99	8,30	8,34	6,95
10 °C	**Ctr**	PHE	-	7,27	7,64	7,85	8,15	8,34	7,93	7,58	7,16	4,44
		PHE	-	7,41	9,35	8,44	8,79	8,86	8,99	8,35	7,53	5,55
10 °C	**PE-100 mass**	PHE	8,00	9,77	10,08	9,19	9,28	7,70	8,40	na	na	na
10 °C	**PS-10 mass**	PHE	9,30	8,02	8,61	8,61	8,43	8,42	8,24	6,46	6,40	4,65
10 °C	**PE-200 mass**	PHE	7,94	9,07	8,59	9,29	8,92	8,87	9,79	na	na	na
10 °C	**PE-10 mass**	PHE	8,05	4,60	5,19	4,73	4,44	5,06	5,64	4,12	sl	2,77
10 °C	**PE-100 SA**	PHE	83,44	8,40	8,33	8,15	7,95	8,08	8,42	6,94	6,33	4,58
10 °C	**PE-200 SA**	PHE	166,78	8,36	8,64	6,72	6,34	7,85	7,94	6,05	6,04	4,28
		PHE	-	7,20	10,04	8,76	7,92	7,85	9,74	8,63	8,58	7,89
20 °C	**Ctr**	PHE	-	6,71	8,16	6,46	7,90	6,85	7,97	7,60	8,42	6,22
		PHE	-	7,08	8,58	7,44	6,46	6,90	8,41	7,41	7,32	6,14
20 °C	**PE-100 mass**	PHE	8,08	8,33	9,56	7,67	8,73	8,35	8,56	na	na	na
20 °C	**PS-10 mass**	PHE	9,30	6,99	7,76	7,15	6,72	7,13	5,20	5,38	5,15	3,28
20 °C	**PE-200 mass**	PHE	8,00	8,06	8,44	8,12	7,59	8,43	7,83	na	na	na
20 °C	**PE-10 mass**	PHE	7,94	4,88	5,43	5,03	sl	sl	5,03	4,71	4,67	2,88
20 °C	**PE-100 SA**	PHE	83,4	8,27	8,15	6,07	6,32	6,85	5,20	5,26	5,11	6,22

20 °C	**PE-200 SA**	PHE	167	7,99	6,53	6,52	5,45	4,97	4,46	3,64	4,55	2,74
		FLA	-	17,2	24,2	23,5	20,4	22,4	26,7	na	na	na
10 °C	**Ctr**	FLA	-	17,0	22,8	22,7	23,8	25,4	26,1	na	na	na
		FLA	-	20,4	26,0	24,6	22,9	24,3	21,1	na	na	na
10 °C	**PE-100 mass**	FLA	8,12	18,8	21,9	22,7	18,2	22,2	24,8	na	na	na
10 °C	**PS-10 mass**	FLA	9,30	17,9	21,2	21,1	16,5	19,4	19,7	na	na	na
10 °C	**PE-200 mass**	FLA	7,99	17,5	24,2	22,7	20,8	21,4	23,2	na	na	na
10 °C	**PE-10 mass**	FLA	7,96	3,88	3,41	4,05	2,84	4,18	5,90	na	na	na
10 °C	**PE-100 SA**	FLA	83,1	13,4	18,7	15,6	14,2	15,5	13,8	na	na	na
10 °C	**PE-200 SA**	FLA	167	18,6	14,7	13,4	10,7	13,88	13,8	na	na	na
		FLA	-	14,6	18,5	17,7	17,2	16,6	18,2	na	na	na
20 °C	**Ctr**	FLA	-	15,2	20,1	16,2	14,5	17,6	20,1	na	na	na
		FLA	-	16,0	16,5	18,4	15,5	14,9	19,1	na	na	na
20 °C	**PE-100 mass**	FLA	8,04	13,6	16,2	17,4	11,6	17,1	16,6	na	na	na
20 °C	**PS-10 mass**	FLA	9,30	12,2	13,1	15,4	14,0	13,6	15,2	na	na	na
20 °C	**PE-200 mass**	FLA	8,06	15,4	17,1	15,6	15,1	17,0	17,2	na	na	na
20 °C	**PE-10 mass**	FLA	7,94	9,15	8,27	9,99	7,88	5,72	9,56	na	na	na
20 °C	**PE-100 SA**	FLA	83,3	14,6	12,3	10,6	3,17	7,08	6,39	na	na	na
20 °C	**PE-200 SA**	FLA	167	15,2	12,6	10,8	6,96	4,96	6,13	na	na	na

na: not analysed

sl: sample lost

SA: surface area

Appendix F: Range-finding study

Table F.1. PAH (phenanthrene= PHE, fluoranthene= FLA) in sample, amount of microplastic (MP) weighed (mg), and concentration of PAH in solution for the range-finding study. The MPs are polyethylene (PE) and polystyrene (PS).

Sample ID	PAH in sample	MP (mg)	Concentration of PAH in solution [ug/L]
Ctr 100% 1	PHE	-	105
Ctr 100% 2	PHE	-	99,5
Ctr 100% 3	PHE	-	112
Ctr 21% 1	PHE	-	12,2
Ctr 21% 2	PHE	-	13,8
Ctr 21% 3	PHE	-	13,7
Ctr 5% 1	PHE	-	16,3
Ctr 5% 2	PHE	-	17,1
Ctr 5% 3	PHE	-	8,45*
PE-10 (0,3 mg) 100%	PHE	0,300	87,3
PE-10 (0,3 mg) 21%	PHE	0,350	13,5
PE-10 (0,3 mg) 5%	PHE	0,340	19,2
PE-10 (0,6 mg) 100% 1	PHE	0,610	50,1
PE-10 (0,6 mg) 100% 2	PHE	0,630	50,9
PE-10 (0,6 mg) 100% 3	PHE	0,620	44,4
PE-10 (0,6 mg) 21%	PHE	0,570	7,71
PE-10 (0,6 mg) 5%	PHE	0,640	14,4
PE-10 (0,9 mg) 100%	PHE	0,900	43,0
PE-10 (0,9 mg) 21%	PHE	0,900	4,53
PE-10 (0,9 mg) 5%	PHE	0,950	11,0
PE-100 (3 mg) 100%	PHE	2,99	77,0
PE-100 (3 mg) 21%	PHE	3,09	11,3
PE-100 (3 mg) 5%	PHE	3,08	19,0
PE-100 (6 mg) 100% 1	PHE	6,03	79,0
PE-100 (6 mg) 100% 2	PHE	6,03	67,3
PE-100 (6 mg) 100% 3	PHE	6,04	83,8
PE-100 (6 mg) 21%	PHE	6,05	6,24

PE-100 (6 mg) 5%	PHE	5,99	17,3
PE-100 (9 mg) 100%	PHE	9,00	62,6
PE-100 (9 mg) 21%	PHE	8,94	7,78
PE-100 (9 mg) 5%	PHE	8,98	13,0
PE-100 (12 mg) 100% 1	PHE	12,0	62,6
PE-100 (12 mg) 100% 2	PHE	12,0	56,0
PE-100 (12 mg) 100% 3	PHE	12,0	62,7
PS-10 (0,23 mg) 100%	PHE	0,230	101
PS-10 (0,23 mg) 21 %	PHE	0,230	11,9
PS-10 (0,23 mg) 5%	PHE	0,230	7,28
PS-10 (0,73 mg) 100%	PHE	0,730	85,4
PS-10 (0,73 mg) 21%	PHE	0,730	11,2
PS-10 (0,73 mg) 5%	PHE	0,730	9,27
PS-10 (2,18 mg) 100% 1	PHE	2,18	50,9
PS-10 (2,18 mg 100% 2	PHE	2,18	46,0
PS-10 (2,18 mg) 100% 3	PHE	2,18	57,2
PS-10 (2,18 mg) 21%	PHE	2,18	4,58
PS-10 (2,18 mg) 5%	PHE	2,18	5,74
Ctr 100% 1	FLA	-	41,1
Ctr 100% 2	FLA	-	35,2
Ctr 100% 3	FLA	-	37,3
Ctr 21% 1	FLA	-	5,86
Ctr 21% 2	FLA	-	5,96
Ctr 21% 3	FLA	-	6,49
Ctr 5% 1	FLA	-	1,26
Ctr 5% 2	FLA	-	1,23
Ctr 5% 3	FLA	-	1,33
PE-10 (0,15 mg) 100% 1	FLA	0,150	13,0
PE-10 (0,15 mg) 100% 2	FLA	0,160	17,6
PE-10 (0,15 mg) 100% 3	FLA	0,150	12,2
PE-10 (0,3 mg) 100%	FLA	0,300	12,0
PE-10 (0,3 mg) 21%	FLA	0,280	2,00
PE-10 (0,3 mg) 5%	FLA	0,290	0,690

PE-10 (0,6 mg) 100%	FLA	0,610	7,20
PE-10 (0,6 mg) 21% 1	FLA	0,640	1,52
PE-10 (0,6 mg) 21% 2	FLA	0,620	1,67
PE-10 (0,6 mg) 21% 3	FLA	0,610	1,46
PE-10 (0,6 mg) 5%	FLA	0,580	0,460
PE-10 (0,9 mg) 100%	FLA	0,910	3,78
PE-10 (0,9 mg) 21%	FLA	0,910	1,05
PE-10 (0,9 mg) 5%	FLA	0,870	0,37
PE-100 (3 mg) 100%	FLA	3,03	23,9
PE-100 (3 mg) 21%	FLA	2,98	5,04
PE-100 (3 mg) 5%	FLA	2,99	1,63
PE-100 (6 mg) 100%	FLA	6,04	25,5
PE-100 (6 mg) 21% 1	FLA	5,99	4,52
PE-100 (6 mg) 21% 2	FLA	6,01	4,66
PE-100 (6 mg) 21% 3	FLA	5,96	3,72
PE-100 (6 mg) 5%	FLA	5,96	0,980
PE-100 (9 mg) 100%	FLA	9,05	25,4
PE-100 (9 mg) 21%	FLA	9,04	4,25
PE-100 (9 mg) 5%	FLA	9,01	0,940
PE-100 (12 mg) 100% 1	FLA	12,0	16,4
PE-100 (12 mg) 100% 2	FLA	12,0	18,8
PE-100 (12 mg) 100% 3	FLA	12,0	19,3
PS-10 (0,23 mg) 100%	FLA	0,230	32,0
PS-10 (0,23 mg) 21%	FLA	0,230	6,17
PS-10 (0,23 mg) 5%	FLA	0,230	1,32
PS-10 (0,73 mg) 100%	FLA	0,730	22,7
PS-10 (0,73 mg) 21%	FLA	0,730	4,98
PS-10 (0,73 mg) 5%	FLA	0,730	1,08
PS-10 (2,18 mg) 100%	FLA	2,18	22,4
PS-10 (2,18 mg) 21% 1	FLA	2,18	4,64
PS-10 (2,18 mg) 21% 2	FLA	2,18	3,33
PS-10 (2,18 mg) 21% 3	FLA	2,18	3,75
PS-10 (2,18 mg) 5%	FLA	2,18	1,08

PS-10 (6,55 mg) 100% 1	FLA	6,55	11,0
PS-10 (6,55 mg) 100% 2	FLA	6,55	12,4
PS-10 (6,55 mg) 100% 3	FLA	6,55	12,1

*: Number outlier. Not used for further calculations.

Appendix G: Isotherms

Table G.1. Sample ID with concentration of phenanthrene, amount of microplastic (MP) weighed (mg), and concentration of chemical in solution for the sorption isotherm study. The MPs are polyethylene (PE) and polystyrene (PS).

Sample ID	MP (mg)		C_{free} [µg/L]		Sample ID	MP (mg)		C_{free} [µg/L]		Sample ID	MP (mg)		C_{free} [µg/L]	
	10°C	20°C	10°C	20°C		10°C	20°C	10°C	20°C		10°C	20°C	10°C	20°C
Ctr 100% 1	-	-	125	88,3	**PE-10 (0,6 mg) 36% 1**	0,570	0,630	32,3	23,3	**PE-100 (9 mg) 13% 1**	9,10	9,03	9,45	7,29
Ctr 100% 2	-	-	127	97,0	**PE-10 (0,6 mg) 36% 2**	0,570	0,590	32,0	21,8	**PE-100 (9 mg) 13% 2**	8,92	8,93	9,50	6,73
Ctr 100% 3	-	-	126	102	**PE-10 (0,6 mg) 36% 3**	0,620	0,570	30,5	24,2	**PE-100 (9 mg) 13% 3**	8,96	8,94	9,97	7,62
Ctr 60% 1	-	-	77,0	54,7	**PE-10 (0,6 mg) 21% 1**	0,590	0,580	20,1	13,3	**PE-100 (9 mg) 8% 1**	9,04	8,93	7,77	8,56
Ctr 60% 2	-	-	75,3	57,0	**PE-10 (0,6 mg) 21% 2**	0,580	0,590	23,0	SL	**PE-100 (9 mg) 8% 2**	8,98	9,00	8,24	8,42
Ctr 60% 3	-	-	76,8	53,5	**PE-10 (0,6 mg) 21% 3**	0,630	0,560	21,1	14,6	**PE-100 (9 mg) 8% 3**	9,03	8,91	8,81	9,26
Ctr 36% 1	-	-	35,0	33,4	**PE-10 (0,6 mg) 13% 1**	0,570	0,560	6,79	5,34	**PE-100 (9 mg) 5% 1**	9,01	9,01	7,09	5,58
Ctr 36% 2	-	-	39,3	34,3	**PE-10 (0,6 mg) 13% 2**	0,620	0,610	6,71	6,82	**PE-100 (9 mg) 5% 2**	8,93	8,98	8,29	5,89

Ctr 36% 3	-	-	38,5	33,5	**PE-10 (0,6 mg) 13% 3**	0,570	0,560	7,14	7,04	**PE-100 (9 mg) 5% 3**	8,99	9,03	7,79	5,08
Ctr 21% 1	-	-	26,8	21,3	**PE-10 (0,6 mg) 8% 1**	0,600	0,600	7,29	8,85	**PS-10 (2,18 mg) 100% 1**	2,18	2,18	104	65,8
Ctr 21% 2	-	-	30,5	20,2	**PE-10 (0,6 mg) 8% 2**	0,570	0,650	7,55	7,54	**PS-10 (2,18 mg) 100% 2**	2,18	2,18	104	64,2
Ctr 21% 3	-	-	28,9	20,8	**PE-10 (0,6 mg) 8% 3**	0,580	0,640	7,70	8,80	**PS-10 (2,18 mg) 100% 3**	2,18	2,18	103	65,1
Ctr 13% 1	-	-	12,5	7,78	**PE-10 (0,6 mg) 5% 1**	0,580	0,570	5,33	5,80	**PS-10 (2,18 mg) 60% 1**	2,18	2,18	53,0	27,1
Ctr 13% 2	-	-	11,3	10,0	**PE-10 (0,6 mg) 5% 2**	0,640	0,590	5,20	6,50	**PS-10 (2,18 mg) 60% 2**	2,18	2,18	53,0	30,6
Ctr 13% 3	-	-	11,6	7,44	**PE-10 (0,6 mg) 5% 3**	0,550	0,560	5,57	6,11	**PS-10 (2,18 mg) 60% 3**	2,18	2,18	52,4	31,3
Ctr 8% 1	-	-	14,6	12,6	**PE-100 (9 mg) 100% 1**	8,92	8,94	102	74,3	**PS-10 (2,18 mg) 36% 1**	2,18	2,18	29,7	17,3
Ctr 8% 2	-	-	13,1	13,5	**PE-100 (9 mg) 100% 2**	9,05	9,02	101	76,8	**PS-10 (2,18 mg) 36% 2**	2,18	2,18	30,1	17,4

Ctr 8% 3	-	-	13,2	12,6	**PE-100 (9 mg) 100% 3**	8,94	9,04	105	71,8	**PS-10 (2,18 mg) 36% 3**	2,18	2,18	30,1	17,2
Ctr 5% 1	-	-	9,45	10,6	**PE-100 (9 mg) 60% 1**	9,08	8,98	62,2	38,7	**PS-10 (2,18 mg) 21% 1**	2,18	2,18	18,6	9,80
Ctr 5% 2	-	-	8,82	9,91	**PE-100 (9 mg) 60% 2**	8,96	8,95	55,0	38,5	**PS-10 (2,18 mg) 21% 2**	2,18	2,18	10,0	9,78
Ctr 5% 3	-	-	10,0	8,98	**PE-100 (9 mg) 60% 3**	8,98	8,93	61,9	38,2	**PS-10 (2,18 mg) 21% 3**	2,18	2,18	19,6	9,77
PE-10 (0,6 mg) 100% 1	0,560	0,630	83,6	74,7	**PE-100 (9 mg) 36% 1**	8,96	8,93	41,1*	23,7	**PS-10 (2,18 mg) 13% 1**	2,18	2,18	7,22	4,56
PE-10 (0,6 mg) 100% 2	0,550	0,610	88,5	74,8	**PE-100 (9 mg) 36% 2**	8,93	9,00	36,6*	22,4	**PS-10 (2,18 mg) 13% 2**	2,18	2,18	7,19	4,62
PE-10 (0,6 mg) 100% 3	0,560	0,590	83,6	73,9	**PE-100 (9 mg) 36% 3**	9,01	8,92	35,1*	24,8	**PS-10 (2,18 mg) 13% 3**	2,18	2,18	6,60	4,00
PE-10 (0,6 mg) 60% 1	0,580	0,580	50,9	SL	**PE-100 (9 mg) 21% 1**	8,95	8,96	21,8	14,4	**PS-10 (2,18 mg) 8% 1**	2,18	2,18	5,00	4,51
PE-10 (0,6 mg) 60% 2	0,580	0,660	49,8	41,1	**PE-100 (9 mg) 21% 2**	9,09	8,95	23,0	14,7	**PS-10 (2,18 mg) 8% 2**	2,18	2,18	6,43	5,74

PE-10 (0,6 mg) 60% 3	0,610	0,580	53,4	39,8	**PE-100 (9 mg) 21% 3**	8,93	8,94	24,9	13,9	**PS-10 (2,18 mg) 8% 3**	2,18	2,18	4,32	6,43
										PS-10 (2,18 mg) 5% 1	2,18	2,18	3,40	3,03
										PS-10 (2,18 mg) 5% 2	2,18	2,18	SL	3,22
										PS-10 (2,18 mg) 5% 3	2,18	2,18	4,27	3,69

*: Number either negative or outlier. Not used for further calculations.
SL: sample lost

Table G.2. Sample ID with concentration of fluoranthene, amount of microplastic (MP) weighed (mg), and concentration of chemical in solution for the sorption isotherm study. The MPs are polyethylene (PE) and polystyrene (PS).

Sample ID	MP (mg)		C_{free} [µg/L]		Sample ID	MP (mg)		C_{free} [µg/L]		Sample ID	MP (mg)		C_{free} [µg/L]	
	10°C	20°C	10°C	20°C		10°C	20°C	10°C	20°C		10°C	20°C	10°C	20°C
Ctr 100% 1	-	-	36,4	26,4	**PE-10 (0,3 mg) 36% 1**	0,280	0,300	3,14	3,01	**PE-100 (9 mg) 13% 1**	8,98	9,06	1,61	1,20
Ctr 100% 2	-	-	34,3	33,9	**PE-10 (0,3 mg) 36% 2**	0,280	0,280	2,60	2,37	**PE-100 (9 mg) 13% 2**	9,01	8,91	1,74	1,33
Ctr 100% 3	-	-	27,6	21,4	**PE-10 (0,3 mg) 36% 3**	0,320	0,290	4,30	2,71	**PE-100 (9 mg) 13% 3**	9,04	8,99	1,68	1,05
Ctr 60% 1	-	-	14,4	19,0	**PE-10 (0,3 mg) 21% 1**	0,280	0,300	1,09	1,64	**PE-100 (9 mg) 8% 1**	9,03	9,10	0,98	0,500
Ctr 60% 2	-	-	17,0	15,3	**PE-10 (0,3 mg) 21% 2**	0,300	0,290	1,04	1,64	**PE-100 (9 mg) 8% 2**	9,10	8,94	0,71	0,530
Ctr 60% 3	-	-	16,2	15,4	**PE-10 (0,3 mg) 21% 3**	0,310	0,340	1,28	1,59	**PE-100 (9 mg) 8% 3**	8,94	9,03	1,23	0,450
Ctr 36% 1	-	-	6,59	6,20	**PE-10 (0,3 mg) 13% 1**	0,370	0,300	0,960	1,00	**PE-100 (9 mg) 5% 1**	9,01	8,96	0,590	1,12*
Ctr 36% 2	-	-	8,62	6,26	**PE-10 (0,3 mg) 13% 2**	0,290	0,310	0,770	1,05	**PE-100 (9 mg) 5% 2**	8,97	9,06	0,480	1,34*
Ctr 36% 3	-	-	7,34	5,73	**PE-10 (0,3 mg) 13% 3**	0,320	0,290	0,780	1,13	**PE-100 (9 mg) 5% 3**	8,99	8,94	0,550	0,480

Ctr 21% 1	-	-	4,47	4,15	**PE-10 (0,3 mg) 8% 1**	0,330	0,350	0,440	SL	**PS-10 (2,18 mg) 100% 1**	2,18	2,18	26,3	20,7
Ctr 21% 2	-	-	4,02	4,27	**PE-10 (0,3 mg) 8% 2**	0,330	0,290	0,400	0,530	**PS-10 (2,18 mg) 100% 2**	2,18	2,18	23,9	17,2
Ctr 21% 3	-	-	6,21	4,46	**PE-10 (0,3 mg) 8% 3**	0,350	0,290	0,380	SL	**PS-10 (2,18 mg) 100% 3**	2,18	2,18	20,0	12,9
Ctr 13% 1	-	-	2,97	2,54	**PE-10 (0,3 mg) 5% 1**	0,300	0,280	0,320	0,360	**PS-10 (2,18 mg) 60% 1**	2,18	2,18	10,9	7,88
Ctr 13% 2	-	-	2,43	2,07	**PE-10 (0,3 mg) 5% 2**	0,370	0,300	0,320	0,360	**PS-10 (2,18 mg) 60% 2**	2,18	2,18	10,9	8,57
Ctr 13% 3	-	-	2,02	2,45	**PE-10 (0,3 mg) 5% 3**	0,320	0,290	0,300	0,370	**PS-10 (2,18 mg) 60% 3**	2,18	2,18	9,66	8,33
Ctr 8% 1	-	-	1,74	1,02	**PE-100 (9 mg) 100% 1**	8,95	8,97	19,98	13,76	**PS-10 (2,18 mg) 36% 1**	2,18	2,18	4,72	3,56
Ctr 8% 2	-	-	2,40	1,23	**PE-100 (9 mg) 100% 2**	9,08	9,08	19,69	12,16	**PS-10 (2,18 mg) 36% 2**	2,18	2,18	4,44	2,63

Ctr 8% 3	-	-	1,47	1,42	**PE-100 (9 mg) 100% 3**	9,09	8,95	19,8	13,9	**PS-10 (2,18 mg) 36% 3**	2,18	2,18	5,08	3,69
Ctr 5% 1	-	-	0,990	1,15	**PE-100 (9 mg) 60% 1**	9,10	8,95	10,67	7,00	**PS-10 (2,18 mg) 21% 1**	2,18	2,18	2,44	1,83
Ctr 5% 2	-	-	0,770	0,770	**PE-100 (9 mg) 60% 2**	8,96	9,14	10,48	6,72	**PS-10 (2,18 mg) 21% 2**	2,18	2,18	2,24	2,12
Ctr 5% 3	-	-	0,750	0,860	**PE-100 (9 mg) 60% 3**	8,96	8,97	8,56	7,46	**PS-10 (2,18 mg) 21% 3**	2,18	2,18	2,67	1,92
PE-10 (0,3 mg) 100% 1	0,310	0,280	7,54	15,8*	**PE-100 (9 mg) 36% 1**	8,97	9,10	4,72	3,18	**PS-10 (2,18 mg) 13% 1**	2,18	2,18	SL	1,23
PE-10 (0,3 mg) 100% 2	0,290	0,310	12,4*	9,34	**PE-100 (9 mg) 36% 2**	9,00	9,10	4,98	2,82	**PS-10 (2,18 mg) 13% 2**	2,18	2,18	1,69	1,06
PE-10 (0,3 mg) 100% 3	0,310	0,320	7,08	8,17	**PE-100 (9 mg) 36% 3**	9,07	9,02	4,60	2,23	**PS-10 (2,18 mg) 13% 3**	2,18	2,18	1,49	1,11
PE-10 (0,3 mg) 60% 1	0,300	0,330	5,31	4,93	**PE-100 (9 mg) 21% 1**	9,06	9,03	4,62*	1,50	**PS-10 (2,18 mg) 8% 1**	2,18	2,18	0,720	0,410
PE-10 (0,3 mg) 60% 2	0,300	0,280	5,34	5,80	**PE-100 (9 mg) 21% 2**	8,98	8,94	2,90	2,11	**PS-10 (2,18 mg) 8% 2**	2,18	2,18	0,580	0,460

PE-10 (0,6 mg) 60% 3	0,280	0,320	5,08	15,4	**PE-100 (9 mg) 21% 3**	9,07	8,92	3,01	1,76	**PS-10 (2,18 mg) 8% 3**	2,18	2,18	0,770	0,770
										PS-10 (2,18 mg) 5% 1	2,18	2,18	0,430	0,340
										PS-10 (2,18 mg) 5% 2	2,18	2,18	0,510	0,240
										PS-10 (2,18 mg) 5% 3	2,18	2,18	0,500	0,340

*: Number either negative or outlier. Not used for further calculations.

SL: sample lost

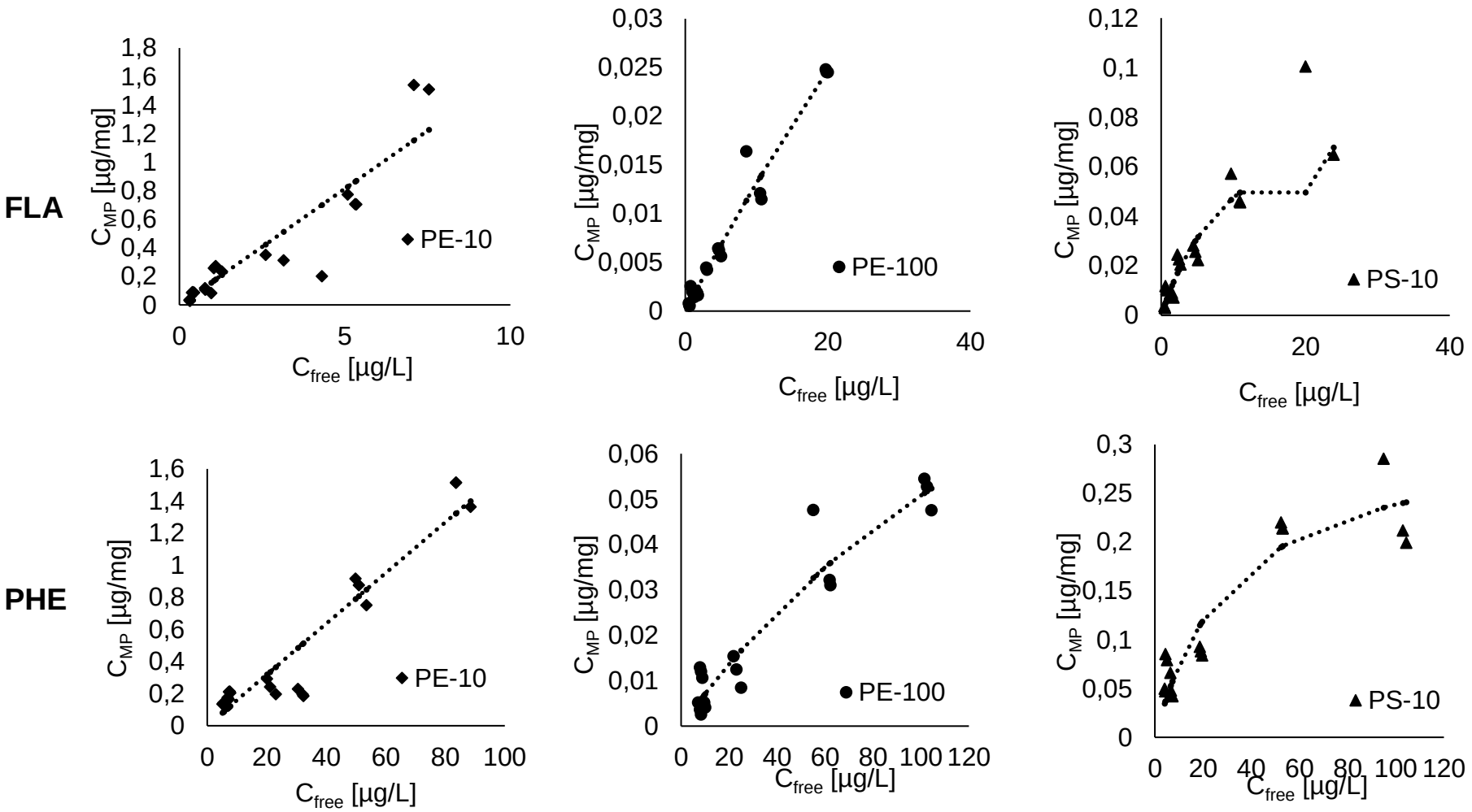

Figure G.1. Adsorption isotherms fitted to the Langmuir model at 10 °C. Model equations and parameters are described in Table 1.1 and fitted parameters in Tables 3.5 and 3.6. Dotted lines show fitting of the Langmuir model to the experimental data.

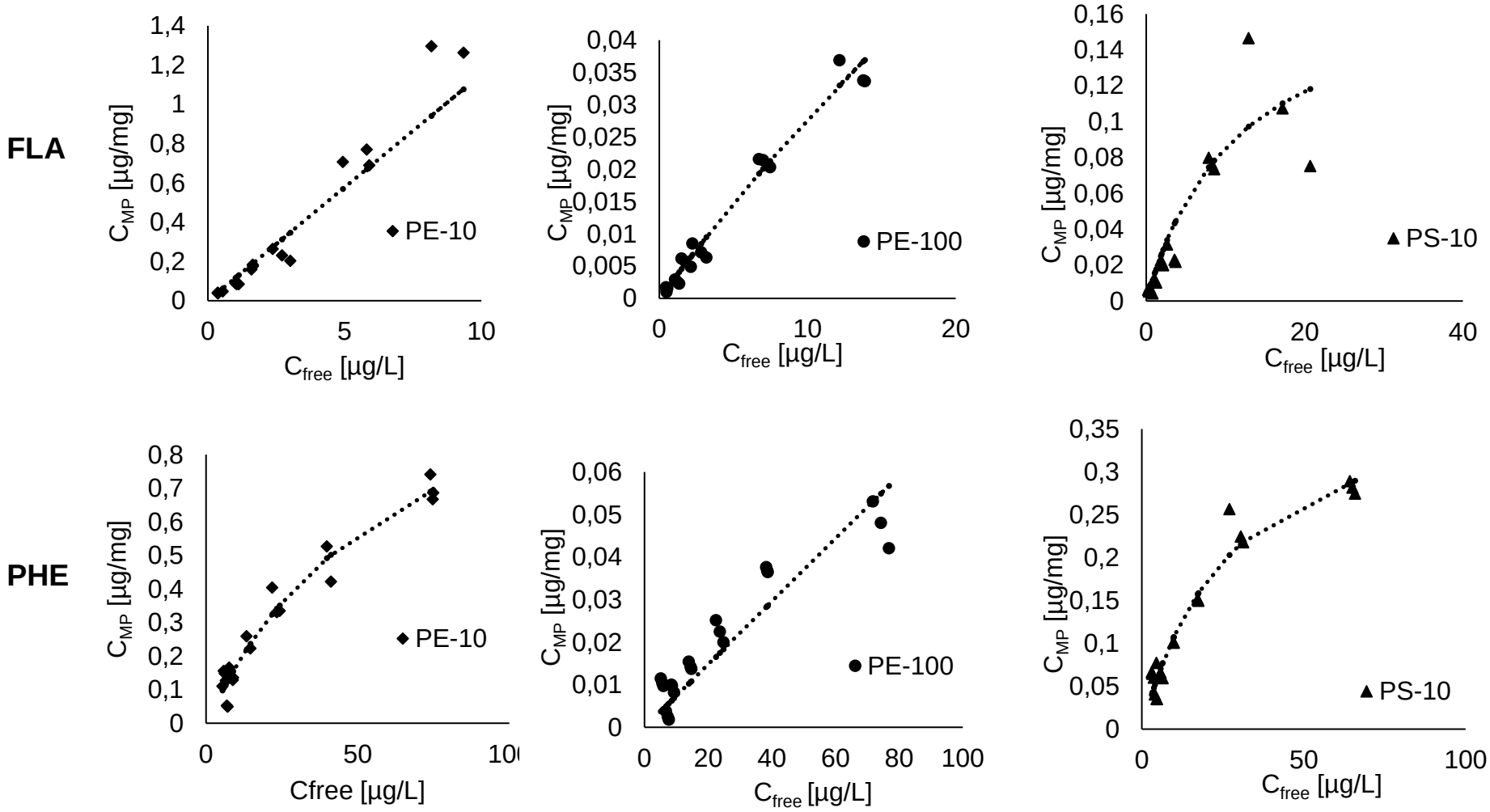

Figure G.2. Adsorption isotherms fitted to the Langmuir model at 20 °C. Model equations and parameters are described in Table 1.1 and fitted parameters in Tables 3.5 and 3.6. Dotted lines show fitting of the Langmuir model to the experimental data.

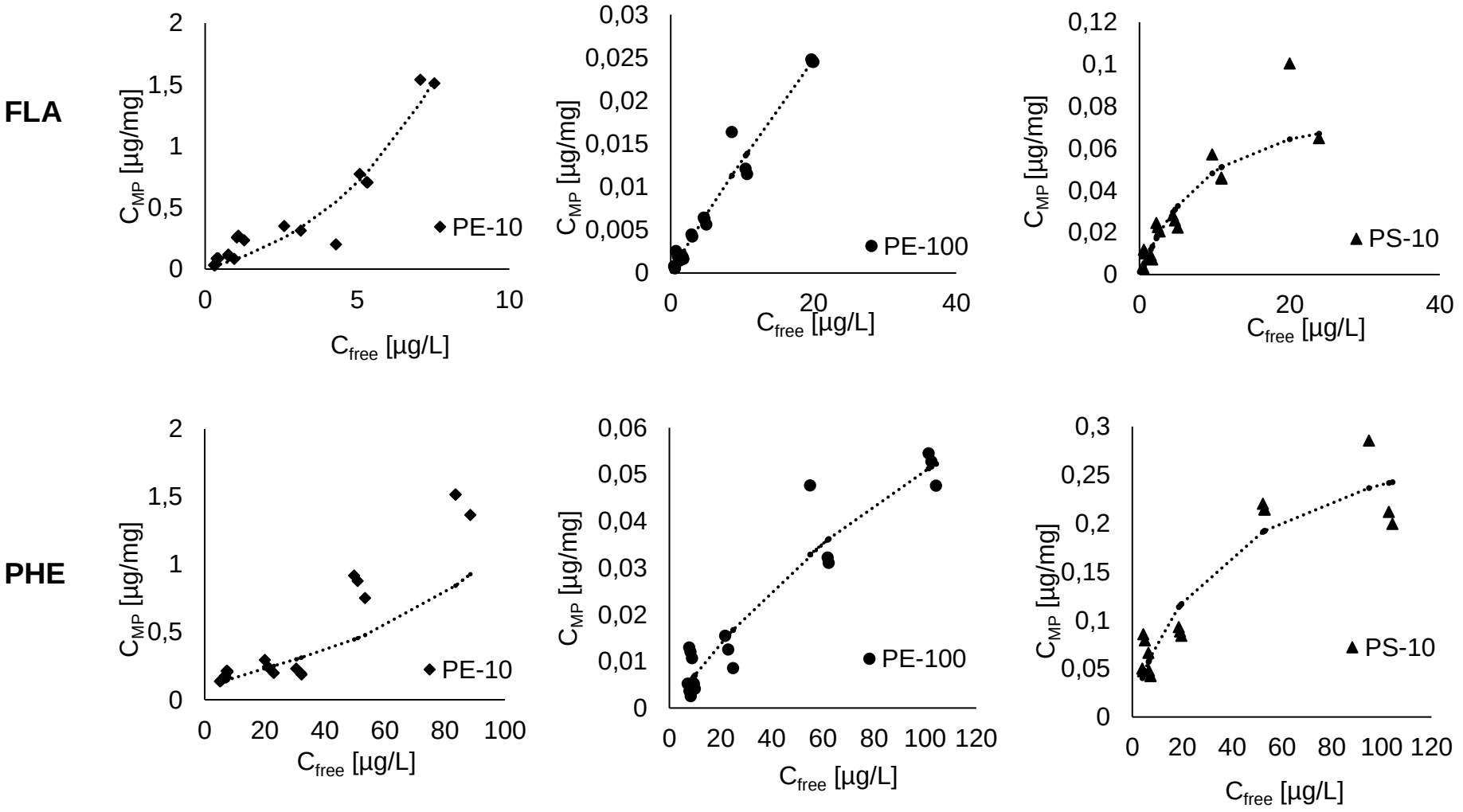

Figure G.3. Adsorption isotherms fitted to the Dubinin Ashtakhov model at 10 °C. Model equations and parameters are described in Table 1.1 and fitted parameters in Tables 3.5 and 3.6. Dotted lines show fitting of the Dubinin Ashtakhov model to the experimental data.

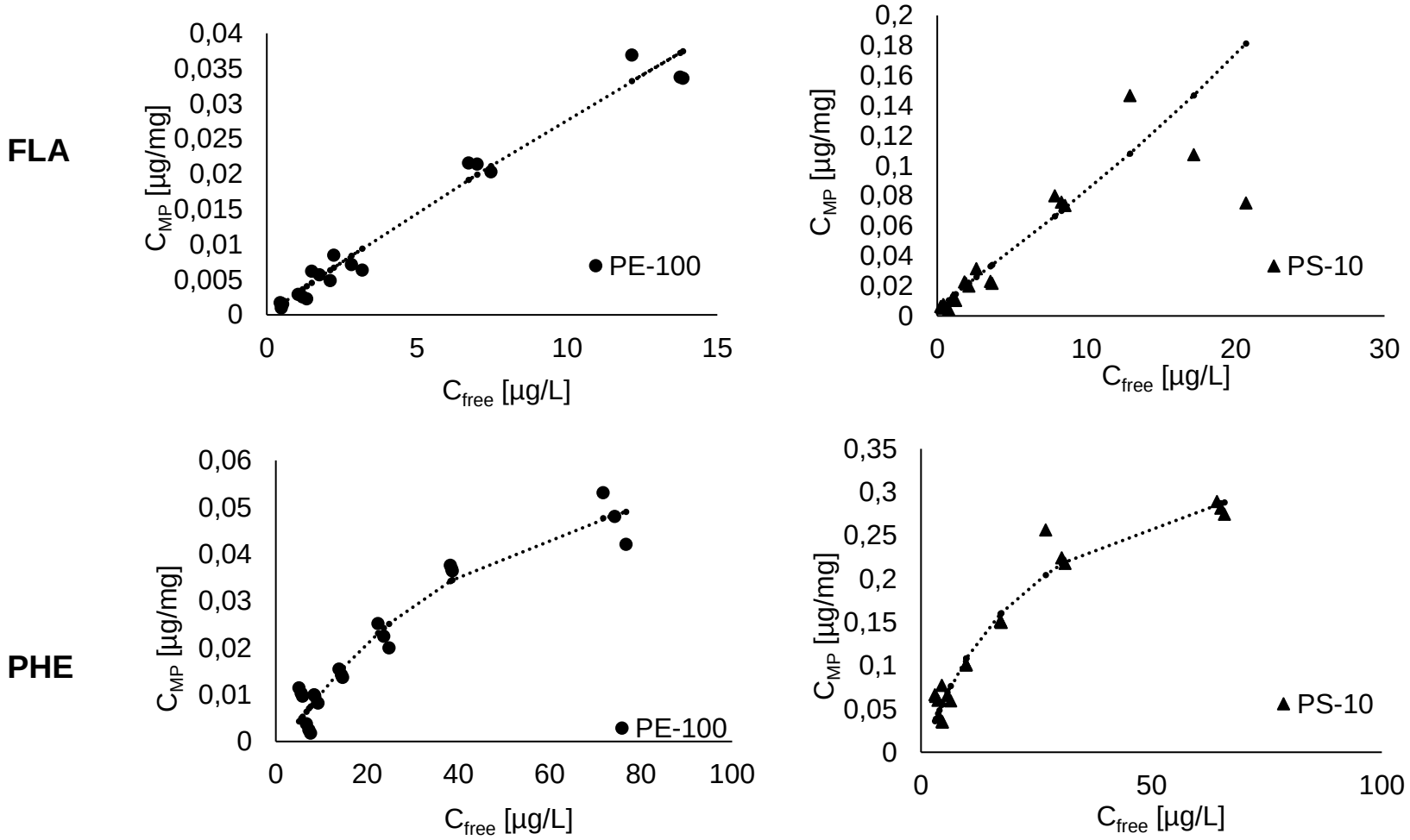

Figure G.4. Adsorption isotherms fitted to the Dubinin Ashtakhov model at 20 °C. Model equations and parameters are described in Table 1.1 and fitted parameters in Tables 3.5 and 3.6. Dotted lines show fitting of the Dubinin Ashtakhov model to the experimental data.

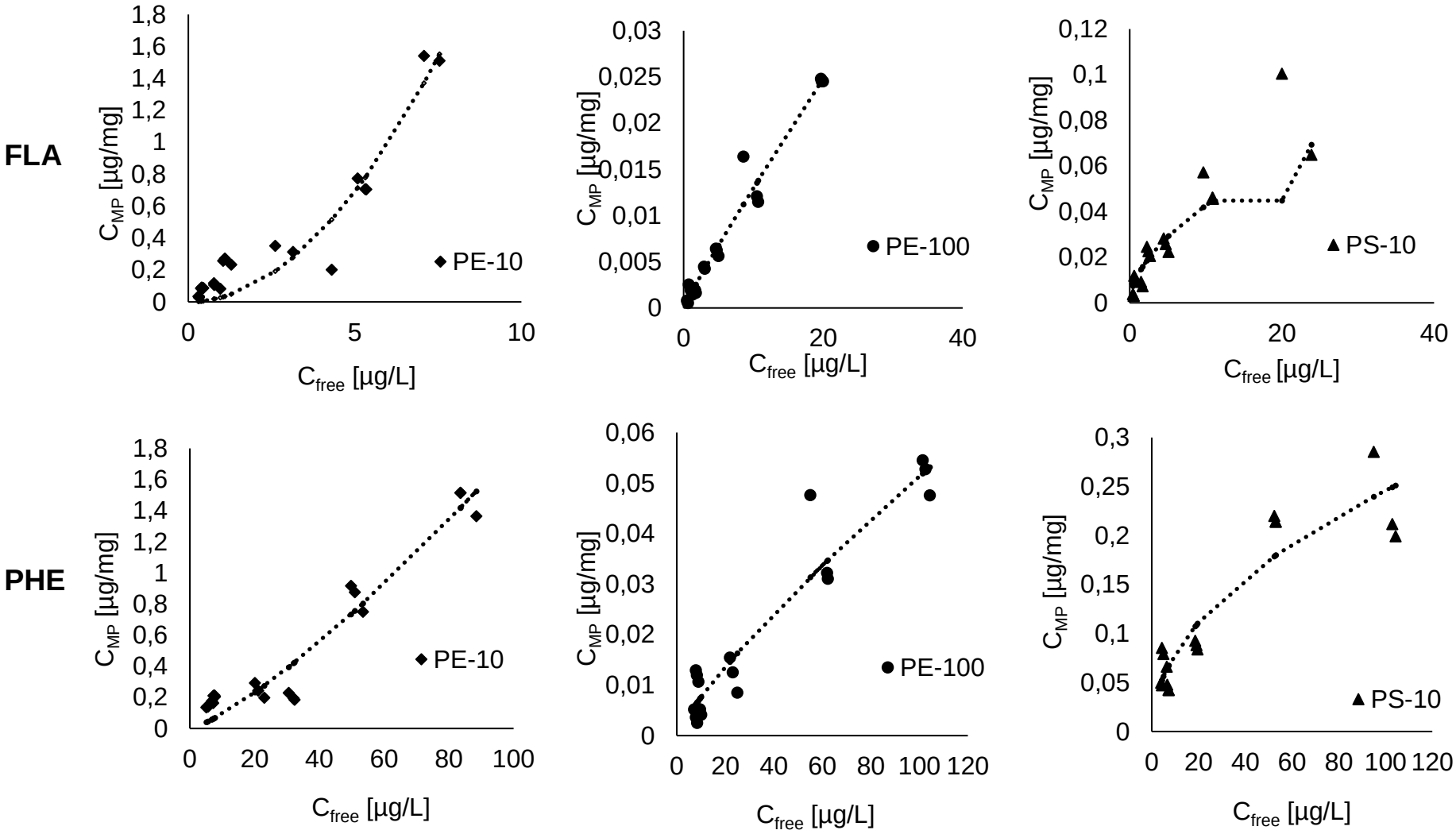

Figure G.5. Adsorption isotherms fitted to the Freundlich model at 10 °C. Model equations and parameters are described in Table 1.1 and fitted parameters in Tables 3.5 and 3.6. Dotted lines show fitting of the Freundlich model to the experimental data.

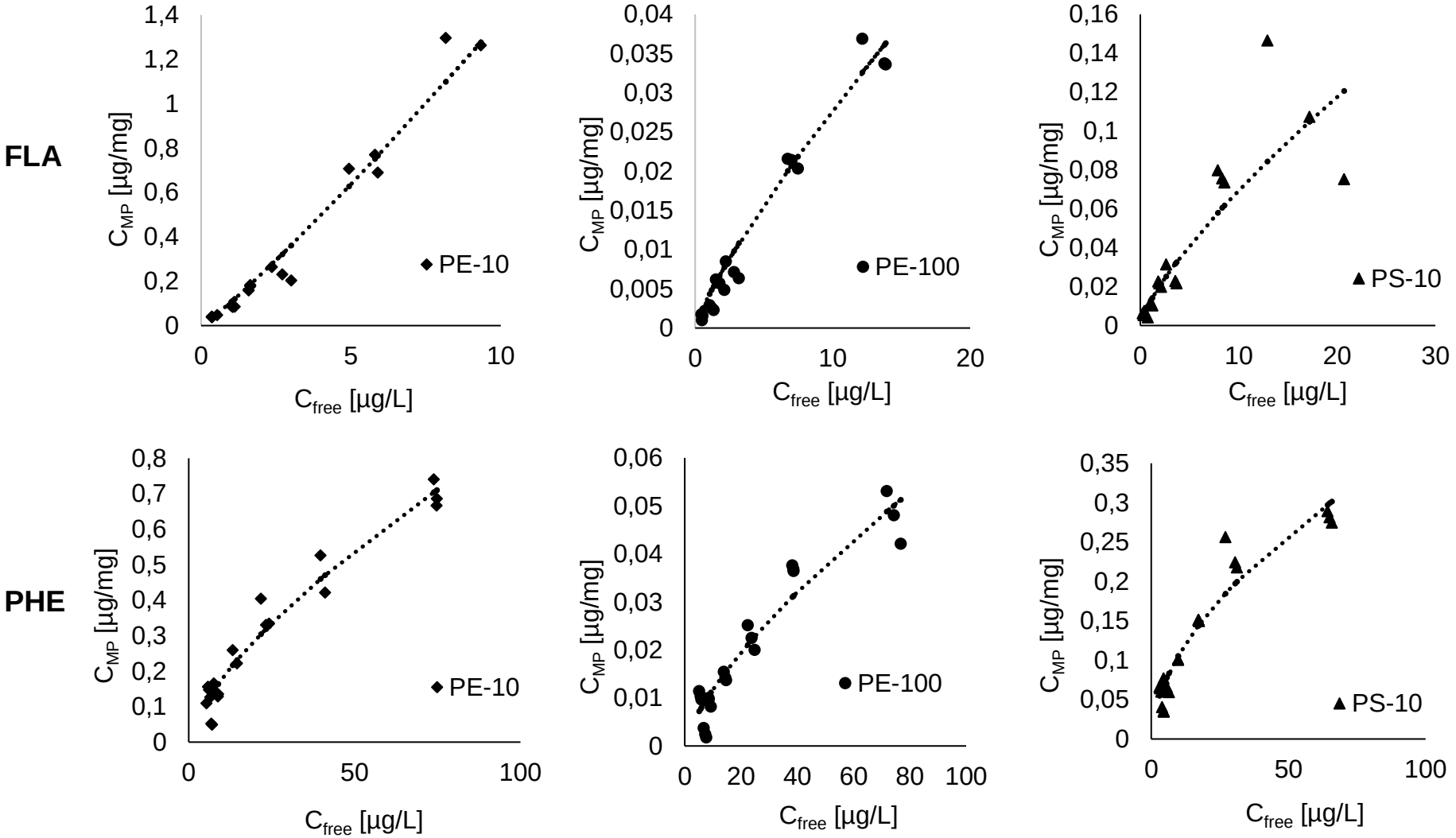

Figure G.6. Adsorption isotherms fitted to the Freundlich model at 20 °C. Model equations and parameters are described in Table 1.1 and fitted parameters in Tables 3.5 and 3.6. Dotted lines show fitting of the Freundlich model to the experimental data.

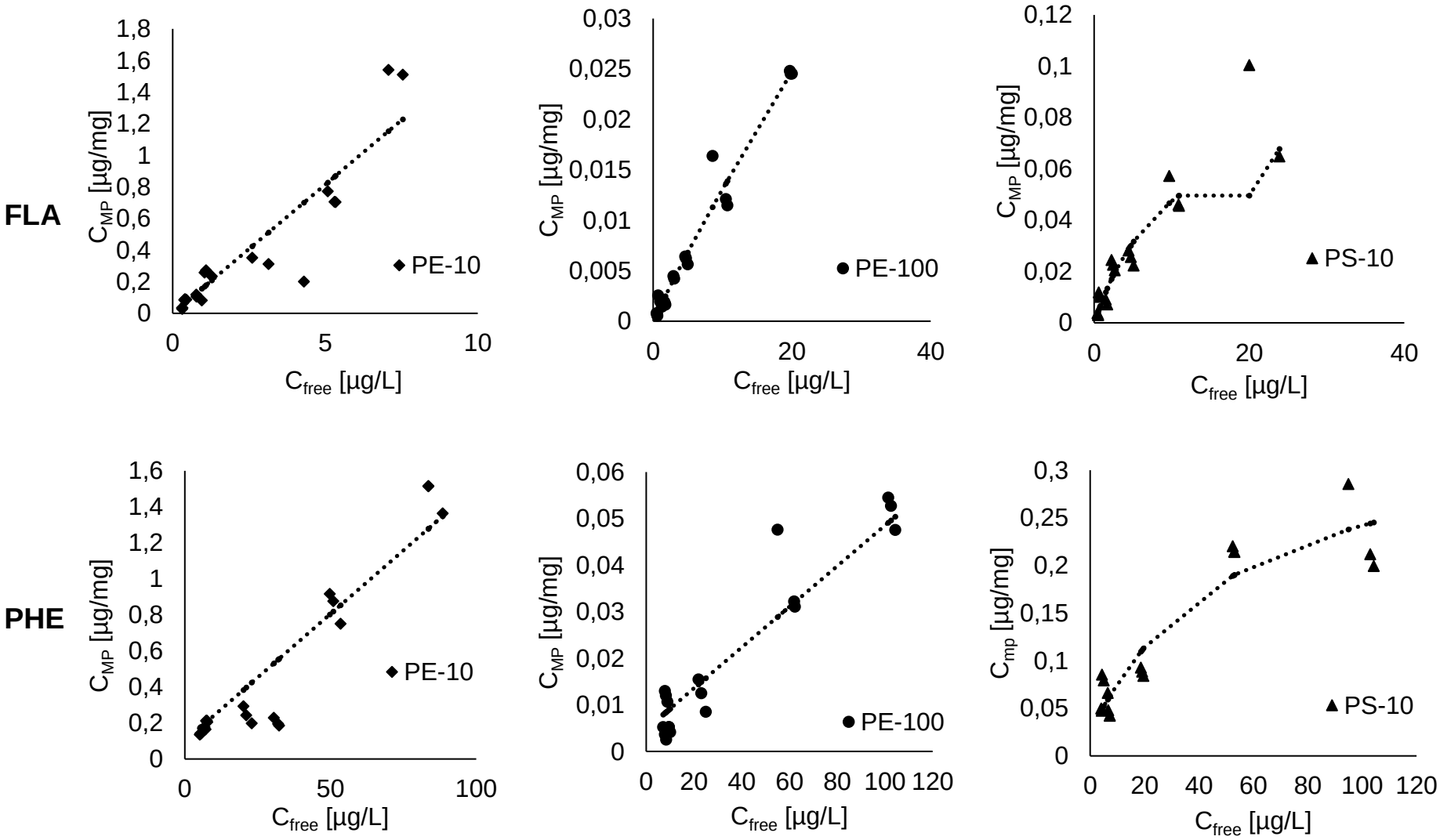

Figure G.7. Adsorption isotherms fitted to the Dual Langmuir model at 10 °C. Model equations and parameters are described in Table 1.1 and fitted parameters in Tables 3.5 and 3.6. Dotted lines show fitting of the Dual Langmuir model to the experimental data.

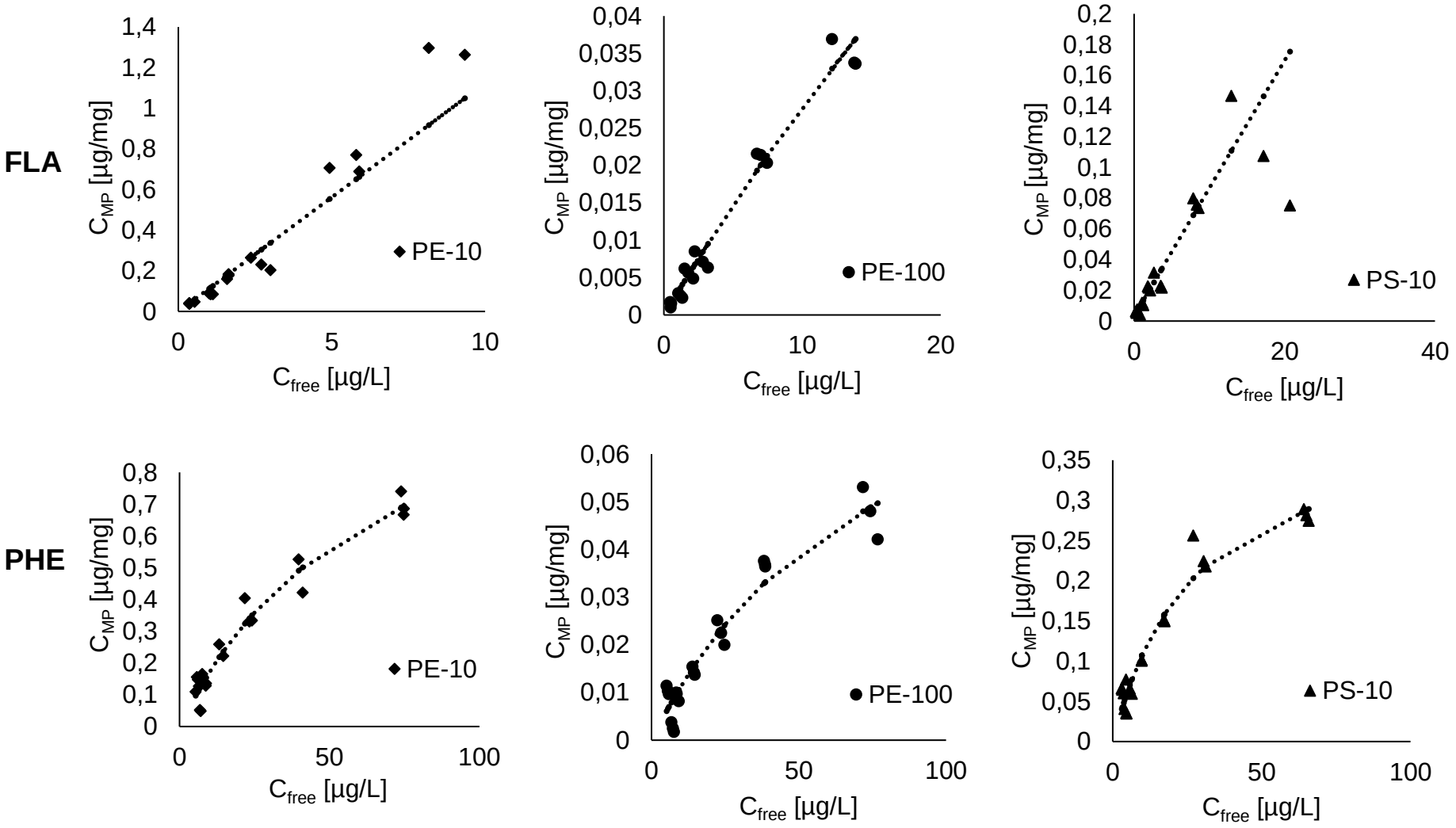

Figure G.8. Adsorption isotherms fitted to the Dual Langmuir model at 20 °C. Model equations and parameters are described in Table 1.1 and fitted parameters in Tables 3.5 and 3.6. Dotted lines show fitting of the Dual Langmuir model to the experimental data.

FLA

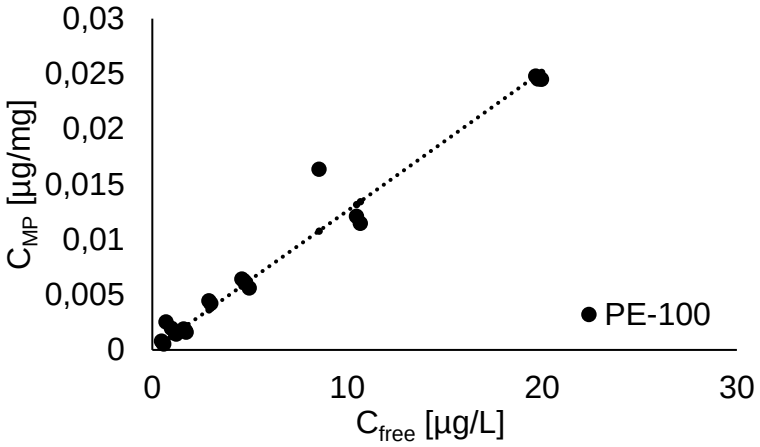

PHE

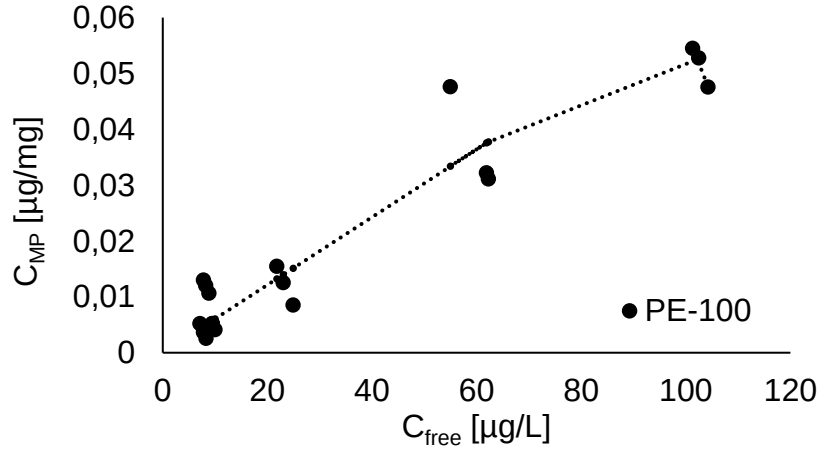

Figure G.9. Adsorption isotherms fitted to the Redlich Peterson model at 10 °C. Model equations and parameters are described in Table 1.1 and fitted parameters in Tables 3.5 and 3.6. Dotted lines show fitting of the Redlich Peterson model to the experimental data.

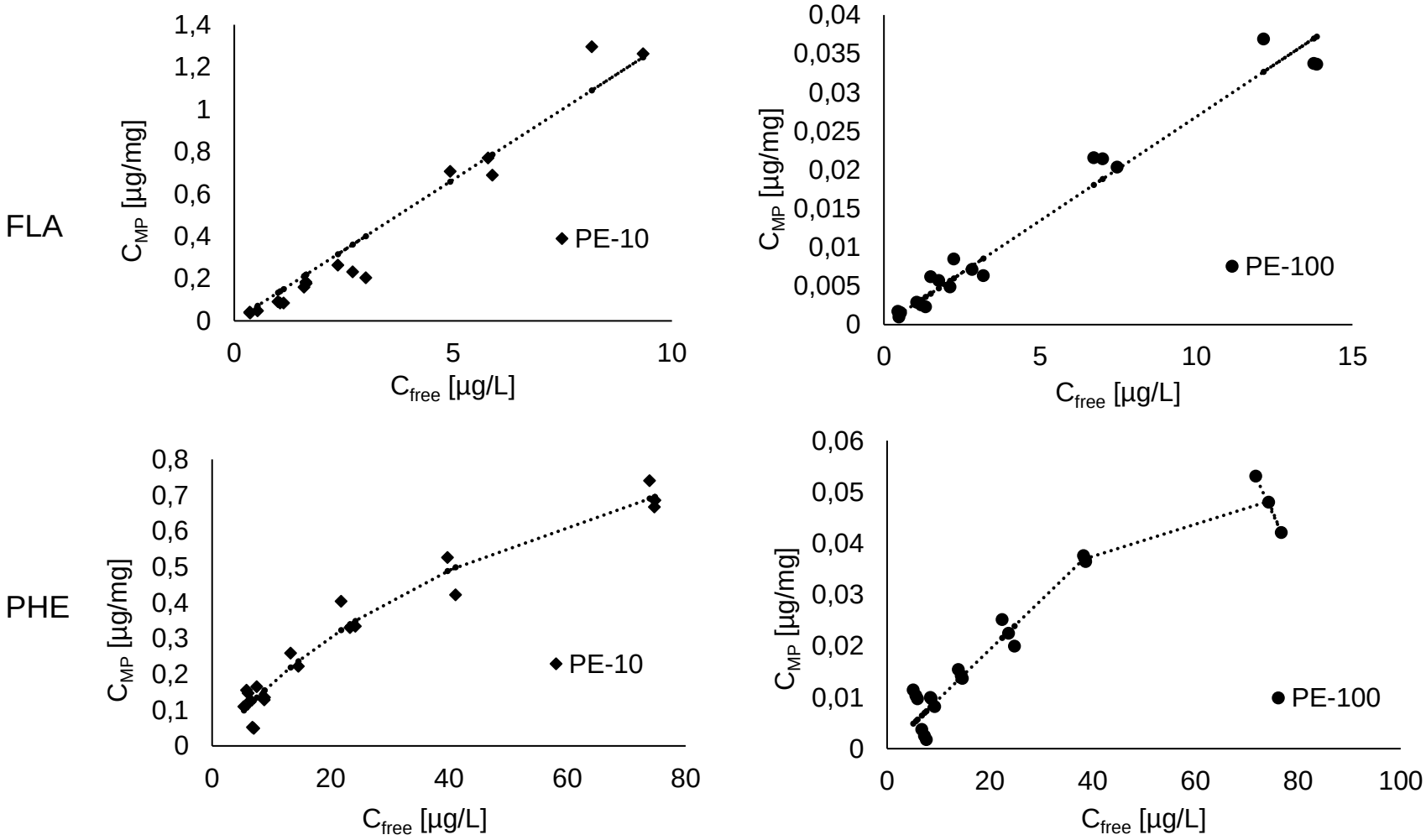

Figure G.10. Adsorption isotherms fitted to the Redlich Peterson model at 20 °C. Model equations and parameters are described in Table 1.1 and fitted parameters in Tables 3.5 and 3.6. Dotted lines show fitting of the Redlich Peterson model to the experimental data.

Table G.3. MWSE and R^2 of the Freundlich, Langmuir, Dual Langmuir, Dubinin-Ashtakhov and Redlich-Peterson models for adsorption isotherms of fluoranthene and phenanthrene to three types of MPs at 10 °C and 20°C.The visual fit of the model is also presented in the table, as representable (r) or not representable (nr) of the experimental data.

	Fluoranthene			Phenanthrene		
	Freundlich					
MP	***R²***	***MWSE***	***Visual fit***	***R²***	***MWSE***	***Visual fit***
PE-10 µm 10°C	0,9776	0,2131	nr	0,9527	0,1906	nr
PE-10 µm 20 °C	0,9999	0,03711	r	0,9991	0,1498	r
PE-100 µm 10°C	0,9999	0,06316	r	0,9999	0,1442	r
PE-100 µm 20 °C	1,000	0,1017	r	0,9999	0,2843	nr
PS-10 µm 10°C	0,9999	0,1469	nr	0,9999	0,06860	r
PS-10 µm 20°C	1,000	0,1040	r	0,9999	0,06820	r
	Langmuir model					
MP	**R^2**	**MWSE**	**Visual fit**	**R^2**	**MWSE**	**Visual fit**
PE-10 µm 10°C	0,9744	0,2138	nr	0,9408	0,1990	nr
PE-10 µm 20 °C	0,9945	0,05389	nr	0,9989	0,1456	r
PE-100 µm 10°C	0,9999	0,06347	r	0,9999	0,1461	r
PE-100 µm 20 °C	1,000	0,05889	r	0,9999	0,3265	nr
PS-10 µm 10°C	1,000	0,1190	r	0,9998	0,08940	r
PS-10 µm 20°C	1,000	0,1401	nr	0,9999	0,05980	r
	Dual Langmuir model					
MP	**R^2**	**MWSE**	**Visual fit**	**R^2**	**MWSE**	**Visual fit**
PE-10 µm 10°C	0,9955	0,4590	nr	0,9673	0,1546	nr
PE-10 µm 20 °C	0,9946	0,05384	nr	0,9989	0,1456	r
PE-100 µm 10°C	0,9999	0,06345	r	0,9999	0,1448	r
PE-100 µm 20 °C	1,000	0,05884	r	0,9999	0,3272	nr
PS-10 µm 10°C	1,000	0,1190	r	0,9999	0,05940	r
PS-10 µm 20°C	0,9999	0,1170	nr	0,9999	0,05930	r
	Dubinin-Ashtakhov model					
MP	**R^2**	**MWSE**	**Visual fit**	**R^2**	**MWSE**	**Visual fit**
PE-10 µm 10°C	0,9408	0,2228	nr	0,9486	160,0	r
PE-10 µm 20 °C	0,9952	0,03051	r	0,9643	0,1400	r

PE-100 µm 10°C	0,9803	0,06685	r	0,9507	159,0	r
PE-100 µm 20 °C	0,9885	0,06101	r	0,8459	0,2293	r
PS-10 µm 10°C	0,9682	0,1269	r	0,9849	159,0	r
PS-10 µm 20°C	0,9742	0,1408	nr	0,9856	0,06500	r

Redlich-Peterson model

MP	R^2	MWSE	Visual fit	R^2	MWSE	Visual fit
PE-10 µm 10°C	0,9845	0,2443	nr	0,9776	0,3100	nr
PE-10 µm 20 °C	0,9946	0,05743	nr	0,9988	0,1498	r
PE-100 µm 10°C	0,9999	0,06718	r	0,9999	0,1544	r
PE-100 µm 20 °C	1,000	0,06251	r	0,9999	0,3446	nr
PS-10 µm 10°C	1,000	0,1244	r	0,9999	0,07363	r
PS-10 µm 20°C	1,000	0,2198	r	0,9999	0,06128	r

The role of microplastics size and type on PAH sorption and bioavailability to copepods

Lisbet Sørensen[1], Emilie Rogers[2], Dag Altin[3], Marianne Unaas Rønsberg[1], Andy Booth[1]

[1]SINTEF Ocean, Norway; [2]Norwegian University of Science and Technology, Norway; [3]Biotrix, Norway

Introduction

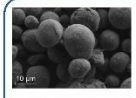

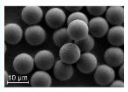

Figure 1. SEM images of PE (top) and PS 10 µm microbeads used in the study.

- Microplastic (MP) may act as a vector for chemical pollutants already present in the environment.
- Polycyclic aromatic hydrocarbons (PAHs) are ubiquitous environmental pollutants, known to cause adverse effects to a variety of marine organisms.
- The relatively high polymer-water partition coefficients of PAHs means they adsorb to MP readily
- Abroad range of marine species have been shown to ingest significant quantities of MP, with extended periods of retention observed in some cases.
- If PAHs are adsorbed to the MPs, this could present an alternative exposure route to PAHs for such species.
- Here, we investigate the sorption kinetics for two model PAHs, fluoranthene (FLA) and phenanthrene (PHE), to polyethylene (PE) and polystyrene (PS) MPs in natural seawater.
- The influence of MP sorption on PAH bioavailability to two marine copepod species (*Acartia tonsa* and *Calanus finmarchicus*) was investigated using PE particles larger and smaller than the ingestion limit.

Materials

PAHs

	SW solubility (µg/L)		LC50 (µg/L)	
	10 °C	20 °C	*Calanus f.*	*Acartia t.*
FLA	28	84	>28	77-84
PHE	159	415	>159	301-331

MPs

	Diameter (µm)	Density (g/cm³)	SA (m²/g)
PS-10	10	1.05	0.833
PE-10	3-16	0.96	0.877
PE-100	90-106	0.96	0.085

PAH-MP partitioning behaviour

- The partitioning of PHE and FLA from seawater to PE and PS MP particles was investigated at 10 and 20 °C.
- Preliminary kinetics experiments showed that equilibration time for fluoranthene at both temperatures was achieved after <5 days, whilst for phenanthrene equilibrium was achieved after <7 days at 10 °C and <9 days at 20 °C.
- For isotherm studies, seawater solutions of PHE and FLA at maximum solubility at 10 °C were diluted to seven concentrations representing 5-100 % solubility (1.67 spacing factor).
- Per mass of polymer, the sorption of PAHs increased by PE-10>PS-10>PE-100. Per surface area of beads, the sorption of PAHs increased by PE-10>PS-10>PE-100.
- Linear, Freundlich, Langmuir, Dual Langmuir, Redlich-Peterson and Dubinin-Ashtakhov isotherms were fitted to the data.

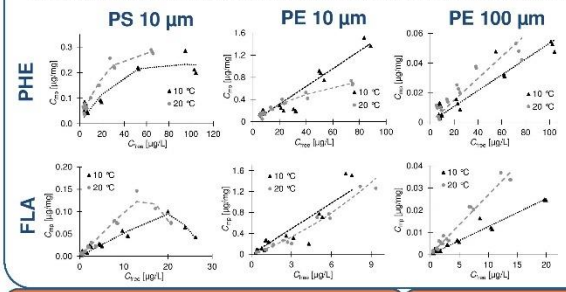

Results

- For PS-10 and PE-10 at 10 °C, Redlich-Peterson best described the sorption, indicating a combination of monolayer and multilayer adsorption.
- For PE-100, a best fit of linear isotherms indicate that the sorption is influenced by absorption
- For PE-10 at 20 °C, a best fit of Dubinin-Ashtakhov indicates higher temperatures allow transitioning of PAHs into micropores.

Figure 2. Sorption isotherms describing uptake of PHE and FLA from seawater to PS-10, PE-10 and PE-100 MPs at 10 and 20 °C.

Methods

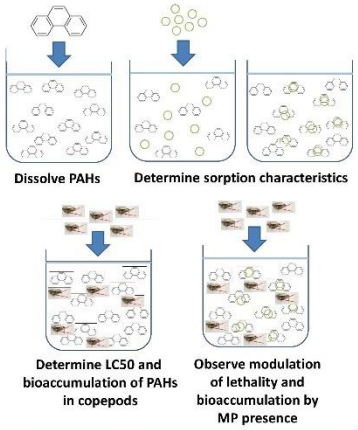

MP ingestion by copepods

Acartia tonsa

Figure 3. Acartia tonsa with 10 µm PE (Dag Altin, Biotrix).

Calanus finmarchicus and *Acartia tonsa* ingested MP ~10 µm diameter, but not MP >90 µm in diameter. Ingested particles were observed both in the body of the organism and encapsulated in faeces.

Calanus finmarchicus

Figure 4. Left: Calanus finmarchicus with 90-100 µm PE that could not be ingested. Right: faeces with ~50 µm PE (top) and ~3-16 mm PE (bottom) encapsulated (Dag Altin, Biotrix).

MP influence on PAH accumulation and toxicity

- The modular effect of PAH sorption to PE-10 and PE-100 on lethality and accumulation of PAHs in copepods was investigated.
- It was hypothesized that ingestible MP could lead to an increased body burden load, compared to non-ingestible MPs.
- The freely dissolved fraction of PAHs (C_{free}) was measured before and after exposure, and the body burden of PAHs in *Calanus finmarchicus* was measured in viable organisms after 4 days exposure.
- While PE-10 reduced C_{free} by ~50 % (49±6 for FLA, 47±5 for PHE), PE-100 reduced C_{free} by 21±5 for FLA and 32±3 % for PHE.
- The difference in C_{free} reduction was not reflected in reduction of lethality and body burden (> 50 % for both MPs).
- This indicates that a negligible amount of MP sorbed PAHs is bioavailable.

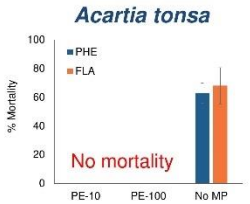

Figure 5. Mortality in Acartia tonsa exposed to MP modulated PAHs

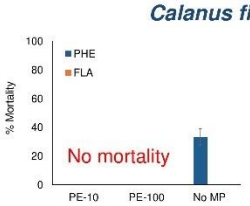

Figure 6. Mortality in Calanus finmarchicus exposed to MP modulated PAHs

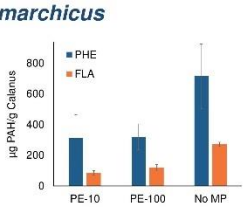

Figure 7. PAH body burden in Calanus finmarchicus exposed to MP modulated PAHs

PLASTOX is supported by national funding agencies in the framework of JPI Oceans and other institutions

https://www.sintef.no/projectweb/plastox/

Follow PLASTOX on Facebook